UNIVERSITY
OF TRENTO - Italy
Department of Materials Engineering
and Industrial Technologies

Doctoral School in Materials Science and Engineering – XXIV cycle

A Smart Solution for Tissue Engineering Applications

Christian Lorandi

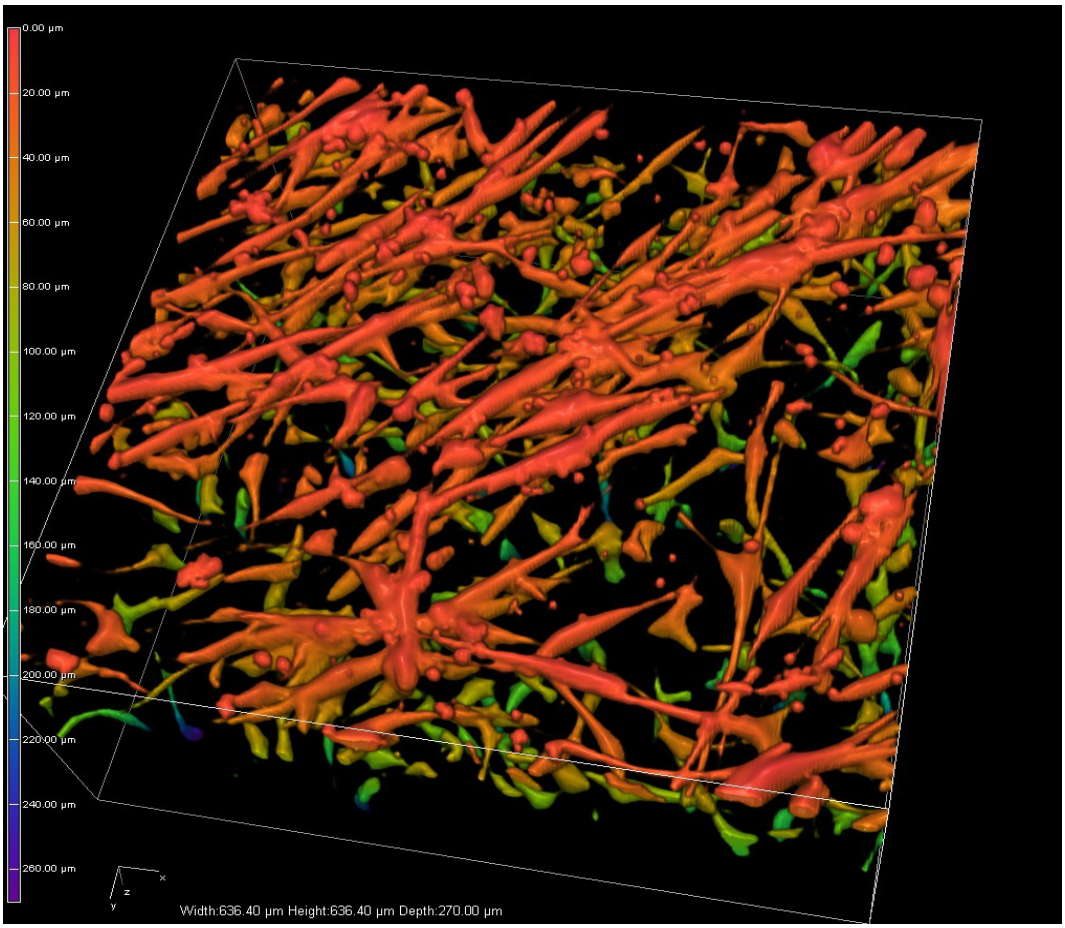

April 2012

Contents

List of Figures

Abstract

Gelatine, which is produced by collagen partial hydrolysis, has been largely used in the biomedical field for a wide variety of applications, which are ranging from drug delivery to wound healing. Its spread depends strongly on its biocompatibility: this natural polymer is indeed non-toxic, non-carcinogenic, non-immunogenic, enzymatically degradable and bioresorbable. In the biomedical field gelatine is mostly used as highly concentrated hydrogel (with a melting point above 43 °C - 45 °C) or cross-linked.

This work investigated the use of uncross-linked gelatine hydrogels, with a melting temperature in the physiological range, for different biomedical applications.

Firstly, it was studied the possibility to produce a solid hydrogel to use as easily removable wound dressing. Once applied to a wound, this patch keeps a moist environment in order to improve the regeneration, while releasing drugs or bioactive factors that it could be preloaded of. Moreover, it can be easily removed, without damages to the wound site and the newly formed tissue, by washing with warm sterile water (37 °C - 39 °C).

Secondly, the gelatine material was investigated as substrate for the so-named cell sheet engineering. With our procedure cell sheets can be grown on the gelatine gel and, successively, they can be integrally transferred to a different surface, with gelatine being removed by melting at 37 °C, without any proteolytic enzyme. The gelatine sheet supporting cells, differently from the "Okano" cell sheet method, could be also directly implanted *in-vivo* without

any need for removal, due to the gentle melting of the gelatine sheet after implantation.

Thirdly, gelatine gels were used as depot to release pro-angiogenic factors *in-vivo*. Due to their ability to absorb aqueous solutions and release them while dissolving / degrading, gelatine gels were loaded with Amniotic Fluid Stem Cells Conditioned Medium and used to evaluate the effect of grow factors in a model of ischemic fasciocutaneous flap.

Additionally, in order to evaluate the *in-vivo* degradation rate of gelatine gels loaded with Platelet Rich Plasma, a preliminary test was performed. The results of this test suggested the possibility to employ the gel films as antiadhesive membranes in surgery.

Since the gelatine hydrogels ability to melt at body temperature is still almost completely unexploited in the medical field, the work described in this thesis was protected by two patent deposits: EP 11 183 232 “Therapeutic use of gelatin hydrogels with a gel-sol transition at body temperature” and EP 11 183 233 “Medical uses of lyophilized polymeric membranes containing blood derivatives”.

Chapter 1

Introduction

1.1 Tissue Engineering

Important results in terms of healing and reconstruction of human tissue have been achieved by extensive research in the medical and engineering fields with a world wide biomaterials market that in 2005 was worth more than 300 billions dollars, with a grow rate of 20% per year.

Tissue engineering and regenerative medicine focuses on the production of new materials and devices able to interact with cells and biological tissue to promote regeneration. Several definitions of Tissue Engineering were given in the past, such as from Langer et al. They defined Tissue Engineering as "an interdisciplinary field that applies the principles of engineering and life sciences toward the development of biological substitutes that restore, maintain, or improve tissue function" [1]. Tissue engineering approaches the problem with the production of scaffolds, which are often preloaded with cells and designed to mimic natural tissue structure and function. On the other hand regenerative medicine usually focuses more on the use of stem cells for the production of new tissue [2].

In the last few years tissue engineering has became a viable option for tissue and organ function replacement thanks to the progress in the field. The

creation of these complex devices, often loaded with cells, requires a three dimensional, porous, biocompatible scaffold. The main role of scaffolds is the promotion of new tissue formation while acting as temporary support for the new forming tissue.

Scaffolds should also preferably be biodegradable and their degradation products should be biocompatible, in order to avoid chronic inflammatory response. Geometry, porosity and chemistry of the device have to allow sufficient permeability, necessary for nutrients exchange, and to avoid stagnation of wastes.

By changing materials and/or fabrication method, scaffold properties can be adapted to the different physical or biological requirements, such as strength, porosity, degradation rate, and surface chemistry. As already said, in most cases scaffolds should be biodegradable, with degradation by-products which, as the native polymers, possess the required biocompatibility with the host tissue [3, 1]. Moreover, in most cases scaffold materials are polymers which can be synthetic or natural.

Synthetic polymers The technology for the production of synthetic polymers offers the possibility to tailor their chemical structure, and therefore their properties on specific needs. Another advantage derives from their degradation mechanism, mostly hydrolytic, hence with a reproducible degradation rate independent of the host. On the other hand, some of them, which are degraded by acid hydrolysis, produce acids as degradation products, leading to an auto-catalytic degradation process, especially in thick samples; the acidic environment induced by degradation may result in inflammatory response or fibrous encapsulation [4, 5, 6].

Most of synthetic polymers used in tissue engineering are polyesters (poly (glycolic) acid [7] , poly (L-lactic) acid [8], poly(D,L-lactic acid-co-glycolic acid [9], poly(ε-caprolattone, poly(propylene fumarate), polyorthoester) [10], but there are also polyanhydrides [11], polycarbonates, poly(ethylene glycol) and poly(ethylene oxide) [12].

Natural polymers Most of natural polymers are enzymatically biodegradable; they often contain biofunctional moieties, which are known to improve cell adhesion, proliferation and differentiation. Even if these properties could appear all positive, some of them may be a problem for the production of scaffolds. In particular enzymatic biodegradability can lead to precocious degradation or to a biostable material, depending on the enzyme levels and activity, which are not constant in the body and can be much different from one patient to another. For this reason the degradation rate could become difficult to predict and tailor.

Natural polymers are further divided into two major classes: polypeptides and polysaccharides. Most known polypeptides are collagen [13], gelatine (which is basically denaturated collagen), elastin [14] and fibrin [15] (mainly obtained by mammalian and fishes), and silk [16] (obtained by insects and arachnids). Collagen is one of the most important component of mammalians tissues, therefore it is easy to understand why it is one of the most studied materials in tissue engineering. On the other hand, the most used polysaccharides are agarose and alginate [17] (derived from algae), chitosan [18] (obtained by partial deacetylation of chitin, found in crustacean and insect exoskeleton), starch [19] (extracted from vegetables), and hyaluronic acid [20] (a glycosaminoglycan (GAG), found in mammalians extracellular matrix).

Biocompatibility and inflammation response The biological response to any living tissue damage is inflammation. Since scaffolds, prosthesis or any other device implantation in the body will cause some kind of injury to the surrounding tissues, inflammation will certainly occur [21]. Moreover, any implant represents a "foreign body" for the host, which causes an amplified inflammatory response [22]. The aim of this response is the protection of the organism, by destroying or isolating the foreign body; to achieve this goal, a series of complex events takes place.

In the first instance, acute inflammation occurs. This cleans the wound site, and provides a provisional matrix. This phase is characterized by vessels

dilation in order to increase the blood flow to the area. Fibrin contained in the blood coagulates and forms a clot, which closes the wound, preventing successive contaminations. Many proteins, such as cytokines and growth factors, are released in the area, while cells, mainly neutrophils and monocytes, are recruited to the injury site [23]. If the foreign body is not eliminated by neutrophils and macrophages, it leads to chronic inflammation [24].

In case of chronic inflammation monocytes, macrophages as well as lymphocytes are still present, new blood vessels are formed to ensure an adequate transport of nutrients, and an increase in the production of connective tissue is observed. In this phase the fibrin cloth previously formed is transformed in highly vascularized granulation tissue by fibroblasts and endothelial cells. Proceeding with the healing process, granulation tissue is substituted for extra cellular matrix (EMC), made of collagen, elastin, glycoproteins and proteoglycans [25].

Moreover, during the inflammation, immune response is carried out by antibodies, complement components, cytokines, chemokines, growth factors and other proteins able to detect a foreign agent and to guide cell recruitment and modifications in order to attack the foreign body.

On this bases, there are some goals that a tissue engineered device has to achieve in order to work properly *in-vivo*:

- restoration of the target tissue with its appropriate function,
- inhibition of macrophages and foreign body response which may degrade the device,
- inhibition of scar and fibrosis formation which may reduce the tissue and the device functionality, and
- inhibition of the immune response, which would cause severe damages to the device itself and surrounding tissues [26, 21].

Cell adhesion and migration Adhesion plays a critical role in the healing process. It is possible to distinguish between two types of adhesion: cell to cell and cell to ECM interactions. Both of them are mediated by trans-membrane receptors, a well as structural and regulatory proteins, which are displayed on the cell surface [27]. Cell to ECM interactions influence cell spatial distribution and migration into tissue and organs. Additionally, cell to cell interactions are necessary to form the three dimensional tissue structure [28].

Three characteristics are shared by all the cell receptors. Firstly, when attached to their ligand, they tend to assemble into clusters. Secondly, they are often linked to cytoskeletal structure, allowing the mechanical binding of the cell to the substrate and mechanical stress transmission. Thirdly, regulatory proteins are associated with receptor clusters, which are regulating cell proliferation and function [29].

Initially, the development of tissue engineered materials focused on obtaining bioinert materials (e.g., titanium, ultra high molecular weight polyethylene...), which had good mechanical properties, and low, a-specific, cell interaction. But it was soon clear that it was not the right path to follow; so devices with a strong cell-material interaction were developed. It was discovered that the increase of cell-device interaction interferes with the natural cell-cell interaction, leading to a suboptimal tissue development. Therefore, new biomaterials were developed trying to balance the two types of interaction. The tailoring of the biological surface properties is often obtained by functionalization of the material by grafting peptides on the surface, inducing an adequate cellular response. In other cases, it is possible to adjust the adhesion just by changing the surface energy (i.e., by changing the hydrophobicity) and the electrostatic charges, modifying the protein adsorption and therefore the cell adhesion [30].

Another important phenomenon affected by cell adhesion is cell migration. Cell migration plays a key role in tissue formation and integration starting from cells seeded on the scaffold. Materials treated to improve cell adhesion, cell migration and in general, biomolecular recognition, often by mimicking

the natural ECM, are called biomimetic [30]. ECM is a complex mixture of proteins produced by the cells. It is part of the tissue, and governs the cell behavior, thus influencing cell migration, growth, division and differentiation. Cell receptors, which are able to detect ECM signals, are located on the cell surface, and pass through the cell membrane. In a living tissue, the ECM is continuously remodelled, to modify the tissue as the need arises. A goal of tissue engineering is to stimulate ECM production to improve tissue regeneration. Increase in the catabolic pathway, which leads to tissue destruction, should be avoided. To improve their biomimetic properties, implanted materials can be functionalized with ECM proteins; in this way, the implant will not be detected as "foreign body". Moreover, in this way, it is also possible to modify the cell response to the material. Sheets of highly organized ECM made of collagen, laminin, proteoglycans and other proteins, called basement membrane, provide an anchor for cells to adhere and spread through specific surface receptors, called integrins [31, 32].

1.2 Gelatine

This research focuses on the exploitation of the physical and chemical properties of gelatine, in order to produce substrates for the tissue engineering. The first known gelatine use dates back to about 8000 years ago. In those days gelatine obtained by boiling animal tissues was used as glue; for the same purpose gelatine was used by the Egyptians around 3000 B.C. The first documented use of gelatine for "medical" purposes is probably dated back to around 1150 A.C. when Hildegard von Bingen, Benedictine Abbess and universal scholar, recommended in her "Physica" frequent eating of broth made from calves feet as relief from joint pain. For centuries gelatine was considered a special food for rich people. During the Napoleonic Wars (19th century), due to the blockade of the French ports by the British navy, gelatine obtained by boiling bones was found to be a protein source to replace meat, which was in short supply.

The revolution in the use of gelatine for biomedical applications happened

in 1833: Mothes, a French pharmacist, patented the manufacture of gelatine capsules to encapsulate drugs. With these capsules, drugs dosing was much easier. Gelatine acted as a barrier from heat, cold and humidity and strongly affected taste: drugs no longer tasted bitter. In the 20th century the use of gelatine in medicine exploded, ranging from sponges for blood absorption during surgeries to gelatine-based substances used as blood replacement agents or plasma expanders [33].

Gelatine is a mixture of proteins obtained by native collagen partial hydrolysis; the content of protein ranges from 85% to 92%, the remainder is constituted by salts and moisture still left after drying [33]. Collagen is a family of proteins (at least 27 types of collagen are known) contained in the connective tissues of animal bodies. About one-third of all the proteins in the human body are collagen. Collagen is structured in triple helices incorporated in rod-like fibrils; these fibrils can also interact with other proteins [34]. The primary structure of type I animal collagen (used for gelatine production) is a sequence of amino acids linked to form chains, of about 100 000 g/mol, which are called α-chains. The α-chain comprises 334 repetitive units of the sequence glycine-X-Y (where X and Y are other amino acids). Glycine covers about 33% of the amino acid component; while proline and hydroxyproline together about 22%. Proline often covers the X-position, while hydroxyproline is almost always in Y-position. The other amino acids (45%) are distributed in X and Y position (some positions are preferred due to steric and electrostatic reasons). Only at the N- and C-terminal ends it is possible to find short chains (15-26 amino acids), which do not fit the glycine-X-Y model. Proline and hydroxyproline are responsible for the secondary structure of collagen: they limit the rotation of the backbone and contribute to the structure of the triple helix. Type I collagen is composed of three α-chains, two of which are identical and one slightly different. Each α-chain is coiled into a left-handed helix with about three amino acids per turn. The three α-chains are then twisted around each other into a right-handed super-helix to form the rigid rope-like structure [35, 33].

Gelatine is produced industrially by treating animal skin (it would be possible to use also bones, but it is more difficult; so, for economical and practical reasons, skin is usually preferred, even if gelatine from bones is different from gelatine from skin) with dilute acids or alkali at a moderate temperature, inducing partial cleavage in the natural cross-linking present in the collagen structure.[1] [2] Due to differences in the cross-linking degree, which depends on the age of the animal, the hydrolysis treatment may vary slightly from one batch to the other. The resulting hydrolyzed proteins mixture, the gelatine, is soluble in warm water. After this step, known as "conditioning process", the warm-water soluble gelatine is extracted by melting it out of the raw material (i.e. the animal skin) through the increase of the temperature of the bath: here an additional thermal hydrolysis step occurs.

Technically, the conditioning process is not mandatory. Gelatine was produced for centuries just by boiling hide and bones; anyway, such a long high temperature process would partially destroy the collagen structure. The collagen structure on the contrary, gentle hydrolysis with diluted acids or alkali allows to keep almost intact, while eliminating the cross-linking.

By controlling type and intensity of the hydrolysis, it is possible to control the molecular weight distribution of the obtained gelatine. The molecular weight distribution is clearly an important parameter since it affects many properties, for example viscosity and the property, which characterize gelatine: the gelling power. Both of them are increased by an increase in the molecular weight. The fraction of molecules around 100 kDa is the most important for gelling power, while viscosity is mostly affected by higher molecular weights (200 kDa - 400 kDa). Gelatine hydrolyzed with alkaline treatment (Type B gelatine) shows a narrower molecular weight distribution (centered on about 100 kDa), when compared to Type A gelatine (obtained by acid hydrolysis),

[1] Gelatine from pigskin is not produced by basic hydrolysis due to the high amount of fat contained, which would be saponificated by the alkali, becoming difficult to separate from the gelatine.

[2] Another way to produce gelatine would be by enzymatic hydrolysis with collagenases, but it is not used so frequently in the industry.

which has a broader distribution. For both gelatine types the molecular weight ranges from about 10 kDa to 400 kDa [33]

Gelation of gelatine gels is a thermal effect; after cooling a gelatine "solution" (a gelatine sol, to be more precise) below its gelation temperature (also called setting temperature), a three-dimensional gel network is formed. The transition is reversible, so it is possible to "melt" the hydrogel (technically it is a gel-sol transition) by heating above a certain temperature, usually called "melting temperature". The gelation temperature is usually considered to be 5°C below the melting temperature. Anyway, this difference in temperature may vary depending on the aging condition and time of the hydrogel. The gelation phenomenon is accompanied by a change in the optical rotation [36]; this has been interpreted as indicating a partial reordering of gelatine molecules into the original collagen helix. The phenomenon is usually called renaturation and is divided into three steps: at first, an intramolecular rearrangement of the imino acid-chain segments occurs, taking on a conformation similar to the one of the same segments found in the collagen. This step, called collagen fold, is responsible for the increase in optical rotation. Then by means of the association of two or three separate chains, the formation of the three dimensional network happens: during this phase crystallite formation, unrelated with the helical region, can be observed with X-Ray diffraction. The third step involves the formation of hydrogen bonds within the helical region, which stabilizes the structure [37]. Gelation is apparently a quick process, but when the quantity of renaturated helices overtime after gelation is analyzed, it is possible to notice an increase in that value. The ratio of new helices created depends on the annealing temperature. The annealing process, numerically expressed by the increase in the helices amount as a function of time, follows a logarithmic law, and supposedly it can continue until all the helices are renaturated [38, 39].

1.2.1 Properties

Gel strength Gel strength, measured as Bloom Value, is an analytical value of the gel firmness and it is considered the most important gelatine character-

istic. According to the European and U.S. Pharmacopoeia, the gel strength (Bloom value) is expressed as: "the mass in grams necessary to produce the force, which, applied to a plunger 12.7 mm in diameter, makes a depression 4 mm deep in a gel having a concentration of 6.67 per cent m/m and matured at 10 °C". Commercial gelatine Bloom value ranges from 50 to 300. Higher gel strength usually means higher melting point, higher gelling temperature, shorter gelling time, and, of course, higher mechanical properties, which mean also lower gelatine concentration to achieve a certain firmness. After the constancy of the product between gelatine concentration and square root of the Bloom value was experimentally observed, an analytical expression correlating them was found to be [33]:

$$C_1 \times \sqrt{B_1} = C_2 \times \sqrt{B_2}$$

with C_1, C_2 and B_1, B_2, respectively concentration and Bloom value of 2 different gelatine solutions. Despite a good degree of correlation, this equation can be used just as a rough indication to predict properties of different gelatines; for accurate values, laboratory tests are needed [33].

Molecular weight distribution As anticipated, molecular weight distribution plays a key role in the assessment of some technological properties of gelatine, like viscosity and gelling power. It is determined by gel permeation chromatography (GPC). The sample (i.e. gelatine) is dissolved into a buffer solution and injected into a gel phase chromatographic column, where, every molecule moves at different speed, depending on the molecular weight. At the end of the column, an UV detector[3] plots the protein concentration on a chromatogram. Through the comparison of the retention time and the area of the picks on the chromatogram with standard samples at known molecular weight, it is possible to reconstruct the molecular weight distribution of the mixture.

[3] In some cases viscometric or light scattering detectors can be used instead.

Melting point The term "melting point" is not exact for gelatine gels: "gel-sol transition temperature" would be more correct since it gives an idea of the type of transition which occurrs. Anyway, as commonly done in literature, also in this thesis the two terms will be used interchangeably. The gel-sol transition temperature of gelatine hydrogels is affected by many parameters, including concentration, molecular weight distribution, pH, thermal history and additives [37]. It is known that by increasing concentration, both setting and melting temperature increase. It is important to remember that melting point and setting point have different values.

As anticipated, gelatine gels are characterized by a continuous annealing process, which involves new helices formation. The formation of new helices and the stabilization of the junctions between different helices with hydrogen bonds increase the stability of the hydrogel, consolidating its structure. This lead to an increase of the melting temperature during the annealing process. The increase of the annealing temperature (taking care not to reach the gel-sol transition) reduces the kinetic of new helices formation, but increases the stability of the junctions. Therefore, more energy is required to melt the hydrogel; for this reason, annealing at higher temperature leads to a gel with higher melting point.[38, 39].

As reported by Osorio et al., there is a dependency of the melting temperature on the pH: the melting temperature is usually maximum for a pH between 6 and 7, and slightly decreases for higher pH values. On the contrary, there is a remarkable decrease in the melting point for pH below 5 [40].

Additives are widely used to modify mechanical and thermal properties of gelatine in the manufacturing of capsules and suppositories. The most used additives for this purpose are glycerol and polyols in general (e.g. sucrose, sorbitol, maltodextrin...), due to their ability to increase the gelatine strength. This kind of additives has also the effect to increase the melting temperature. On the contrary, electrolytes usually reduce both strength and melting point. Aldehydes, as well as carbodiimides and genipin, are often considered additives: they react with gelatine inducing chemical cross-linking. Cross-linked gels loose

their ability to melt [37].

1.3 Objectives

The aim of this research is to develop a gelatine based hydrogel to be used for wound healing. The gel should be used as cell culture substrate, able to deliver cells *in-situ*, and should be easily removable after the treatment. It should also be effective in delivering growth factors if surgically implanted into a patient with impaired wound healing.

1.3.1 Specific Objectives

- Develop a hydrogel solid at physiological temperature, and able to melt at higher (but still harmless) temperature to be used as easily removable bandage,
- culture cells on the surface of that hydrogel,
- transfer cells cultured on the hydrogel on a different surface, and later, remove the hydrogel by melting,
- load the hydrogel with growth factors and use it as depot,
- tune the melting temperature and degradation/dissolution kinetic of the hydrogel to be suitable as anti-surgical adhesions.

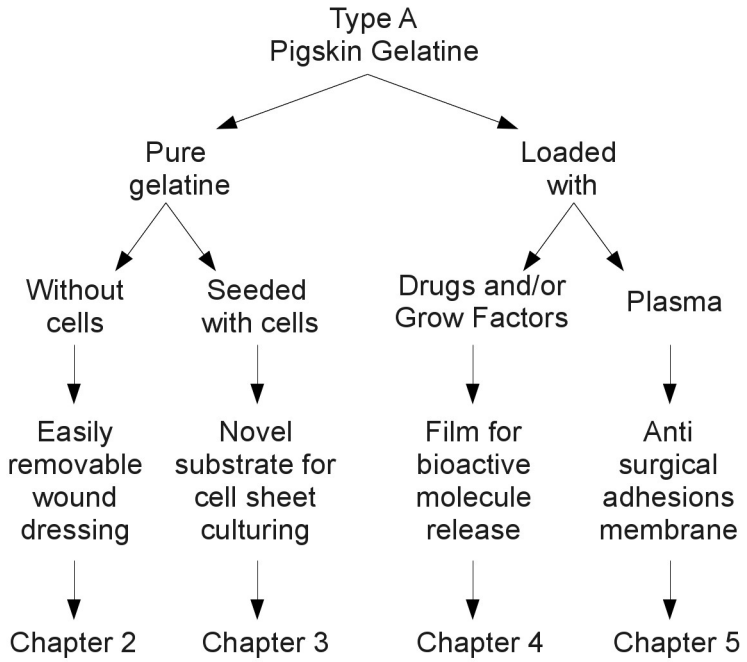

Figure 1.1: the scheme shows the uncross-linked hydrogel applications which were studied in this work.

Chapter 2

Membranes for Wound Covering

2.1 Introduction

One big issue in medicine is the removal of bandages which are stuck to an open wound or sore. Indeed, when it is necessary to remove the dressing to check the wound, bandage removal typically causes also detachment of the clot stuck to the bandage itself. This, in turn, causes bleeding, interruption of the wound healing process, partial destruction of the new formed tissue and pain for the patient. The problem becomes even more important in case of chronic wounds, as in case of diabetes.

In the field of wound dressing an uncountable number of different treatment options can be found. Moreover, new products and technologies are constantly developed. Some of them are improvements of older products, others are the results of completely new studies. While traditional wound dressing are mainly focused on keeping the wound clean, new products try to alter the wound environment to optimize healing conditions.

While plain gauze is still the most used dressing, devices able to keep the wound moist and protected have been developed in order to achieve better healing conditions. The big spread of plain gauzes is certainly related to the low cost, the ease of use and the versatility. Impregnated gauzes can also provide

better moisture conditions and have reduced adhesion to the wound surface. To increase the autolytic debridement, occlusive dressing were developed, such as Tegaderm^{TM} and Duoderm^{TM}. For heavily exudative wounds, absorptive products, mainly hydrogel based, were developed. Although the higher cost of these products compared to traditional gauzes, they seem to bring an overall reduction of the cost per wound, due to a minor number of replacements per day and faster healing, resulting in a shorter treatment period.

Gelatine sponges have been very useful in the treatment of severe burns and as a dressing for many types of wounds, such as pressure sores, donor sites, leg ulcers and decubitus ulcers, as well as for *in-vitro* tests. US 4,659,572 describes a burn wound-adherent dressing material as composed of a complex with gelatine and a water-soluble resin, aimed at controlling water-loss and minimizing the intrusive of exogenous micro-organisms. The gel protection remains on the wound 7 or more days, and is removed after the starting of the healing process, when skin grafting is allowed to take place. In US Patent Application 2005/0036955, a moldable, bioresorbable, biocompatible, unallergenic cross-linked gelatine derivative dressing for the prevention of post extraction alveolar osteitis pain is defined along with methods for the gel use. The dressing is placed at the time of surgery and acts as a bone covering obtundant and physiologic scaffolding for the conduction of normal alveolar bone healing sequence of fibroblast ingrowth, blood vessel formation, and reossification of the extraction site defect. US 5,895,412 describes an apparatus and method to boost and enhance wound closure in tissue by flowing a heated sealant, such as gelatine, on the wound. This creates an effective barrier against further blood leakage and, upon cooling, the sealant readily adheres to the tissue to seal the wound.

For wound protection and skin healing, extensive investigation has been carried out on the hydrophilic and water absorbing properties of gelatine as a clinical wound dressing [41].

Traditional or prior art gels act as a matrix for controlled release, but they do not act for an almost immediate release. In topical uses, such as in wound

healing, it is better to have the release of a high concentration of the adjuvant agents (such as platelet rich plasma, PRP) in a short time. Further, if the gel melts naturally at body temperature or is washed away with a warm solution (38 °C - 40 °C), the wound is not affected. By contrast, if there is the necessity to remove a solid gel, which is stuck to the wound, its removal provokes both pain and the reopening of the wound.

Moreover, there is the need for a gelatine hydrogel, which allows the contact between platelet derived components (including, but not limited to PRP and platelet lysate (PL), platelet poor plasma (PPP), cryoprecipitate (CRYO) alone or together with other therapeutic agents) and wounded skin or organ injury, on which the platelet components can release growth factors and enhance their healing properties. In particular, in skin treatment, an immediate contact of all available platelet components with the skin injuries would favor both the repairing process and the growth of regenerated skin. If the skin injury is continuously in contact with fresh platelet components (including PRP and PL) by mean of a suitable delivery system, rapid regeneration will occur, even when replacing the delivery system [42, 43].

There is also the need for a gel film that can be easily placed as a protecting barrier against infection on skin wounds or injuries that is not painful to remove. The gel may contain biologically active agents and may be used on skin wounds or lesions due to burning or to relieve bedsore or metabolic ulcers. Removal of the film is often painful given the adhesion of the gel onto the wounds. A hydrogel system which is in a gel state at the temperature of the skin (33 °C) but "melts" when water at a temperature compatible to the body (36 °C - 38 °C) is poured onto it, would be removed easily and without pain.

Moreover, the hydrogel system needs to be composed of biocompatible, bioresorbable and biodegradable materials, preferably from natural sources (not synthetic) and not chemically modified, such as cross-linked. Among the materials, pure gelatine (not cross-linked) has proven to possess the characteristics of being biocompatible, bioresorbable and biodegradable. It also has a

better biocompatibility than other natural products, such as albumin [44].

The use of gelatine gels and cross-linked collagen gelatines has been investigated, so far, as "depot" systems, which slowly release the biologically active agents for a prolonged release. However, gelatine matrix degradation is observed in such gels. The degradation occurs after a long period of time and in different forms, such as enzymatic erosion and dissolution,. The degradation kinetic depends on the application site (i.e., from 6 - 8 hours in ophthalmic applications, where the elimination is in general very fast, to 7 - 10 days in other body districts, such as skin).

Gelatine-based systems have a common characteristic: they are solid at 37 °C, with a melting temperature- (i.e., a gel-sol transition temperature) much higher than the body temperature (the melting temperature is usually at least 43 °C - 45 °C or more). The commercial advertisements for gelatine focuses also on this point. They stress that gelatine melting point is to be considered a quality index. In other words, a higher melting point is advertised as both an index of good gelatine and a sign of good stability. It is also advertised that gelatines will lose activity, denature and degrade when the temperature is substantially higher than their melting point. Thus, the loss of activity will mainly occur with low melting gelatines.

Therefore, the right choice for the gelatine to be used in the above medical applications is to select the one with a melting point as high as possible. There is still the need for an improved gelatine hydrogel, which allows the easy removal of the gelatine gel films, or other forms, from wounded skin (burning, bedsore) without any damage or pain.

Since gelatine has a gel-sol transition temperature comprised between 30 °C and 37 °C, it could be a good candidate as material for the making of bandages easy to remove. In order to use gelatine gels as wound dressing, it is necessary to have a gel-sol transition temperature higher than the skin temperature, which is typically below 33 °C - 34 °C (it depends on the body part, on the temperature of the environment and there are differences between subjects). To better understand gelatine properties a study on the factors which influence

the transition temperature has been carried out.

Gel-sol transition temperature of gelatine gels is influenced by several factors: the first, and most important factor, is the source of gelatine. Gelatine from mammalian collagen shows a gel-sol transition temperature, which ranges from 30 °C to 37 °C, while the one of gelatine from fishes typically ranges from about 10 °C to 28 °C, depending on fish species and on the temperature of the water, where they live [45]. For this reason, gelatine from porcine skin was selected for this research.

Gelatine gels are also influenced by the gel water content (i.e gelatine concentration). As a matter of fact, an increase in water content causes a decrease in the gel-sol transition temperature [40]. The water content can be controlled in different ways, depending on the technique used to prepare the hydrogel: if the gel is prepared by solution casting, the final concentration of the gel will be the same of the solution, while, if it is prepared through water absorption from dry gelatine, the water content will depend on the soaking time and the absorption kinetic. Equilibrium value and absorption kinetic, as explained in section 2.3.4, depend on temperature.

The pH of the gelatine solution is another important factor, which affects gelation and gel-sol transition: lowering the pH usually induces a reduction of the melting temperature. However, changes are more relevant in the range 3 - 6, so keeping pH around 7 is sufficient to avoid gel-sol transition temperature reduction[40].

The gel-sol transition temperature of the gelatine hydrogel is greatly affected by the thermal history both of the gel itself, and of the gelatine used [38, 46, 47, 48].

2.2 Materials and Methods

In order to develop a device able to resist the body temperature, but easy to remove by melting, gelatine hydrogels at different concentrations were produced. As anticipated, thermal properties of gelatine hydrogels are greatly

affected by the their thermal history. In order to exploit the results obtained by Djabourov et al. [39], one tried to increase the thermal resistance of the gelatine gels by annealing them at 29 °C for 48 hours. For a complete description of the production process please refer to section 2.2.1.

2.2.1 Gelatine Preparation

The procedure used for gelatine sample preparation was optimized in 6 steps, described below:

1. Sterilization Dry gelatine powder was sealed in Polypropylene falcon tubes and sterilized by γ-ray radiation (dosage: 25 Gy) by Gammarad Italia s.p.a.

2. Dissolution Gelatine solution was prepared by soaking sterile gelatine powder in sterile water or cell culture medium for 10 minutes, at room temperature, to allow gelatine swelling, by absorbing a certain amount of liquid. The suspension was then placed in a 37 °C bath for 1 hour, and stirred every 20 minutes by using a vortex mixer until a clear gelatine solution was obtained. To reduce bubbles and foam on the surface (induced by the stirring process), the solution was finally centrifuged at 2300 relative centrifugal force (rcf) for 5 minutes. After centrifugation, the gelatine solution was placed again into the 37 °C bath for 10 minutes, in order to avoid gelation in the pipette during the casting process.

3. Casting and Gelation Gelatine solution at 37°C was cast into polystyrene tissue culture plates (TCPs); different plate sizes and solution volumes were used, depending on the need. To induce gelation, the solution was kept for 24 hours in an incubator, at room temperature (20°C) and at 100% relative humidity (RH).

4. Annealing Gelatine gels, prepared as previously described, were moved to a 29°C oven, at 100% RH, and maintained in this condition for 48 hours. The annealing process performed at 29 °C for 48 hours induces the formation of stable triple helices, which leads to an increase of the gel-sol transition temperature, if compared with the one of the untreated gels [39].

5. Freeze drying To produce a gelatine sponge, the gel produced by solution casting, as described in step 3, was frozen at -80°C for 24 hours and freeze-dried for 3 days at -50 °C, and 0.1 mbar. Resulting sponges can be stored for months in a dark, dry place at room temperature, and, when necessary, they can be rehydrated just by soaking in water, culture medium or plasma derivatives.

6. Drying Gelatine gel, produced by solution casting as described in step 3, was dried in a ventilated drying oven at 50°C. After 48 hours, a solid, transparent and brittle film was obtained.

Also in this case, the samples can be stored for months in a dark, dry place at room temperature, and, when necessary, they can be rehydrated just by soaking in water, culture medium or plasma derivatives.

2.2.2 Mechanical Compression Test

Stiffness of gels 5%, 10% and 15% gelatine in water, prepared as described in section 2.2.1, step 3, and of others, at the same concentrations, prepared as described in 2.2.1, step 4, was tested according to ASTM standard D695-10. Samples were cut in cylindrical shape (diameter: 0.5 inch; height: 4 mm), and tested by means of an Instron 4502 (testing speed: 1.3 mm/min), working at 23 °C and 33 °C, in a thermostatic chamber at 100% RH. Three samples per type per temperature were tested.

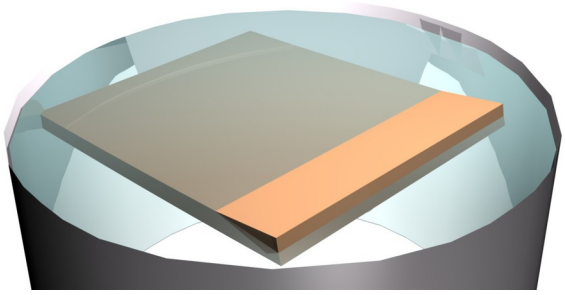

Figure 2.1: Rapid cooling device. It is composed by a copper plate immersed in liquid nitrogen, the hydrogel was leaned on the non-immersed area

2.2.3 Samples Preparation for Scanning Electron Microscopy

In order to analyze the gel porosity, samples, prepared as described in section 2.2.1 step 4, were frozen with a high cooling rate and observed at the Field Emission Scanning Electron Microscope (FE-SEM). The high cooling rate was achieved by a self constructed device, constituted of a copper plate (4x40x50 mm), immersed into liquid nitrogen, leaving only a small area ((10x40 mm) exposed to the air, as shown in figure 2.1. Gelatine gels were placed on the exposed area of the plate, achieving a high cooling rate due to the low temperature of the liquid nitrogen (-195.79°C), and the high conductivity of the copper. After samples were completely frozen, they were cryo-fractured, exposing the inner part, moved to a lyophilizer, and freeze-dried at -50°C and 0.1 mbar, for 24 hours. Once removed from the lyophilizer, samples were immersed in silver-paste (except for the face to observe) to increase the conductivity with the stub. They were then observed by using the FE-SEM (Supra 40, Zeiss), through the detection of Secondary Electrons.

2.2.4 Dynamic Scanning Calorimetry (DSC)

The influence of concentration and annealing on the gel-sol transition of a gelatine hydrogel was studied by using Differential Scanning Calorimetry (DSC, Mettler DSC 30). DSC is a thermoanalytical technique, which measures the

difference in thermal flow between a sample and a reference, to maintain both of them at the same temperature. The analysis is typically carried out heating (or cooling) both the sample and the reference at some rate. The difference in thermal flow is then plotted as a function of the temperature; in this way it is possible to identify at which temperature a some change in the heat flow happens. Changes in the thermal flow are caused by transformations in the material; some of them are exothermic (e.g. crystallization), others are endothermic (e.g. fusion, boiling). By analyzing the thermogram shape (and knowing the possible transitions, which can occur in the material), it is possible to infer which transformation happened at each temperature (e.g. glass transition is a flex, melting is an endothermic peak).

Analysis on gelatine samples were performed increasing the temperature from 2 °C to 60 °C in order to be sure to include the gel-sol transition for each concentration and annealing treatment. The heating rate was set to 1°C/min since, from preliminary tests, there was no appreciable difference reducing this rate. Only one scan was performed, since the first scan induces a gel-sol transition, which modifies the material irreversibly.

2.2.5 Water Absorption

Water absorption quantification test was performed by soaking gelatine gels, films, or membranes, in water, at room temperature (20 °C). After 15 minutes, 30 minutes, 60 minutes, 2 hours, 4 hours, 6 hours and 24 hours, samples were strained and weighted. The water uptake was calculated as a percentage increase in weight, compared with the initial weight of the sample, according with the formula:

$$\text{WaterUptake} = \frac{W_{wet} - W_{dry}}{W_{dry}} \cdot 100$$

Gelatine Conc.	Annealing	E at 23°C (KPa)	E at 33°C (KPa)
5		6.9 ± 1.8	2.7 ± 0.6
5	YES	7.0 ± 1.7	2.6 ± 0.9
10		34.9 ± 2.3	2.9 ± 0.3
10	YES	34.7 ± 1.9	2.8 ± 0.8
15		79.6 ± 3.0	23.2 ± 3.0
15	YES	79.9 ± 2.6	22.9 ± 3.1

Table 2.1: Mechanical compression of gelatine gels, performed according to ASTM standard F2900-11.

2.3 Results and Discussion

2.3.1 Mechanical Compression Test

In order to evaluate the influence of concentration, annealing and temperature on the gelatine gel stiffness, compression tests were performed, according to ASTM standard D695-10-11, as described in section 2.2.2. Concentrations used to perform the tests were 5%, 10% and 15% gelatine in water. Tests were performed at 23 °C and 33 °C, 100% RH.

Results As shown in table 2.1, the stiffness is greatly affected by both concentration and temperature. Testing temperatures were chosen below the melting temperature. However, the decrease in stiffness at 33°C, especially for diluted samples, is evident, even if melting was not reached.

On the contrary, annealing does not affect the stiffness at all.

2.3.2 Gel micro- and nano-structure

Micro- and nano-structure of gelatine hydrogels were analyzed by the Scanning Electron Microscope (FE-SEM). Gels were prepared as described in section 2.2.1, rapidly frozen at -195.79°C on a copper plate, and freeze-dried. Samples were then included in silver paste, to increase the conductivity between them and the stub, and observed by using the FE-SEM. For the complete protocol,

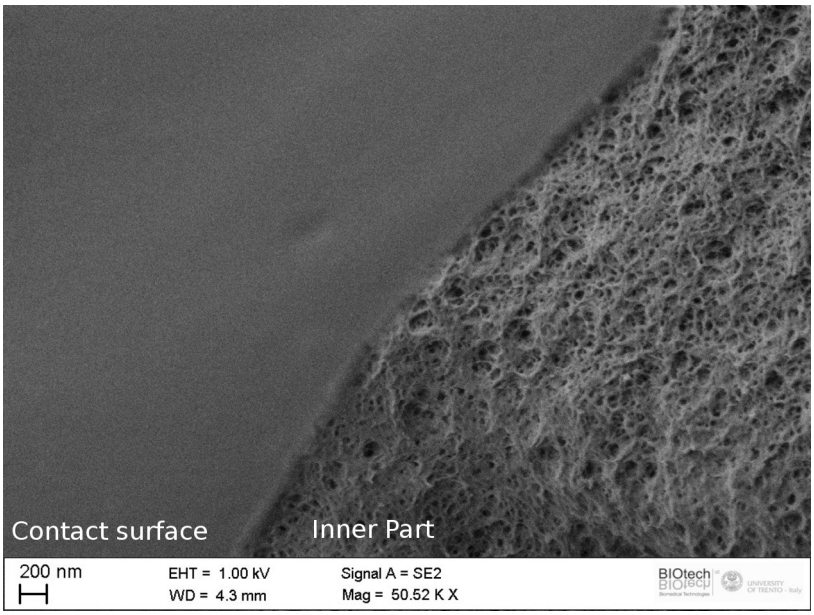

Figure 2.2: gelatine sample FE-SEM image acquired on the cryofracture area, near the surface in contact with the copper plate (smooth area): the gel porosity is clearly visible.

please refer to section 2.2.3.

Results Figure 2.2 shows the nanostructure near the surface in contact with the copper plate (i.e., the smooth area visible on the image). The size of the small fibers is compatible with the one of collagen fibers, as reported in literature [49]. Due to the extremely quick freezing process used, the porosity observed near the surface can be supposed to be the gel porosity, since it should not be affected by ice crystal growth.

The image acquired in the central part of the sample (figure 2.3) shows big pores, with small fibers on the boundary. These big pores were produced by the growth of ice crystals during the freezing process, because of the low cooling rate, and thus they can be considered an artifact. No appreciable morphological differences were detected between normal and annealed gels.

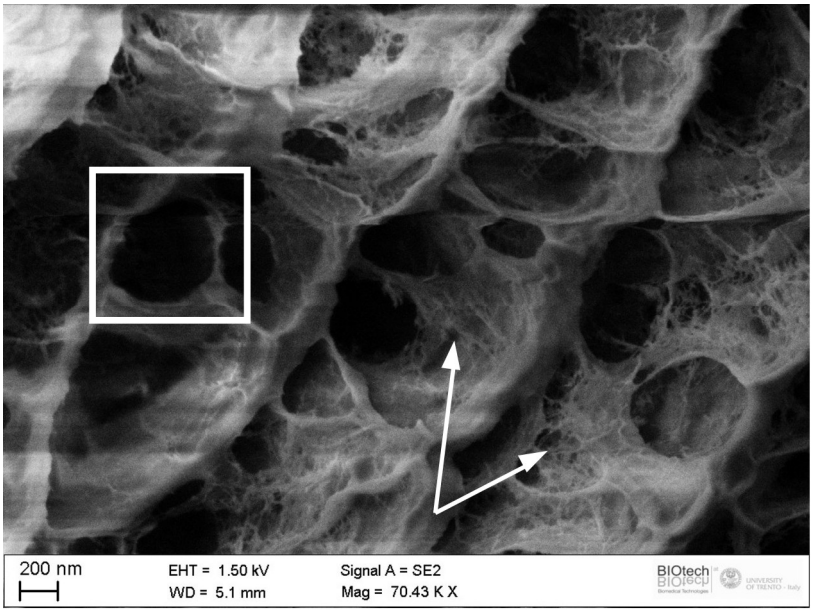

Figure 2.3: gelatine sample FE-SEM image acquired on the cryofracture area, far from the surface in contact with the copper plate: the big porosity is due to ice crystal growth during the freezing process (square). Small fibers of collagen are visible on the bottom of the big pores (arrows).

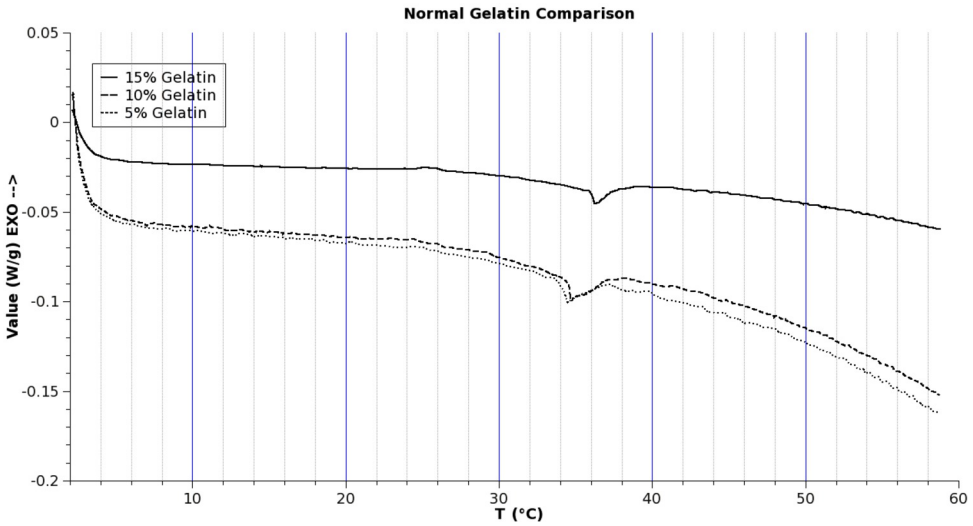

Figure 2.4: DSC comparison between untreated gelatine gels (heating rate: 1°C/min): the endothermic peak indicates the gel-sol transition.

2.3.3 Differential Scanning Calorimetry

In order to evaluate the influence of concentration and annealing treatment on gelatine gels, two batches of gelatine gels prepared as shown respectively in sections 2.2.1 , step 3 (for untreated samples) and step 4 (for annealed samples), were analyzed by DSC, as described in section 2.2.4. Three concentrations per batch were chosen: 5%, 10% and 15% in weight.

Results As shown in figures 2.4 and 2.5, the increase of the concentration from 5% to 15% rises the melting temperature of the untreated gelatine from about 34 °C to about 36 °C, while for annealed samples there is a smaller difference, from about 37 °C to 38 °C.

A more interesting comparison is the one between annealed and untreated samples, prepared with the same concentration. As shown in figures 2.6, 2.7 and 2.8, the melting temperature of annealed samples is about 2 °C higher than the one of untreated samples. Comparing the three figures it is also possible

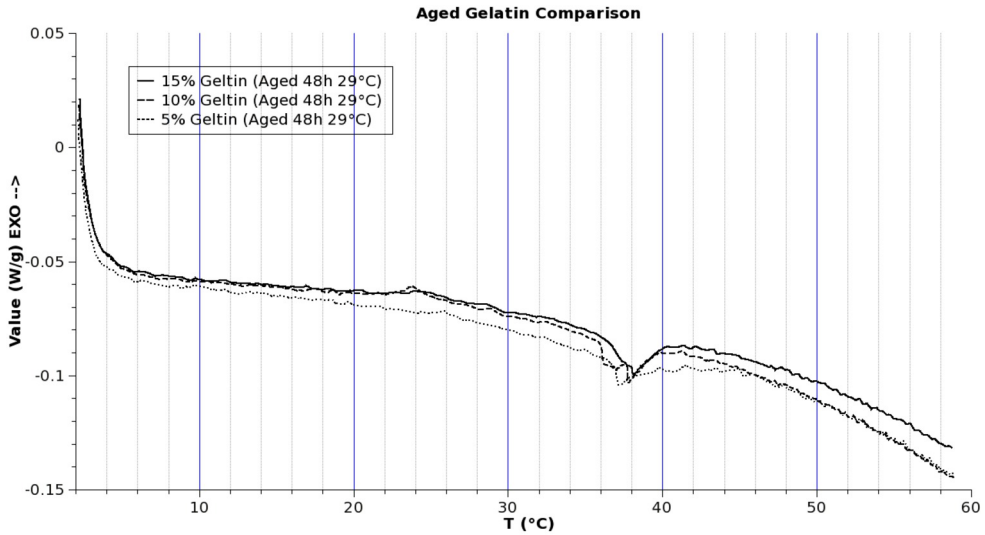

Figure 2.5: DSC comparison between annealed gelatine gels (heating rate: 1°C/min): the endothermic peak indicates the gel-sol transition.

to notice that the increase in melting temperature of the most concentrated sample (figure 2.8) leads to a broadening of the pick: a possible explanation for this broadening could be the presence of a wider distribution of bonding energy, in the gelatine. Weaker bonds break at lower temperature while stronger at a higher one. This wider distribution can depend on the fact that at a higher concentration, chain mobility is partially impaired by other chains: for this reason some of them cannot reach the more stable condition induced by the annealing process.

2.3.4 Water Absorption

In order to understand the behavior of a gelatine gel immersed in cell culture medium and tailor the soaking time of a freeze-dried gelatine bandage, a water absorption test was performed on both dried gelatine gels (prepared as described in section 2.2.1, step 6), and freeze-dried gelatine membranes (prepared as described in section 2.2.1, step 5). The tests were performed as

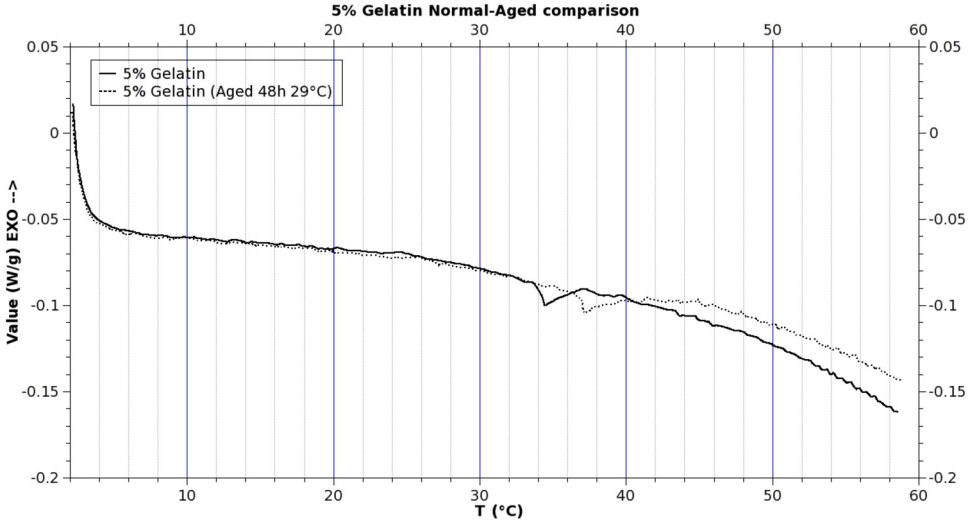

Figure 2.6: DSC comparison between 5% untreated and annealed gelatine gels (heating rate: 1°C/min).

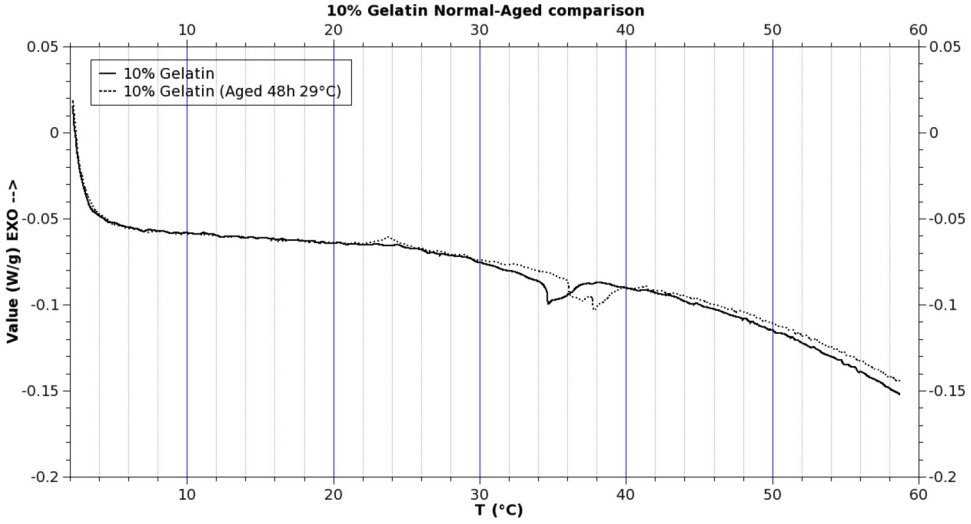

Figure 2.7: DSC comparison between 10% untreated and annealed gelatine gels (heating rate: 1°C/min).

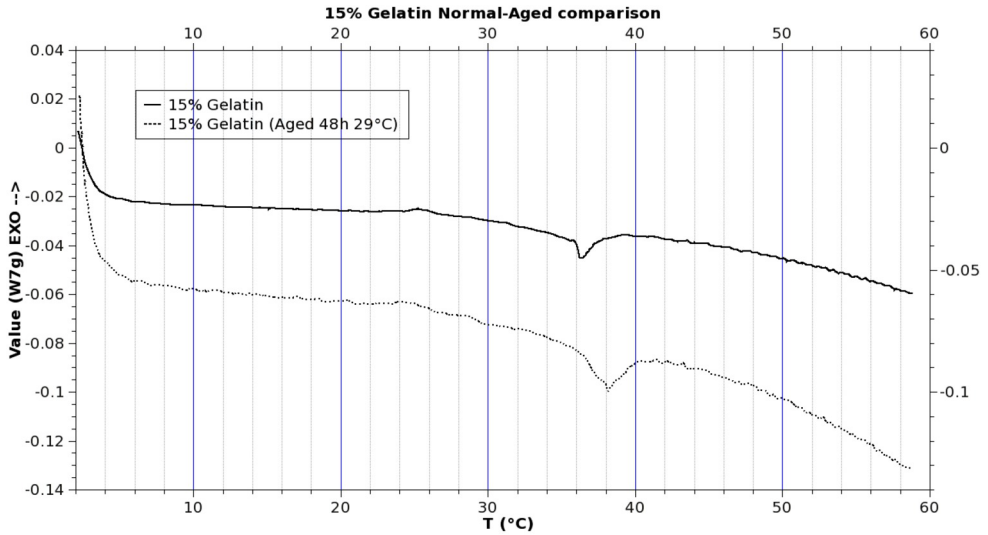

Figure 2.8: DSC comparison between 15% untreated and annealed gelatine gels (heating rate: 1°C/min).

described in section 2.2.5

In figure 2.9 the water uptake curve is shown as a logarithmic plot.

The logarithmic kinetic for the dried sample is evident. On the other hand, the water uptake of the freeze-dried is comparable to the dried one in the first 2 hours; successively it seems to increase more rapidly. This difference on the kinetic could be explained referring to the porosity of the freeze-dried sample. When it is immersed in water, the water is initially not able to enter the pores, since the porosity on the surface is small, the gelatine surface is hydrophobic and the water surface tension is too high to allow water to enter those hydrophobic pores. When gelatine absorbs water, the surface changes and so its wettability. As a consequence, the water is able to diffuse and fill the porosity. Once pores are filled, the contact area between gelatine and water is bigger than in the case of the compact gel. For this reason the absorption kinetic increases. This data interpretation is also confirmed by the observation of the freeze-dried sponge while it is absorbing water. Initially the presence of

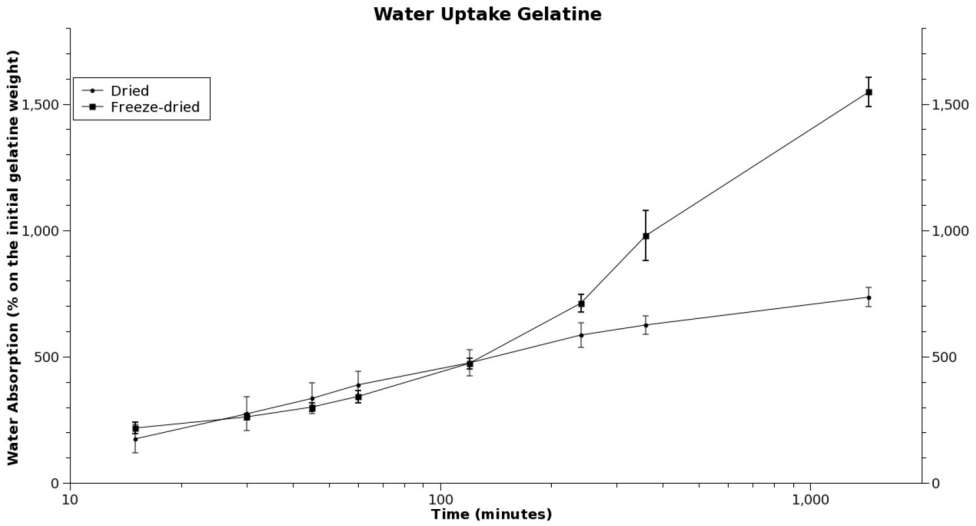

Figure 2.9: Water Uptake in dried gelatine and freeze-dried sponges.

micrometric air bubbles inside the wet sponge is clear, but after 2 hours it is possible to notice a reduction of the bubbles, which continues until each pore is filled.

Similar experiments were carried out with medium and PRP and they gave the same results.

2.4 Conclusions

Due to their ability to protect the wound, absorb exudates and maintain moist the environment, cross-linked or highly concentrated gelatines are extensively studied as wound dressing materials. While cross-linked materials have lost their ability to melt, the highly concentrated uncross-linked ones present a melting temperature over 45 °C. In this work it was analyzed the possibility to produce uncross-linked gelatines, with a melting temperature between 35 °C and 40 °C. As shown in section 2.3.4, these gelatines can absorb, quite quickly, large amounts of water. This property can be exploited to produce dry gelatine

bandages, which can be stored at room temperature and rehydrated when necessary. Moreover, the possibility to absorb liquids is an important property once gelatine is used to dress wounds, especially in case of highly exudative wounds.

A consequence of the annealing process on gelatine gels is an increase of the gel-sol transition temperature, without the addition of chemicals. Technically, it involves a sort of cross-linking, which, in this case, is thermo-reversible, as previously discussed in section 1.2. Therefore, the possibility to melt the gel is not impaired as in the case of chemical and dehydrothermal cross-linking.

However, the most interesting property of the studied gelatine, is the possibility to remove it from the wound by melting / washing with warm sterile water. This allows the detachment and removal of the wound dressing without damaging the newly formed tissue. Additionally the pain for the patient during the removal of gelatine membranes is greatly reduced, if compared with traditional gauzes.

Chapter 3

Cell Sheet Engineering on Gelatine

3.1 Introduction

Aim of this work, as already anticipated, was to culture confluent cell layers on gelatine hydrogel surfaces, in order to realize easily transferable cell sheets. Since fibroblasts are of great importance in the wound healing process, it was decided to start working with this cell type. In particular, MRC-5 cell line was chosen and used as a model. In future work they could be changed with other cell types in order to solve different problems.

Gelatine hydrogels, used as substrate for cell sheets, can be melted at physiological temperature, as shown in section 2.3.3. This characteristic allows to easily remove them by melting, once the cell sheet is transfered on the surface, which has to be treated. Indeed, it is sufficient to use warm sterile water (37 °C - 40 °C) to completely dissolve gelatine hydrogels in a few minutes, after the cell sheet has adhered to the target surface. Moreover, if implanted into the body, gelatine takes less than one week to dissolve/degrade without the need of removal, since gelatine is reported to be non-toxic, biocompatible, non-carcinogenic and non-immunogenic (please, refer to chapter 5 for more

details and explanations) [50].

Due to the possibility to quickly remove gelatine by melting and washing it, it is possible to apply several cell sheets, possibly made of different cell types, one above the other, in order to face up a particular problem. This technique would allow to obtain a thicker tissue made of stacked cell sheets, similar to what was described by Yamato et al. [51]. An interesting example is the use of fibroblasts followed by keratinocytes, for ulcer and burn treatments.

Cell culturing on a surface is the only way to allow cells to rapidly adhere to an injured area. Indeed, if cells are inside a matrix, they cannot be rapidly transferred on a target region: it becomes, therefore, necessary to leave the whole scaffold in place to allow the slow cell migration process.

The main problem when culturing cells on gelatine, is the cell culture process itself. Indeed, gelatine, when immersed in water (or in a culture medium), continuously absorbs the liquid (chapter 2.3.4); the increase in water content reduces the gel melting temperature below the standard cell culture temperature (37 °C). As a consequence, cells cannot be cultured at 37 °C on normal gelatine hydrogels immersed in culture medium.

Different approaches have been tried in order to increase gelatine gel gel-sol transition temperature: most of them were focused on partial cross-linking (e.g. dehydrothermal treatment, cross linking with 1-ethyl-3-(3-dimethylaminopropyl)-carbodiimide(EDC)), others relied on blending with hydrogels with higher gel-sol transition temperature (e.g. agar-agar), but none of them worked for the purpose. Cross-linking led in fact to the loss of the gel-sol transition, while blending did not increase the melting temperature at all. Only two alternatives were then possible: cell culture on cross-linked gelatine (renouncing to the gel-sol transition), and cell culture at reduced temperature.

3.2 State of the Art

Cell-sheet engineering was developed by Okano et al. to overcome polymeric scaffold and cell suspension limitations. The target was to reconstruct tissues

starting from cell sheets instead of single cells. Although cell suspension injection achieved some results in small animals, it does not seems to be suitable for large tissue reconstruction, due to the low percentage of cells really integrating into host tissues.

The main advantage of cell sheets, compared with traditional tissue engineering, is the absence of scaffolds. Scaffolds are useful to culture cells *in-vitro*, but, when implanted *in-vivo,* they often present some limitations. One of them is the degradation time, ranging from weeks to months. During degradation, the space occupied by the scaffold is filled with proliferated cells and deposited ECM. However, ECM deposition in tissues, following an implant and consequently an inflammation, often results in fibrosis. Furthermore, for some applications, scaffolds impair organ functionality, as it happens in the case of opaque scaffolds for corneal regeneration.

From a histological point of view, many organs are structured as intimately associated cell sheets. For example, liver comprises interconnected layers of hepatocytes and endothelial cells.

Temperature-responsive Tissue Culture Plates Traditionally, cells are harvested using proteolytic enzymes, such as trypsin or dispase. These enzymes cleave protein bonds between cells and culture substrate. Unfortunately, these enzymes destroy also cell-cell and cell-ECM bonds. To overcome this problem, temperature-responsive culture dishes were developed. A temperature-responsive polymer, poly(N-isopropylacrylamide)(PNIPAAm), was grafted onto the surface of TCP. At 37 °C, the surface is hydrophobic, such as standard TCPs, and allows cell culture, but under 32 °C it becomes hydrophilic, inducing cell detachment without any needs of proteolytic enzymes. Avoiding enzymes, cell-cell junctions and receptor proteins are not affected by the process. Therefore, cells can be harvested as continuous cell sheet. Harvested cell sheets can then be transferred into other TCPs, implanted *in-vivo*, or stacked on other cell sheets to form thicker layers.

One of the most interesting applications of cell sheet engineering shown by

Okano et al. was the regeneration of ocular surfaces. Limbal stem cells were isolated from the patients and expanded on temperature-responsive culture dishes. Once continuous layers were formed, they were detached from the TCP by reducing the temperature under 32 °C. The harvested cell sheets were continuous and easily manipulated. They were then moved on corneal stromas of injured eyes. The sheets adhered to the new surfaces without the need of suture. In all the patients an increase in the visual acuity was observed.

Traditional tissue engineering tried to produce scaffolds for the culture of cardiomyocytes. However, there were problems related to the stiffness of the material, which hampered the dynamic pulsation of the cardiomyocytes. Okano et al. showed that layering several cell sheets of confluent cardiomyocytes allowed the production of pulsatile myocardial tissue. Synchronous tissue pulsation indicates good conductivity between different lamina sheets. A stack of four sheets was sufficient to see the spontaneous pulsation with naked eyes. Most recent cell sheet applications include treatment of esophageal ulceration, periodontal tissue, lung air leak and pancreatic islet tissue.

At the moment cell sheet technology presents some limitations in the production of 3D constructs. Although it is possible to stack cell sheets to form three dimensional tissues, it is difficult to achieve cell survivability into thick layers, mainly due to insufficient nutrient diffusion and waste accumulation in the central part of the layer. Actually, the highest thickness for *in-vivo* cell survivability is approximately 80 μm [52]. Therefore, to achieve higher thickness, a polysurgery approach is necessary, adding cell sheets once the previous is vascularized [52]. To overcome this limitation and allow *in-vitro* culture of thicker tissues, the production of a capillary-like structure has been explored. This particular structure has been achieved adding micro-patterning technique to the cell sheet engineering [53].

Cell sheet engineering demonstrated to have a wide-range potential for tissue reconstruction. With the addition of the recently studied micropatterning techniques, it could be possible to extend cell sheet technology to thick heterogeneous and vascularized tissues .

3.3 Materials and Methods

3.3.1 Cell Subcultivation

In order to subcultivate the fibroblasts (MRC-5) cells (please refer to section 3.1 for the explanation of this cell line choice), a commonly used protocol was followed. It consists of few steps, which are briefly described below.

Before reaching confluence fibroblast (MRC-5) cells were subcultivated in a polystyrene tissue culture flask, under normoxia (air plus 5% CO_2), using a seeding density of $1 \cdot 10^4$ cells/cm^2. The medium composition is showed in table A.1. The medium was changed twice per week. The cells were then detached, after rinsing 2 times in phosphate buffered saline (PBS), using trypsin 0.05% - EDTA 0.02% in PBS for 3 minutes at 37°C. After that, trypsin was quenched by adding a volume of culture medium four times the trypsin one. Cells were counted in a Bürker chamber and cell viability was measured by trypan blue exclusion. Cell suspension density was successively adjusted depending on the need.

3.3.2 Cell culture on EDC cross-linked gelatine

1. Cross-linking In order to produce a gelatine substrate without gel-sol transition, and in order to evaluate the possibility of culturing cells on it and, successively, transferring the obtained cell layer to a target surface, gelatine gels 15% gelatine in water were prepared as described in section2.2.1, step 4. After the annealing procedure, gels were soaked in a solution 2% of EDC in water for 15 seconds, at room temperature; then, they were extracted from the solution and rinsed with abundant water to remove the unreacted reagent. EDC was chosen as cross-linker, because of its water solubility and its ability to cross link proteins, and, since it is a zero-lenght cross-linker (i.e. after the cross-linking process, no EDC residual chains will remain attached to the protein). Successively, samples were left in water for 2 hours; water was changed frequently in order to allow reaction products diffusion and elimination. It

was not possible to produce the gelatine gel using culture medium, instead of water, due to changes (e.g. pH) induced by the medium. These do not allow the EDC to react and cross-link the gelatine without the addition of N-hydroxysulfosuccinimide (Sulfo-NHS). It was preferred to avoid the use of NHS and Sulfo-NHS in order to reduce the number of residual substances potentially cytotoxic in the hydrogel.

2. Cell Culture In order to evaluate the possibility of culturing cells on cross-linked gelatine hydrogel surfaces, and successively transfer the obtained cell layer to a target surface, cross-linked gelatine gel was prepared as previously described. Before cell seeding the cross-linked gel surface was soaked in cell culture medium (table A.1) for 2 hours, in order to allow the diffusion of the medium inside the gel, and protein adsorption on the surface, which increases cell adhesion.

Fibroblast (MRC-5) cells were seeded on the cross-linked surface at a cell density of $1 \cdot 10^4$ cells/cm^2 and incubated at 37 °C in culture medium. The culture was checked every 24 hours by using a phase contrast microscope. An empty well per plate was seeded with the same amount of cells, as control. 6 hours after seeding, the samples and the control were covered with medium to ensure the cells proper hydration.

After the formation of a confluent layer (i.e. after 84 hours), samples were moved to a new TCP with seeded side down, ensuring a good contact between the cell layer and the TCP. After an incubation of 24 hours, the cross-linked gelatine gels were removed and the presence of an adherent cell layer on the plate was checked by using both a phase contrast microscope and a confocal laser microscope.

3.3.3 Cell culture protocol development

To develop a new protocol for cell culturing on gelatine gels, a multi-step procedure was followed during which the preliminary results obtained were used to optimize the following steps.

1. Cell culture at different temperature Gelatine gels prepared as described in section 2.2.1, step 4, were seeded with fibroblasts (MRC-5), at a seeding density of $1 \cdot 10^4$ cells/cm^2. Samples were divided into three groups and incubated respectively at 31 °C, 32 °C and 34 °C for 24 hours into multi-well TCPs. An empty well per plate was seeded with the same amount of cells, as control. 8 hours after seeding, the samples and the control were covered with medium to ensure the cells proper hydration. 2 hours, 8 hours and 24 hours after seeding, the samples were observed at the phase contrast microscope.

2. Cell culture on dry surface Gelatine gels prepared as usual (section 2.2.1, step 4), were seeded with fibroblasts (MRC-5), at a seeding density of $1 \cdot 10^4$ cells/cm^2. The samples were then incubated at 31 °C into multi-well TCPs. As before, an empty well per plate was seeded with the same amount of cells, as control. After 2 hours cell adhesion was checked by using a phase contrast microscope. Half samples were then re-incubated at 31 °C in "dry" conditions (i.e. without adding any liquid medium), the others were re-incubated at 31 °C in standard culture conditions (i.e. immersed in the culture medium). All the samples were observed after 2 hours, 8 hours, 24 hours and 48 hours by using the phase contrast microscope.

3. Cell culture on barely wet surface Also in this case gelatine gels were prepared as usual (section 2.2.1, step 4), and seeded with fibroblasts (MRC-5), at a seeding density of $1 \cdot 10^4$ cells/cm^2. The samples were then incubated at 31 °C into multi-well TCPs, in which it was prepared the usual control well. After 6 hours cell adhesion was checked by using a phase contrast microscope. Samples were then kept at room temperature for 15 minutes to allow gelatine to cool down. Successively 100 μL of medium, at room temperature, were added to each sample (well diameter: 34 mm), before re-incubating at 31 °C. The adding of new medium (100 μL) to each sample was repeated twice per day following the same protocol. All the samples were observed every 24 hours by using the phase contrast microscope.

4. Cell seeding density test Gelatine gels were prepared following the usual procedure described in section 2.2.1, step 4. Cells, previously subcultured as described in section 3.3.1, were seeded on sample surfaces at different seeding density: $1 \cdot 10^4$ cells/cm^2, $2 \cdot 10^4$ cells/cm^2, and $4 \cdot 10^4$ cells/cm^2. Samples were then incubated at 31°C, and cultured re-wetting the surface twice per day as described above (section 3.3.3, step 3).

5. Cell culture - optimized procedure Gelatine gels were prepared following the procedure described in section 2.2.1, step 4. They were then seeded with fibroblasts (MRC-5), previously subcultured as shown in section 3.3.1, with a seeding density of $2 \cdot 10^4$ cells/cm^2. Successively the samples were incubated at 31 °C in multi-well TCPs. An empty well per plate was seeded with the same amount of cells, as control. After 6 hours, cell adhesion was checked by using a phase contrast microscope. Samples were then kept at room temperature for 15 minutes to allow gelatine to cool down. Successively 100 μL of medium, at room temperature, were added to each sample (well diameter: 34 mm), before re-incubating at 31°C. The adding of new medium (100 μL) to each sample was repeated twice per day following the same protocol. Once per day, just before one of the two medium additions, samples were firstly placed at room temperature for 15 minutes. Successively they were completely immersed in culture medium at room temperature for 10 minutes. After this, all the liquid medium was removed and 100 μL of medium were added, as usual, before re-incubating at 31 °C. All the samples were observed every 24 hours by using the phase contrast microscope.

3.3.4 DNA quantification - PicoGreen

In order to evaluate the cell proliferation on the samples cultured at 31 °C, three DNA quantification tests were performed (before the seeding, after 24 and after 72 hours of culture). For these analyses, the Quant-iT PicoGreen dsDNA Assay Kit (Invitrogen, cat. n. P11496) was used. The aim of this assay is the quantification of the DNA content in a sample. The DNA content

is directly related to the number of cells on the sample. After DNA extraction, by destroying cell and nuclear membranes, PicoGreen is used as fluorescent staining for the fluorimetric analysis.

Fibroblasts (MRC-5) were seeded on 6 gelatine samples at a seeding density of $1 \cdot 10^4$ cells/cm^2.

2 of them were immediately melted at 37°C and centrifuged at 1300 rcf for 10 minutes, to separate the cells from the gelatine. After removing the gelatine, the cells were moved to 2 empty wells, covered with 500 μL Triton-X 0.05%, and stored at -20 °C. These samples were used as reference.

The other 4 samples were incubated at 31 °C and cultured as described in section 3.3.3 step 5.

24 hours after seeding 2 incubated samples were melted and centrifuged as the reference samples. The cells separated through centrifugation were moved to 2 empty wells, covered with 500 μL Triton-X 0.05%, and stored at -20 °C.

48 hours later the 2 remaining samples were melted, centrifuged and frozen as previously described.

48 hours after the freezing of the samples, both reference and cultured samples were thawed at room temperature, transferred to 1.5 mL tubes, and sonicated for 10 seconds by using Hielscher UP400S, (cycle: 1, amplitude: 40%) to break cells and nuclei. Tubes were soaked in ice just after sonication, in order to avoid DNA denaturation.

A calibration curve was prepared by mixing respectively 400, 200, 100, 40, 20, 10, 4, 0 μL of DNA lambda (2 μg/mL), with 0, 200, 300, 360, 380, 390, 396, 400 μL of TE buffer. Both the DNA lambda and the TE buffer were provided with the DNA Assay Kit.

A 96-well plate was prepared with the 8 standards for the calibration curve (3 wells per concentration), the 2 references (2 wells per sample), and the cultured samples (2 wells per sample), loading 100 μL per well.

Successively, 100 μL of PicoGreen working solution, provided by the DNA Assay Kit, were added to each well.

After 3 minutes of incubation at room temperature, standards and samples

were read on a fluorescent plate reader (TECAN Infinite M200, excitation wavelength: 485 nm, emission wavelength: 538 nm).

A calibration curve was built using the average values of the 8 standards. Samples DNA content was then evaluated by interpolation on this curve. Samples frozen after seeding and samples cultured were compared in order to evaluate the increase in the cell number during the culture.

3.3.5 Cell Viability and 3D distribution

Fibroblast (MRC-5) cells were seeded on 15% gelatine hydrogel prepared as described in chapter 2.2.1 step 4, and cultured for 21 days following the procedure shown in section 3.3.3, step 5. After this, samples were washed three times with PBS and incubated with Calcein AM 4mM for 10 minutes at 31 °C before analyzing them by using the Confocal Laser Microscope (Nikon A1, excitation wavelength: 488 nm, detection wavelength: 525 nm).

3.3.6 Histological Analysis

Cell-sheets cultured on gelatine at 31 °C as described in section 3.3.3 step 5, for one week, were rinsed in PBS, cut in 4 pieces, and soaked in 10% formalin neutral buffered (HT501128 Sigma) for 24 hours for fixation.

Dehydration After fixation samples were rinsed in water for 4 hours, then dehydrated and prepared for inclusion in paraffin by immersion in a sequence of different solutions:

- 50% ethanol, 1 hour
- 50% ethanol, 1 hour
- 70% ethanol, 1.5 hours
- 70% ethanol, 1.5 hours
- 70% ethanol, 1.5 hours

- 96% ethanol, 1 hour
- 96% ethanol, 1 hour
- 100% ethanol, 1 hour
- xilene, 15 minutes
- xilene, 15 minutes.

Inclusion and Cut Samples were then immersed in liquid paraffin at 60 °C for 2 hours, allowing it to penetrate into the samples. After that time samples in paraffin were left to solidify in the fridge (3 °C). Once solidified, samples were cut in 5 μm thick histological sections, with cuts parallel and perpendicular to the cell sheet plane. Paraffin was then removed from the cut samples by immersion in xilene for 10 minutes. Samples were then rehydrated by immersion in a sequence of ethanol solutions at decreasing concentrations:

- 100% ethanol, 5 minutes
- 100% ethanol, 5 minutes
- 90% ethanol, 5 minutes
- 70% ethanol, 5 minutes

and then soaked in water for 5 minutes. Samples were then divided into two groups and stained with hematoxylin and eosin (H&E) and van Gieson staining.

H&E staining The staining process was performed by soaking in a sequence of different solutions:

- Mayer's hematoxylin (1g/L), 10 minutes
- warm water, until violet tone
- eosin G, 30 sec

- distilled water, 10 sec
- ethanol 70%, 5 sec
- ethanol 80%, 5 sec
- ethanol 90%, 5 sec
- ethanol 100%, 10 sec
- ethanol 100%, 10 sec
- xilene, 10 sec
- xilene, 10 sec

van Gieson staining The staining process was performed by soaking in a sequence of different solutions:

- Weigert's iron hematoxylin stainng solution, for 15 minutes
- rinse in distilled water
- wash in running water, 10 minutes
- rinse in distilled water
- Van Gieson's staining solution, 1 minutes
- rinse in distilled water
- rinse in ethanol 70%
- dehydrate rapidly in ethanol 100%
- xilene, 10 sec

Dehydration Stained samples (both H&E and van Gieson) were then dehydrated by soaking in a sequence solutions:

- ethanol 50%, 5 minutes
- ethanol 70%, 5 minutes
- ethanol 90%, 5 minutes
- ethanol 100%, 5 minutes
- ethanol 100%, 5 minutes
- xilene, 5 minutes
- xilene, 5 minutes

Observation Pictures of the samples prepared as described above were acquired by using the optical microscope (Zeiss Axiotech).

3.3.7 Cell Transferring

Because of gelatine future applications, it was necessary to develop a procedure to transfer cells cultured on gelatine gels from sample surfaces to a different substrate (figure 3.1). The optimized transfer method consists of few steps:

1. Fibroblasts (MRC-5) were seeded with a seeding density of $2{\cdot}10^4$ cells/cm^2 on gelatine gels, prepared as usual (section 2.2.1, step 4). All the samples were incubated and cultured following the optimized method described in section 3.3.3, step 5.

2. 72 hours after seeding, the transfer procedure started: gels were moved to a new TCP with the seeded side down, maintaining the cell layer in contact with the polystyrene TCP.

3. Before carrying on with cell incubation under standard conditions (37 °C, 100% RH, normoxia), samples were analyzed by using the optical microscope

4. In order to monitor both gelatine melting and adhesion process, cells were checked again by using the optical microscope after a 60-minute incubation.

5. 90 minutes after the beginning of the transfer, melted gelatine was removed and samples rinsed with warm medium (37 °C), before carrying on the incubation at 37 °C (immersed in medium, in standard cell culture conditions).

6. In order to remove any residual gelatine, medium was changed again 90 minutes after step 5, and cells were observed with the optical microscope.

7. The analysis was repeated 24 and 48 hours after the transfer.

8. After the last check by using the optical microscope (48 hours), cells were rinsed with PBS, stained with Calcein AM 4mM for 10 minutes ant 37 °C, and observed with the fluorescence microscope.

3.4 Results and Discussion

3.4.1 Cross-linked gelatine

The use of an EDC cross-linked gelatine, which does not swell when soaked in culture medium and does not undergo gel-sol transition at the culture temperature, allows cell culture on this kind of gelatine in standard conditions [54]. The drawback is the impossibility to detach the cells by melting the gelatine.

Ultra-thin cross-linked gelatine gels were produced following the method described in section 3.3.2 step 1, and used as substrate for fibroblast culture (section 3.3.2). As already told, this procedure allowed to obtain a gelatine

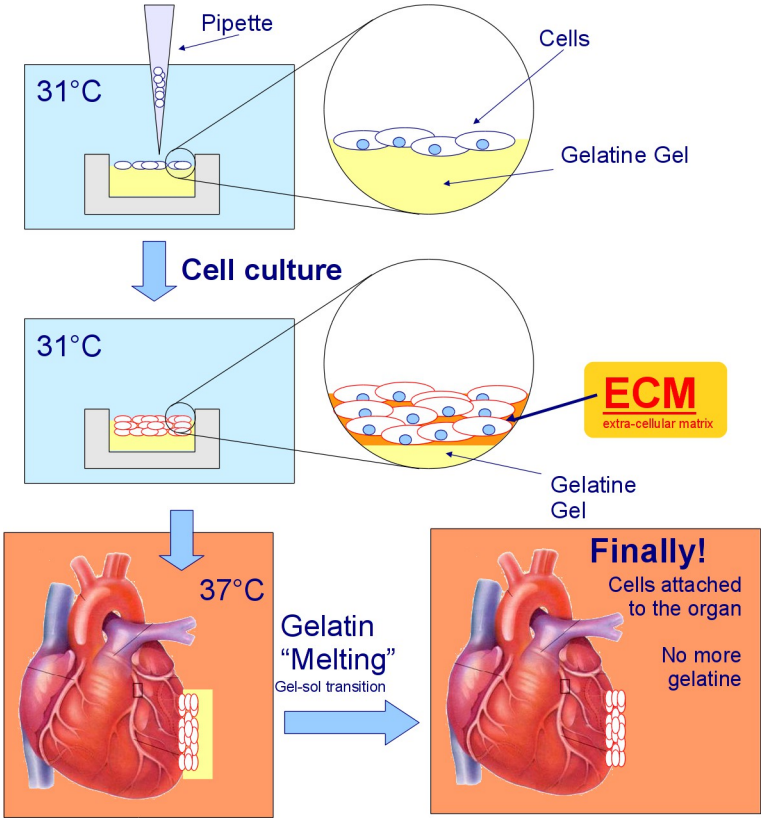

Figure 3.1: scheme of the cell sheet transferring process.

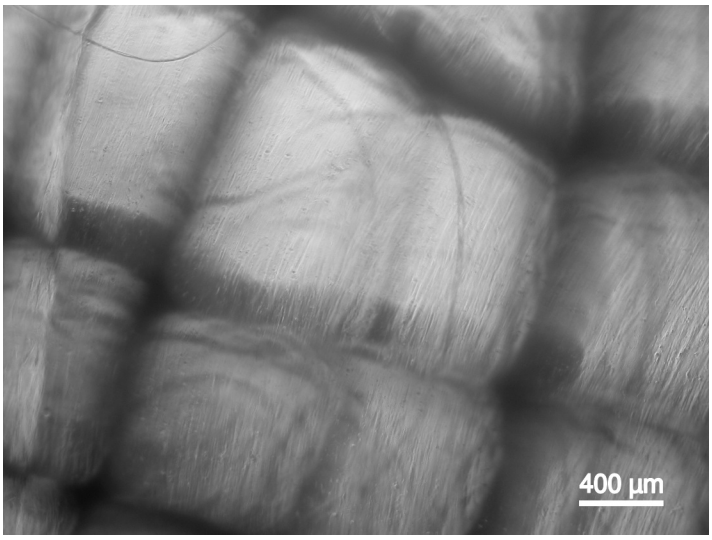

Figure 3.2: Confluent fibroblasts (MRC-5) on EDC cross-linked gelatine after 84 hours after seeding.

with only the superficial cross-linked layer, due to the short soaking time in the cross-linking solution. It was therefore possible to remove the inner part of the substrate by melting, but not the thin cross-linked layer, which is the culture substrate.

Cells grown on cross-linked gelatine surface reached confluence in 84 hours. Figure 3.2 shows the layer of confluent fibroblasts, which are aligned with the gelatine surface roughness (the big visible network is a cotton lint placed under the gel in order to handle it easily). Unfortunately, due to gel thickness and surface bending, caused by the swelling of its internal part (uncross-linked), it was not possible to observe the cells with the phase contrast microscope.

When placed on the polystyrene TCP for the transfer step, cells could not to completely detach from the cross-linked gelatine and adhere to the plate surface in a short time. Therefore, it was not possible to transfer cells using this culture substrate. As a consequence, the choice to use cross-linked gelatine as fibroblast culture substrate was given up.

3.4.2 Cell culture protocol development

Since the use of cross-linked gelatine as a substrate for fibroblast cell sheet culturing was given up, it was necessary to develop a novel cell culture technique, able to avoid (or at least reduce) water absorption by gelatine. This is necessary because water absorption causes a reduction in the gelatine concentration, which leads to a reduction of the gel-sol transition temperature and, as a consequence, to the "melting" of the substrate during the culture. The substrate melting during the culturing process would cause cell detachment, followed by cell sinking into the gel and finally cell adhesion to the bottom of the TCP, making the whole process useless. The first parameter which had to be changed was the culture temperature, since it was not possible to culture cells on uncross-linked gelatine at 37 °C. Successively it became necessary to change the medium addition (i.e., cell feeding) technique, in order to improve the quality of cell culture after 24 hours. Finally, due to its increased melting temperature (please, refer to section 2.3.3), gelatine prepared as described in section 2.2.1 step 4, was chosen to perform cell culture tests.

1. Temperature Reduction Since temperature plays a key role determining gelatine gel properties, it was necessary to find the best temperature at which to perform the cell culture.

There were no reliable analytical methods to determine how the temperature should be changed in order to achieve the best result; a try and error approach was therefore chosen, in which cultures at different temperatures were compared. Tests were performed at a temperature some degrees below the gelatine melting temperature in order to avoid the melting of the surface exposed to the liquid medium, which otherwise would swell, thus lowering its gel-sol transition temperature.

Cells were then cultured on annealed samples (section 2.2.1 step 4) at 31 °C, 32 °C and 34 °C, as described in section 3.3.3 step 1, and observed by using the phase contrast microscope after 2, 8, and 24 hours.

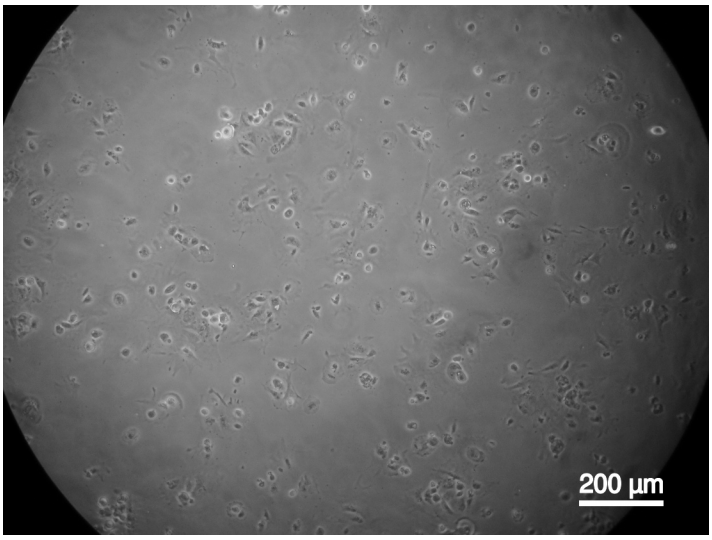

Figure 3.3: fibroblasts (MRC-5) cultured on gelatine at 31 °C. The image was acquired 2 hours after seeding.

Results Comparing the images acquired 2 hours after seeding (figures 3.3, 3.4 and 3.5) no difference could be observed between samples cultured at 31 °C and 32 °C. Both samples showed signs of cell adhesion: attaching to the surface, indeed, cells started to elongate. On the contrary, on the sample cultured at 34 °C there was no evidence of elongation, which usually indicates a lower degree of adhesion or a lower cell activity. The differences in the number of cells appearing in the images were not related to the culturing conditions or seeding density used, but they were only due to the fact that the images were acquired on different areas.

8 hours after seeding, (figures 3.6, 3.7, and 3.8) there were still no difference between samples cultured at 31 °C and 32 °C: adhesion increased and cells elongated further. However, signs of adhesion could now be observed also on the sample cultured at 34 °C, mainly as deformation of cells caused by focal adhesion. The substrate did not seem to be stiff enough to sustain cell spreading.

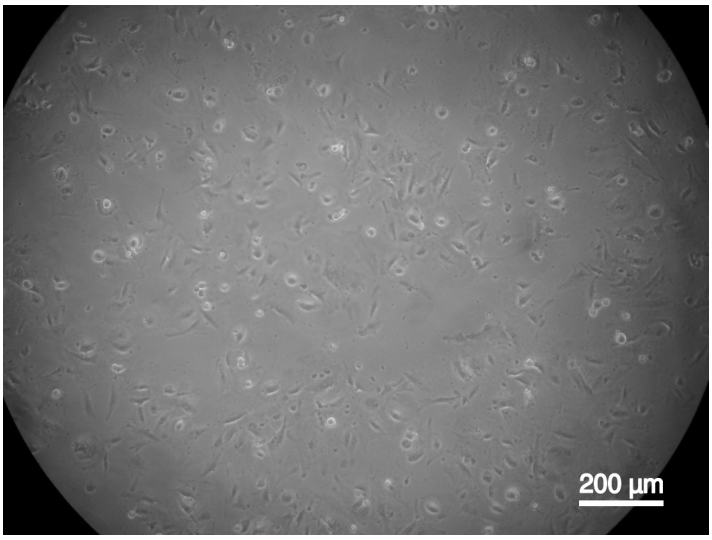

Figure 3.4: fibroblasts (MRC-5) cultured on gelatine at 32 °C. The image was acquired 2 hours after seeding.

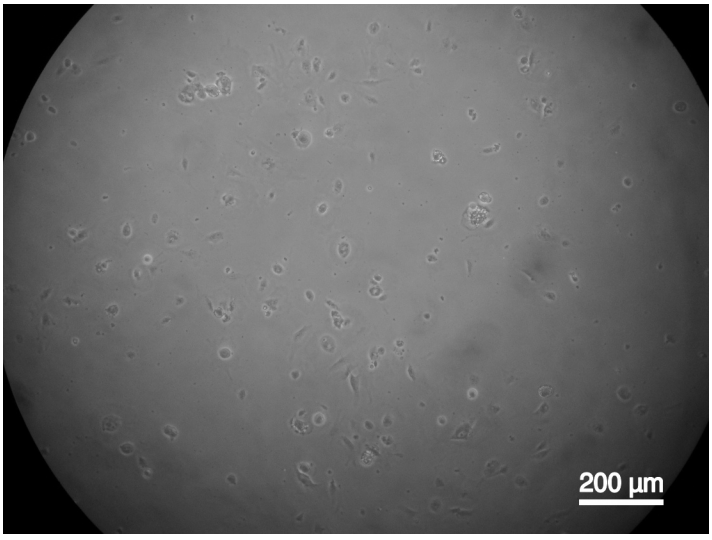

Figure 3.5: fibroblasts (MRC-5) cultured on gelatine at 34 °C. The image was acquired 2 hours after seeding.

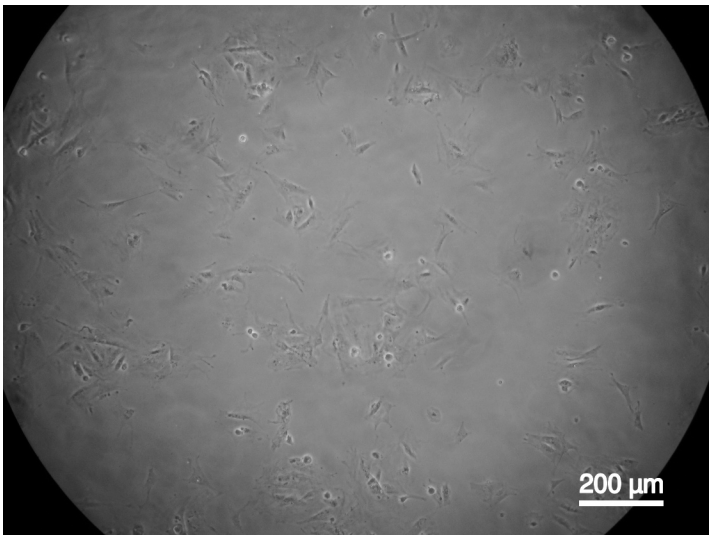

Figure 3.6: fibroblasts (MRC-5) cultured on gelatine at 31 °C. The image was acquired 8 hours after seeding.

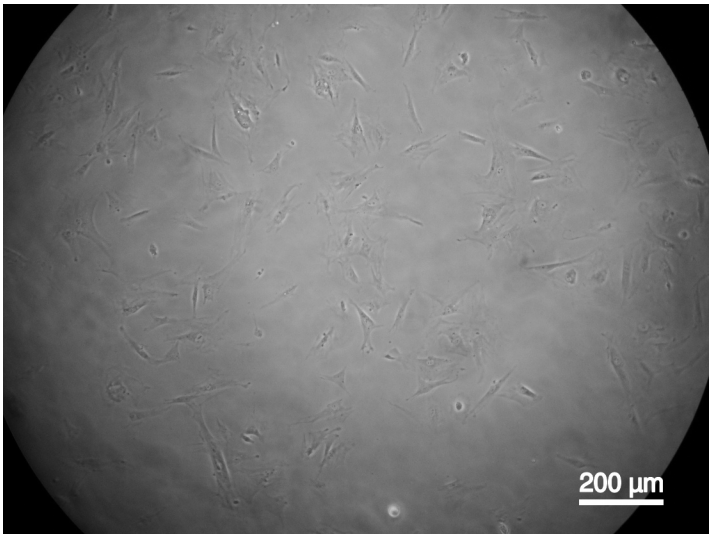

Figure 3.7: fibroblasts (MRC-5) cultured on gelatine at 32 °C. The image was acquired 8 hours after seeding.

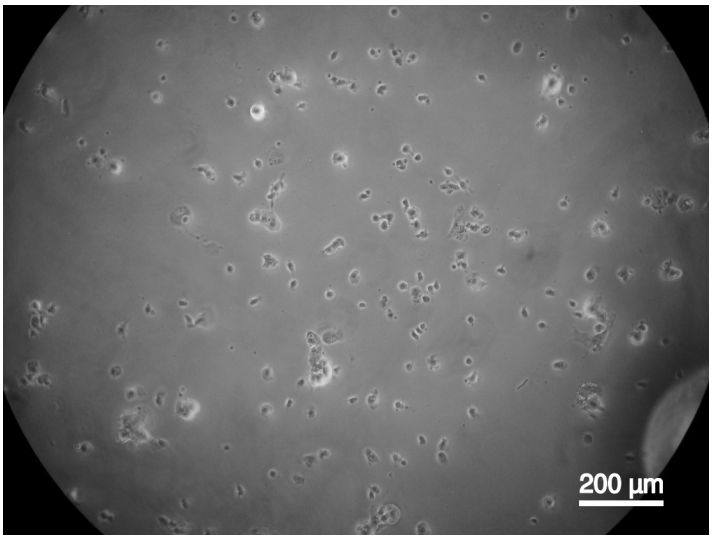

Figure 3.8: fibroblasts (MRC-5) cultured on gelatine at 34 °C. The image was acquired 8 hours after seeding.

24 hours after seeding, both round and spread cells were visible, on the sample cultured at 31 °C (figure 3.9). Spread cells were correctly attached to the gelatine surface, while round ones were less adhered or showed a lesser degree of activation. On samples cultured at 32 °C and 34 °C, the spreading was much lower: cells were almost round in shape, which indicates poor adhesion, probably due to too soft a substrate.

48 hours after seeding (figure 3.12), also the sample cultured at 31 °C showed a reduction in the amount of spread cells, indicating a certain degree of cell detachment probably caused by the swelling of the gelatine gel.

2. Cell Culturing on Dry Surface Once the best culture temperature was found, another problem became evident: after some days during which samples were cultured at reduced temperature and in standard culture conditions (i.e., samples were immersed in culture medium, in a polystyrene multi-well TCP), gelatine swelled absorbing medium and the cell sheets which formed on

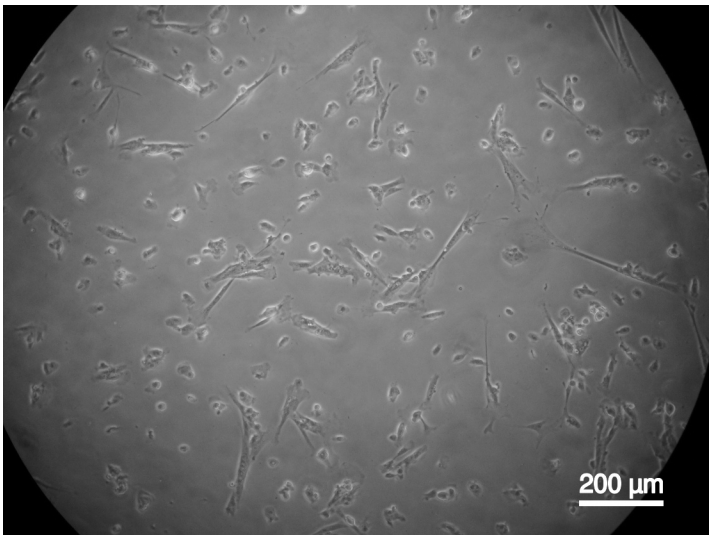

Figure 3.9: fibroblasts (MRC-5) cultured on gelatine at 31 °C. The image was acquired 24 hours after seeding.

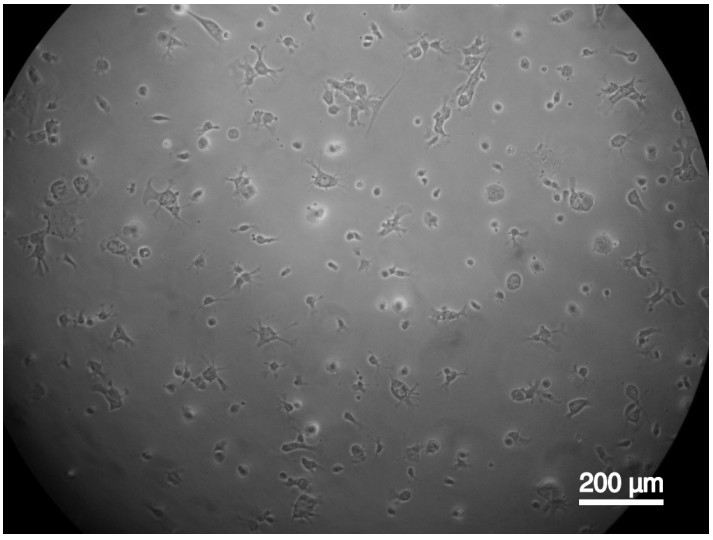

Figure 3.10: fibroblasts (MRC-5) cultured on gelatine at 32 °C. The image was acquired 24 hours after seeding.

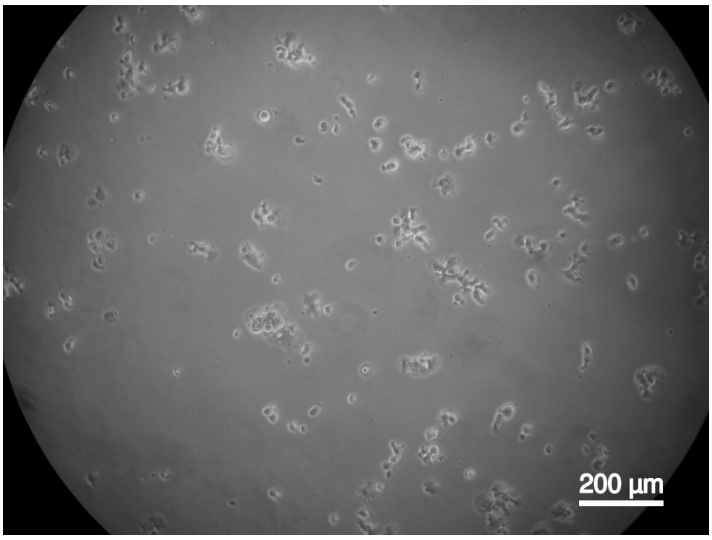

Figure 3.11: fibroblasts (MRC-5) cultured on gelatine at 34 °C. The image was acquired 24 hours after seeding.

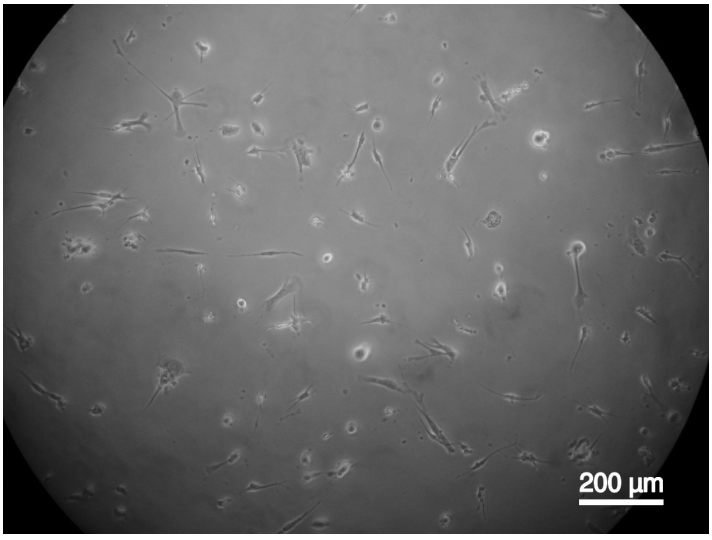

Figure 3.12: fibroblasts (MRC-5) cultured on gelatine at 31 °C. The image was acquired 48 hours after seeding.

the substrate surface detached themselves and shrunk (similar contraction for detached cell sheets was observed by Matsuda et al. [55]). Considering that:

- cells are seeded on a hydrogel constituted by 85% of cell culture medium,
- and the sample is inside an incubator which provides an environment with 100% relative humidity (RH),

a new culture method was developed, in order to overcome the issue previously described. This new method consisted of culturing human fibroblasts on a gelatine surface at 31 °C, with no medium covering the surface.

Fibroblasts (MRC-5) cultured at 31 °C on the surface of a dry annealed gelatine gel, were compared with cells cultured on gelatine immersed in culture medium (section 3.3.3 step 2).

Results Dry samples presented a good cell spreading, comparable with the one shown by samples cultured in standard conditions (at 31 °C) up to 8 hours after seeding (figures 3.13 and 3.14). To the naked eyes it was possible to notice that the surface was still slightly wet, due to the medium contained in the drop used for cell seeding.

After 24 hours (figure 3.15) cells on dry samples were mostly round, and to the naked eyes, it was possible to notice the total dryness of the surface. This excessive dryness was partially due to gelatine absorption and swelling, and partially to evaporation from the gel surface. Despite of the presence of water inside the incubator in order to maintain 100% RH, a certain degree of evaporation was noticeable. The round shape of the cells was in this case a symptom of sufferance induced by the surface dryness.

In figure 3.16a it is also possible to notice the effect of drying after 24 more hours: cells were mostly suffering, while cells on the wet surface (figure 3.16b), were partially round but in good conditions.

At the end of the test some mL of medium were added to a dry sample, as shown in figure 3.17: 24 hours after the medium addition, cells started to spread again, but with an unusual shape.

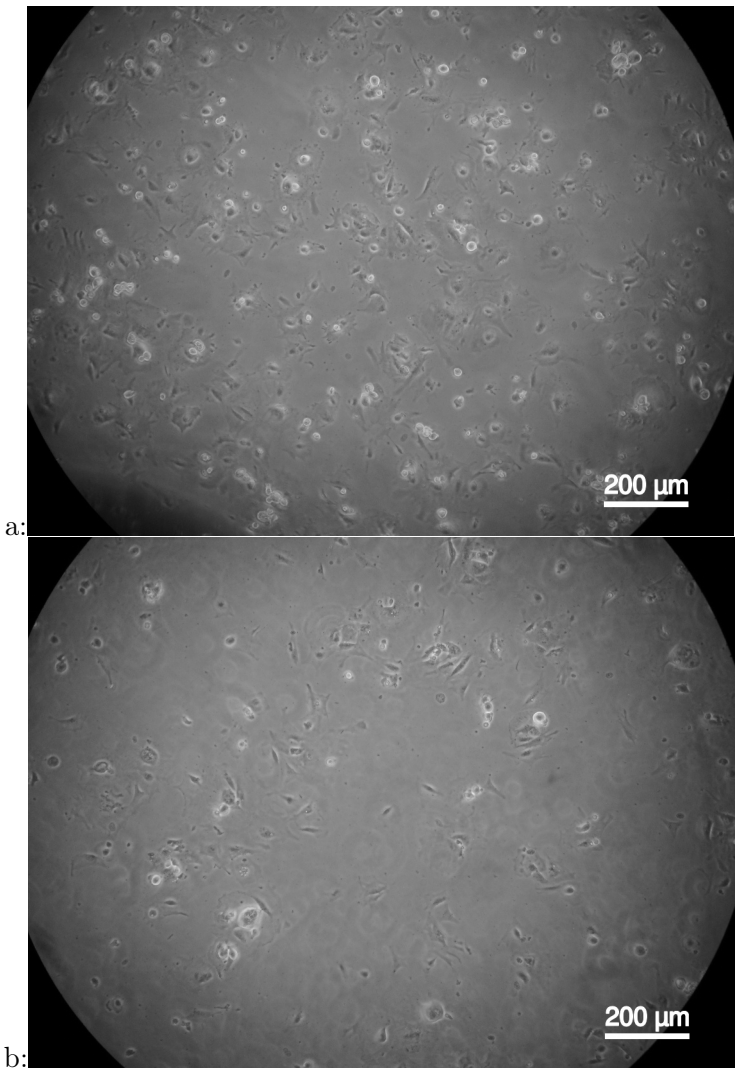

Figure 3.13: fibroblasts (MRC-5) on a dry sample (a), and on a wet samples (b). The images were acquired after 2 hours culturing at 31°C, by using the phase contrast microscope.

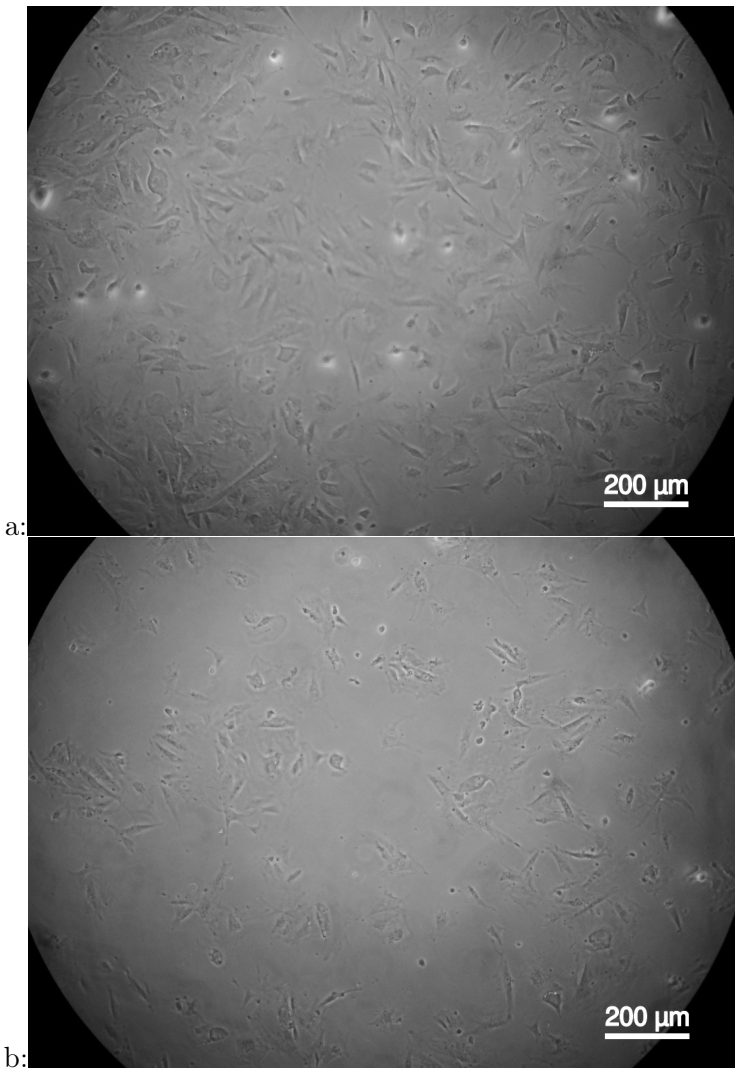

Figure 3.14: fibroblasts (MRC-5) on a dry sample (a), and on a wet samples (b). The images were acquired after 8 hours culturing at 31°C, by using the phase contrast microscope.

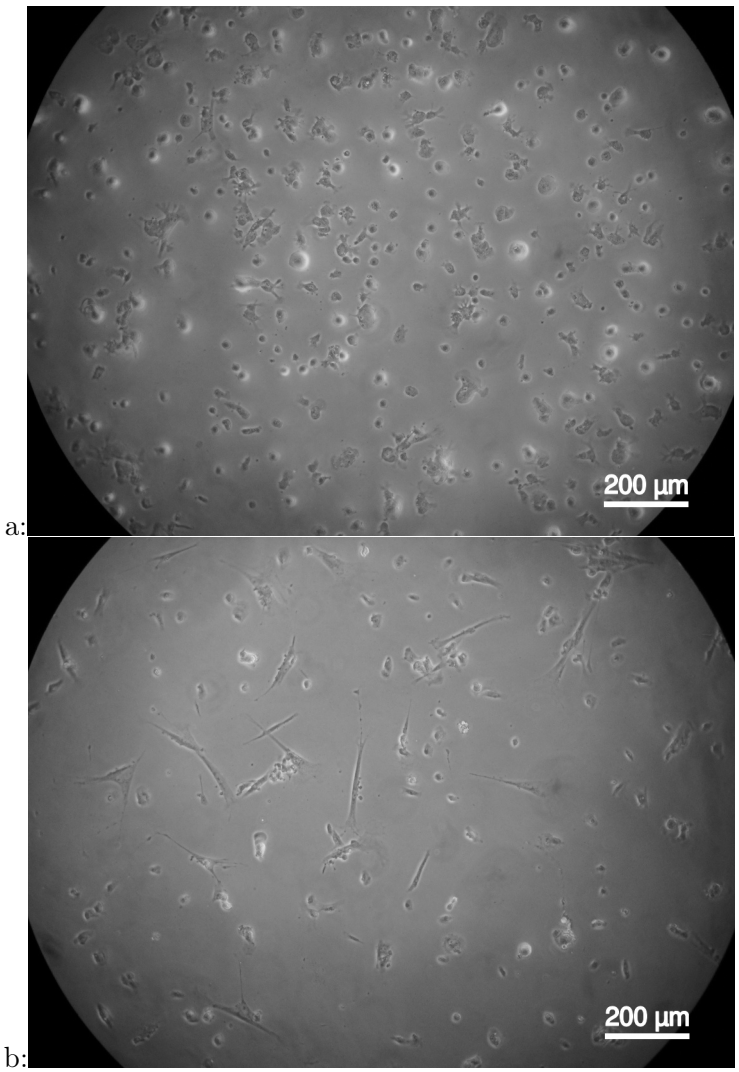

Figure 3.15: fibroblasts (MRC-5) on a dry sample (a), and on a wet samples (b). The images were acquired after 24 hours culturing at 31°C, by using the phase contrast microscope.

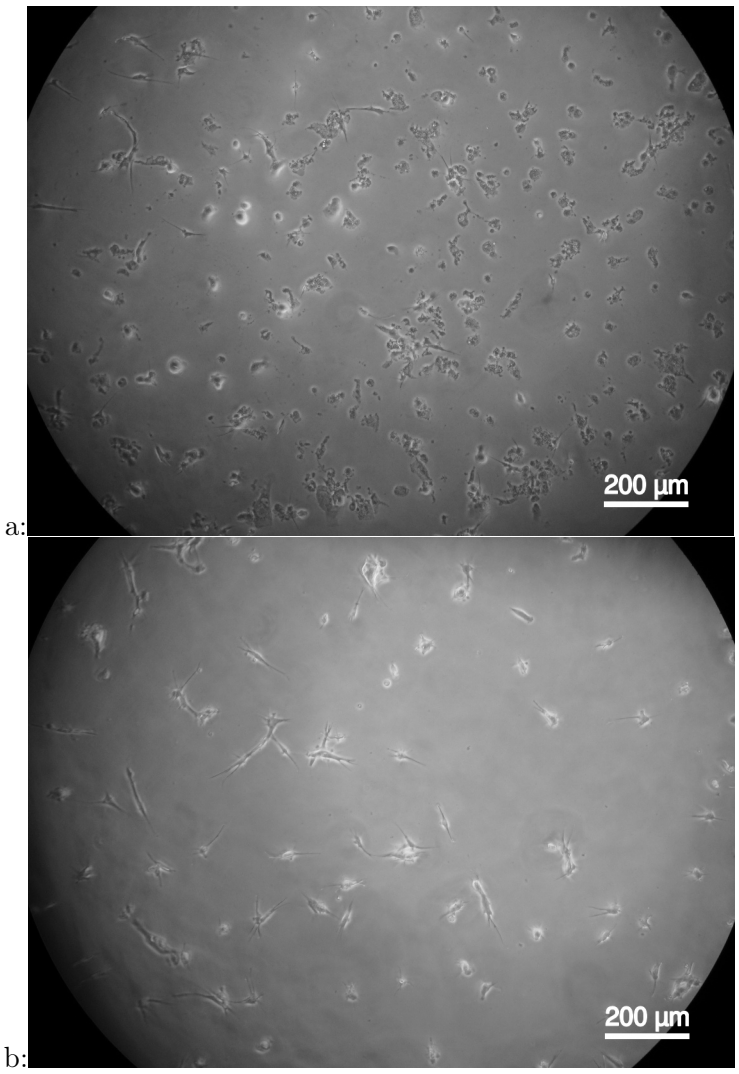

Figure 3.16: fibroblasts (MRC-5) on a dry sample (a), and on a wet sample (b). The images were acquired after 48 hours culturing at 31°C, by using the phase contrast microscope.

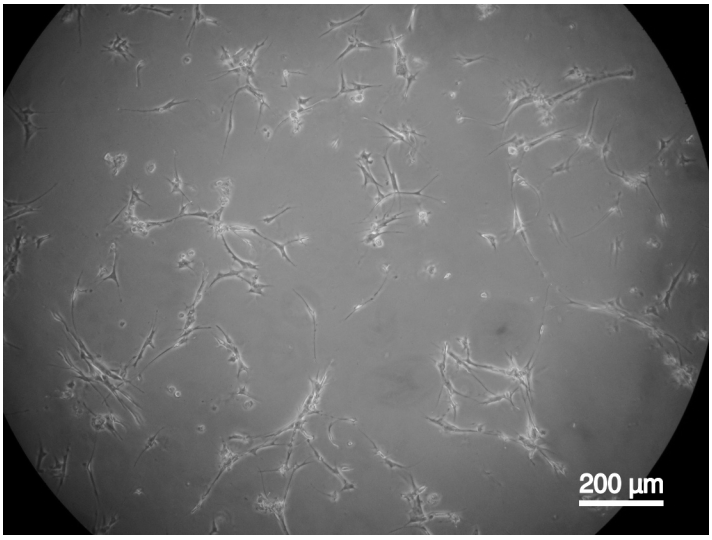

Figure 3.17: fibroblasts (MRC-5) cultured on a dry surface for the first 24 hours, and immersed in medium for the next 24. The image was acquired at the end of the culture (i.e., after 48 hours), by using the phase contrast microscope.

3. Cell Culturing on Barely Wet Surface As previously shown, the cell culturing on dry gelatine ran properly until the surface did not dry too much (i.e., for a time ranging from 24 to 48 hours). For this reason, new culture conditions were developed to maintain the right amount of liquid on the sample surface, without suffering of an excessive swelling of the gelatine. It was decided to perform, twice a day, small medium additions on the sample surface. Preliminary tests showed a certain degree of cell detachment associated with each medium addition. This phenomenon was interpreted as the reaction to the quick swelling of the warm gelatine (31 °C) caused by the medium addition. For this reason, prior to adding medium, samples were cooled down to room temperature for 15 minutes. In order to avoid thermal shock, also the added culture medium was heated to room temperature.

Fibroblasts (MRC-5) were cultured on annealed gelatine (section 2.2.1 step 4) at 31°C, adding twice a day 100 μL of medium on the surface at room temperature, as described in section 3.3.3 step 3. Cultured samples were observed by using the phase inversion microscope every 24 hours.

Results After the first 24 hours of incubation on a "barely wet" surface (figure 3.18) a significant difference in the cell behavior, in terms of adhesion and spreading, was observed. Cells which previously reverted to round shape in 48 hours (please refer to the test on dry sample and on completely immersed in medium described in steps 1 and 2), in this case maintained for weeks their elongated shape, typical of adherent fibroblasts. Moreover, no remarkable differences could be observed between samples with different culture times (figures 3.18 to 3.21).

4. Seeding Density Seeding density is an important parameter in most of cell cultures, in particular when cells are cultured at a reduced temperature, since cell proliferation is much reduced in relation to cultures performed at standard temperature (37 °C) [56, 57], as successively described in section 3.26. Moreover, fibroblasts are known to stop proliferation and migration when they

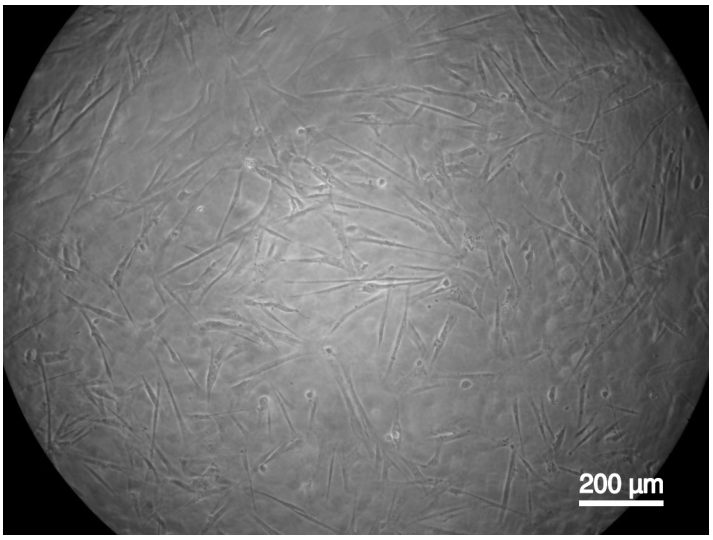

Figure 3.18: fibroblasts (MRC-5) cultured on a "barely wet" gelatine at 31 °C. The image was acquired 24 hours after seeding by using the phase contrast microscope.

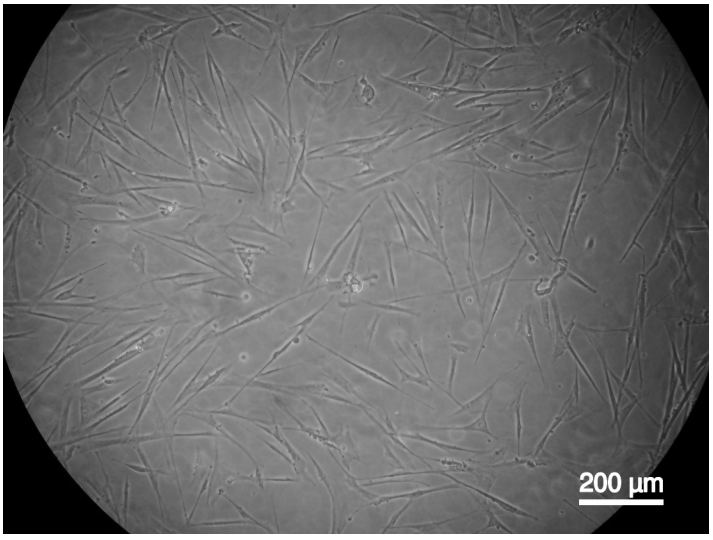

Figure 3.19: fibroblasts (MRC-5) cultured on a "barely wet" gelatine at 31 °C. The image was acquired 48 hours after seeding by using the phase contrast microscope.

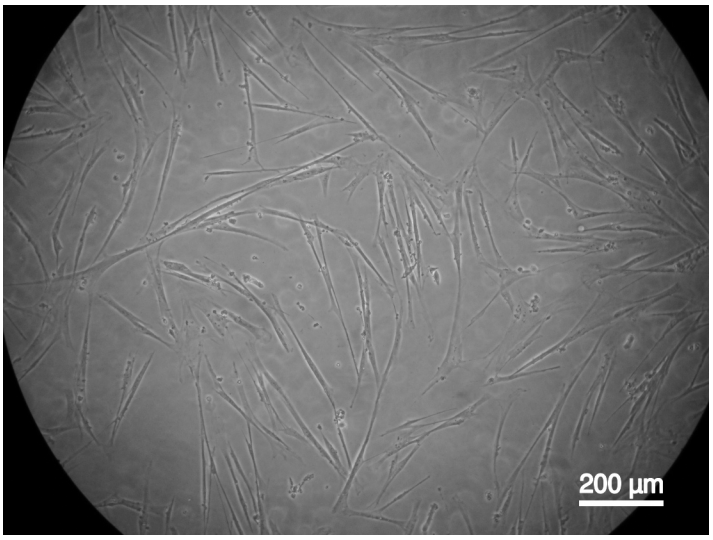

Figure 3.20: fibroblasts (MRC-5) cultured on a "barely wet" gelatine at 31 °C. The image was acquired 72 hours after seeding by using the phase contrast microscope.

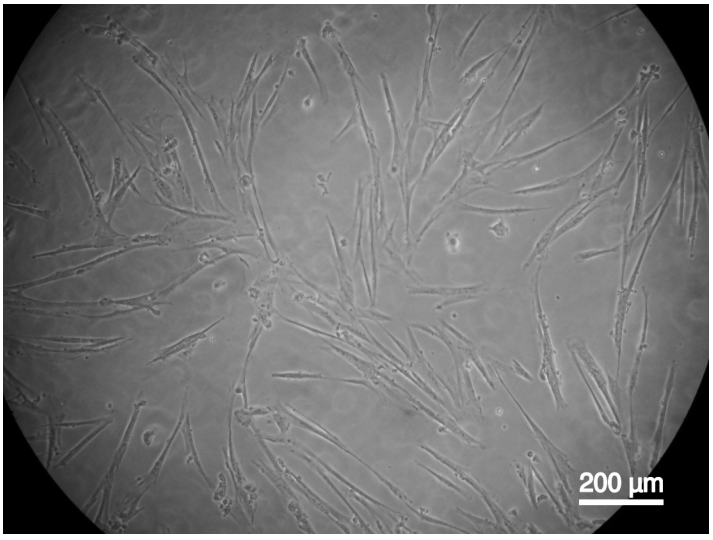

Figure 3.21: fibroblasts (MRC-5) cultured on a "barely wet" gelatine at 31 °C. The image was acquired 96 hours after seeding by using the phase contrast microscope.

get in contact each other: this phenomenon was called "contact inhibition" by Abercrombie and Heaysman [58, 59, 60, 61]. Since the aim of this work was to obtain a confluent layer of fibroblasts, bound to each other in order to hold together during the transfer process, the seeding concentration should be almost as much as the cell density at confluence. This allows cells to reach confluence in short time, in order to trigger the ECM production to reinforce the cell sheet before transferring.

To determine the best seeding density value, cells were seeded on the sample surface at 3 different seeding densities: $1 \cdot 10^4$ cells/cm^2, $2 \cdot 10^4$ cells/cm^2 and $4 \cdot 10^4$ cells/cm^2. Successively, they were incubated at 31 °C with wet surfaces, which were re-wet twice a day, as described in step 3 (please, refer to section 3.3.3 step 4 for the details).

Results It is known that 24 hours after seeding, cells cultured at 31 °C show a very low proliferation rate [56, 62]; therefore this culture time was taken as reference for seeding density comparison.

In figure 3.22 it was possible to notice that cells seeded at $1 \cdot 10^4$ cells/cm^2 were not enough to reach confluence in 24 hours.

On the contrary, cells seeded at $2 \cdot 10^4$ cells/cm^2 (figure 3.23) formed an almost confluent layer, as required.

It was interesting to observe what happened when cells were seeded at higher density. At $4 \cdot 10^4$ cells/cm^2 (figure 3.24), cells formed a multilayer structure, well spread on the surface.

Unfortunately, continuing the culture, the limit became evident. After 48 hours of culture, multi-layered cells detached from the surface, and collapsed in a huge cell cluster made of cells mostly round in shape (figure 3.25). After this contraction, the layer diameter was usually 1/3 of the initial diameter (i.e., when cells were attached and spread).

5. Cell Culture - optimized procedure Cell culture procedure developed in step 3 represented an improvement of the protocol used for cell culturing

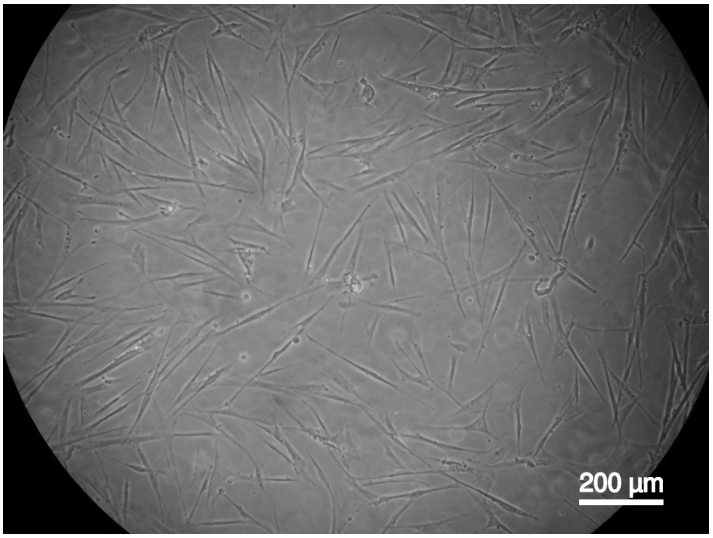

Figure 3.22: MRC-5 on gelatine, 24 hours after seeding, seeding density $1 \cdot 10^4$ cells/cm^2, cells spread, unable to reach confluence.

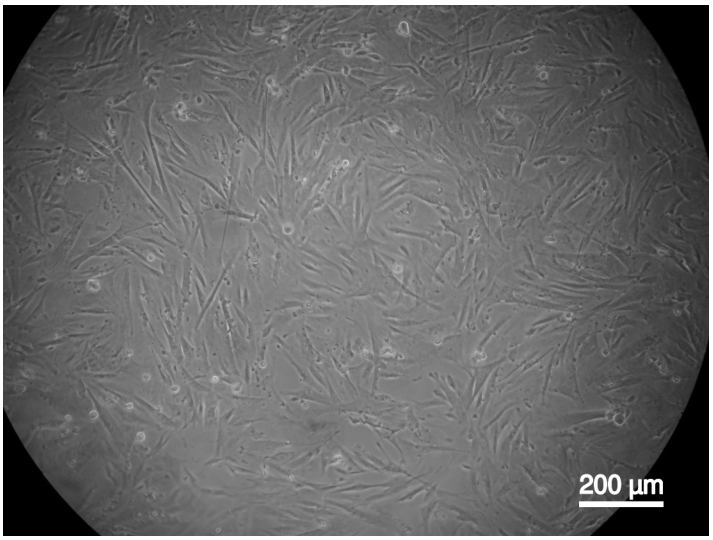

Figure 3.23: MRC-5 on gelatine, 24 hours after seeding, seeding density $2 \cdot 10^4$ cells/cm^2, cells spread forming a monolayer.

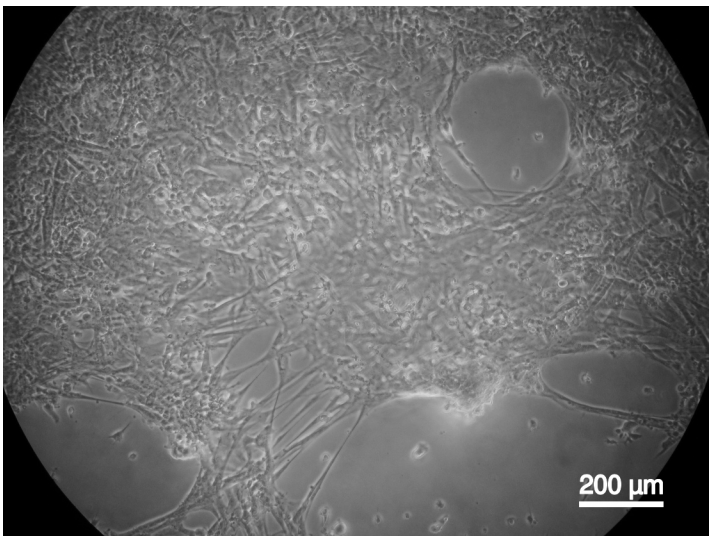

Figure 3.24: MRC-5 on gelatine, 24 hours after seeding, seeding density $4 \cdot 10^4$ cells/cm^2, cells spread and formed a multilayer structure.

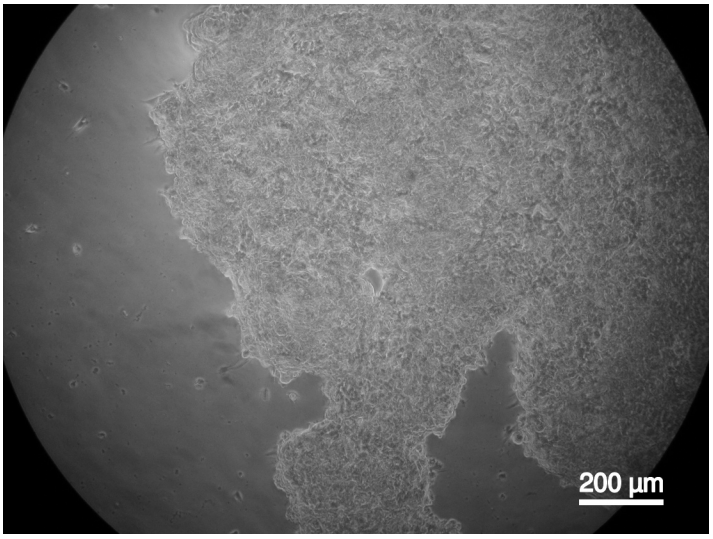

Figure 3.25: MRC-5 on gelatine, 48 hours after seeding, seeding density $4 \cdot 10^4$ cells/cm^2, the cell sheet has detached and contracted forming a huge cell cluster.

on gelatine at reduced temperature, since the use of this protocol allowed to culture cells on thermo-reversible gelatine almost as it were cultured on a TCP.

Anyway, to improve the method, it was necessary to develop a procedure for the replacement of the medium contained in the gelatine. The same medium remains inside the gelatine for several days while culturing, an obvious reduction of nutrients overtime (partially consumed by cells, and partially naturally degraded, e.g. L-glutamine), together with a waste stagnation occur.

The only way to replace the culture medium inside a gelatine substrate, without detaching the cells seeded on the surface, was by exploiting the diffusion, at a temperature at which gelatine does not swell too much. Therefore, it was decided to add another step to the culture protocol.

Once a day gelatine samples were removed from the incubator and left at room temperature for 15 minutes. Then they were soaked in culture medium at room temperature for 10 minutes. Successively they were extracted and a culture medium addition was performed as explained in step 3, before re-incubation at 31 °C. Please, refer to section 3.3.3 step 5 for a more detailed description of the procedure.

3.4.3 DNA quantification

In order to evaluate the cell proliferation on the samples cultured at 31 °C, the DNA content of samples incubated on gelatine at 31 °C for 24 and 72 hours, was compared with the DNA content of the ones analyzed just after seeding. The DNA content is directly related with the number of cell in the sample; therefore, it was possible to determine the increase of the cell number during the culture. For the detailed protocol, please refer to section 3.3.4.

Results In figure 3.26 the slight increase in the cell number after 24 hours of cell culturing at 31 °C is shown. On the contrary, no increase in the DNA quantity can be detected after the successive 48 hours of culture. This reduction in the mitotic activity, after 24 hours of culture at reduced temperature, is reported also by Enniga et al. and Thompson [56, 57]. However, the spread

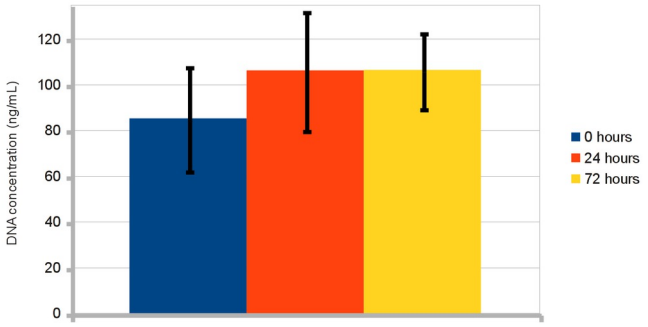

Figure 3.26: DNA quantification results: cells cultured at 31 °C for 24 hours showed a slight increase in number if compared with the reference sample. 48 hours later the cell number seems to be unchanged.

of the DNA content data, which is probably related to the difficulty to harvest the cells after the centrifugation step, does not allow to exclude a small increase in the number of cells even after 24 hours of culture.

3.4.4 Cell viability and migration

Culturing cells on a gelatine substrate, for a relatively long time, in non standard conditions of temperature and feeding (as described in section 3.3.3 step 5), led to the necessity to check the cell viability. Different techniques are used to analyze standard samples; but due to the special conditions required for cell culture on gelatine (mainly for the impossibility to incubate at 37 °C), it was chosen to use the confocal laser microscope after staining with calcein acetoxymethyl ester (AM). This because the analysis of samples stained with calcein AM not only allows to evaluate the cell viability, but also to observe shape and three-dimensional cell distribution on the surface and inside the hydrogel.

Calcein AM is a non-fluorescent, hydrophobic compound, able to enter the membrane of live cells with intact membranes. The hydrolysis of Calcein AM by endogenous intracellular esterases produces calcein (figure 3.27), a hy-

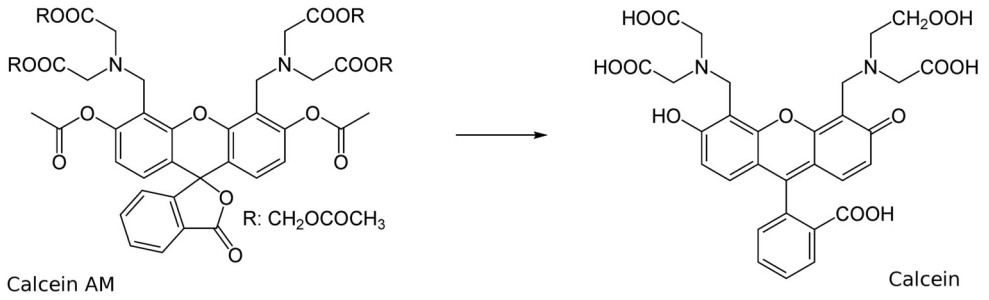

Figure 3.27: calcein acetoxymethyl ester (non fluorescent) esterases reaction which produces calcein (fuorescent).

drophilic strongly fluorescent compound which, due to its hydrophilicity, is retained in the cytoplasm. Moreover, calcein AM does not stain dead cells, and is rapidly lost under conditions that cause cell lysis. For these reasons, stained cells are certainly still living.

In order to test the survivability of fibroblasts cultured on gelatine at reduced temperature, fibroblasts (MRC-5) were seeded on 15% gelatine and cultured for 21 days, following the procedure described in section 3.3.5. Successively living cell distribution was observed by using the confocal laser microscope.

Results In figure 3.28 the stacked view of the gelatine sample (i.e., from above) is shown.

These cells were not only on the surface, but also partially penetrated into the gel during the culture period, as shown in figures 3.29 and 3.30, which are 3D reconstruction of the same part of the gel. This penetration was not assignable to an excessive swelling and to a consequent softening of the gel, because in this case cell detachment would be evident. On the contrary fibroblasts aligned perpendicularly to the surface, as in figure 3.30, indicated cell migration.

In figure 3.31, different cell orientations at different depths are evident.

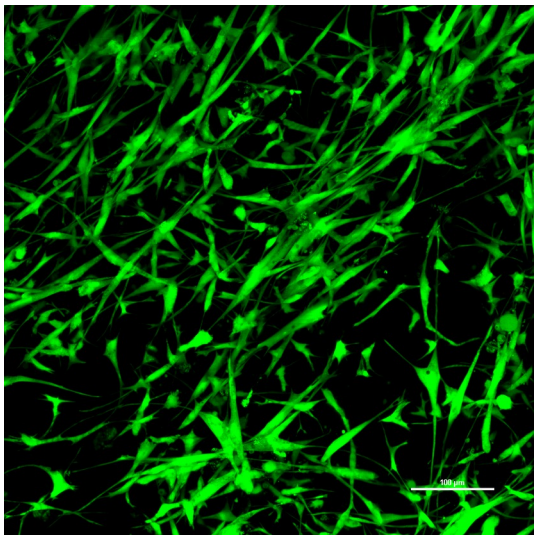

Figure 3.28: stacked view of a full thickness sample of fibroblasts (MRC-5) cultured on gelatine at 31°C for 21 days. The image was acquired after seeding by using the confocal laser microscope.

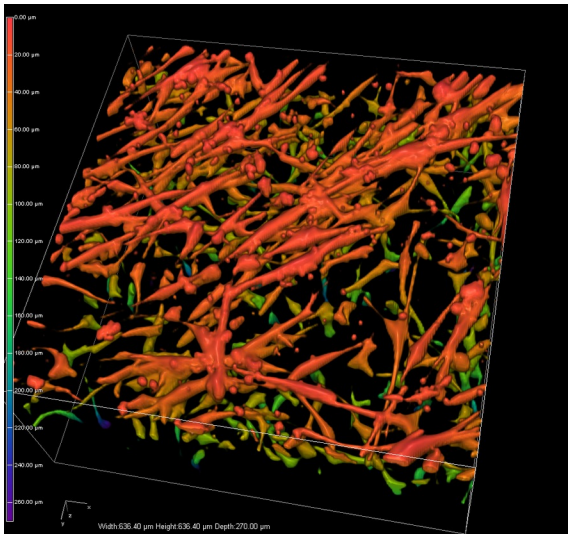

Figure 3.29: 3D reconstruction (top view) of a full thickness sample of fibroblasts (MRC-5) cultured on gelatine at 31°C for 21 days. The image was acquired after seeding by using the confocal laser microscope.

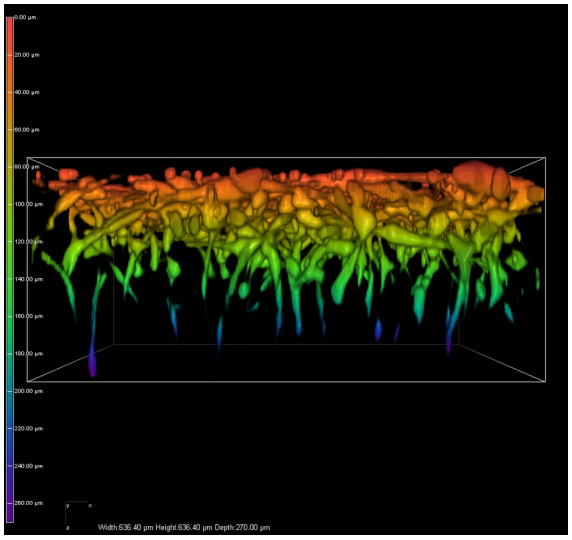

Figure 3.30: 3D reconstruction (side view) of a full thickness sample of fibroblasts (MRC-5) cultured on gelatine at 31°C for 21 days. The cell penetration depth is about 140 μm. The image was acquired after seeding by using the confocal laser microscope.

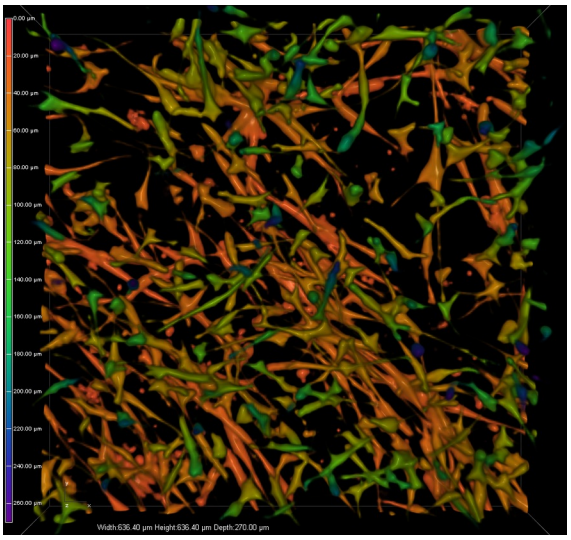

Figure 3.31: 3D reconstruction (bottom view) of a full thickness sample of fibroblasts (MRC-5) cultured on gelatine at 31°C for 21 days. The image was acquired after seeding by using the confocal laser microscope.

3.4.5 Cell Sheet Histology

In order to analyze the morphology of the cell sheets cultured on gelatine at 31 °C, histological analyses were performed.

For the histological tests, fibroblasts (MRC-5) were cultured at 31 °C on gelatine hydrogels for 7 days following the procedure described in section 3.3.3 step 5. Successively, the samples were fixed in formalin, dehydrated and embedded in paraffin. Samples were then cut in slices 5 μm thick, with both horizontal and vertical cross-section as shown in figures 3.32 and 3.33. Histological sections were stained with hematoxylin and eosin (H&E), and van Gieson staining, in order to show the cell distribution. The detailed protocol followed for the histological preparation was described in section 3.3.6.

Results The first interesting result deduced by means of this test was reached before cell fixation: the sample cut (figure 3.34) showed the presence

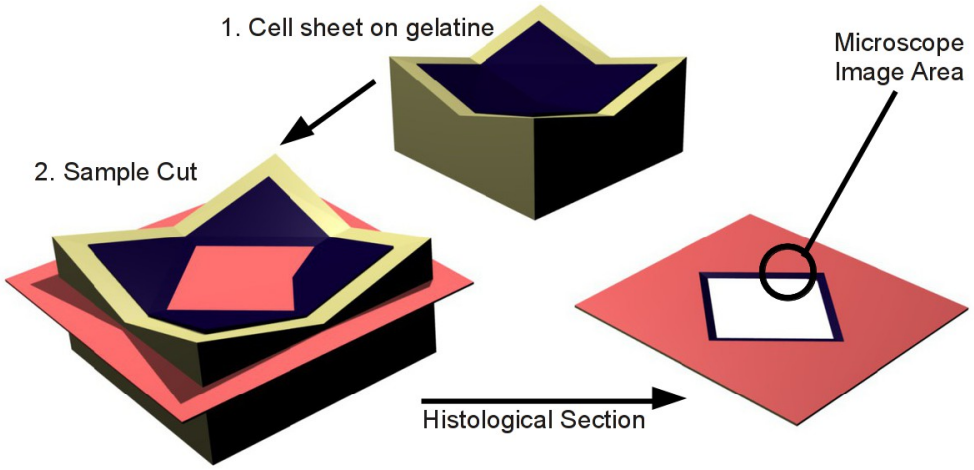

Figure 3.32: scheme of the horizontal cross-section (gelatine in yellow, cell-sheet in black, and the plane of section in red).

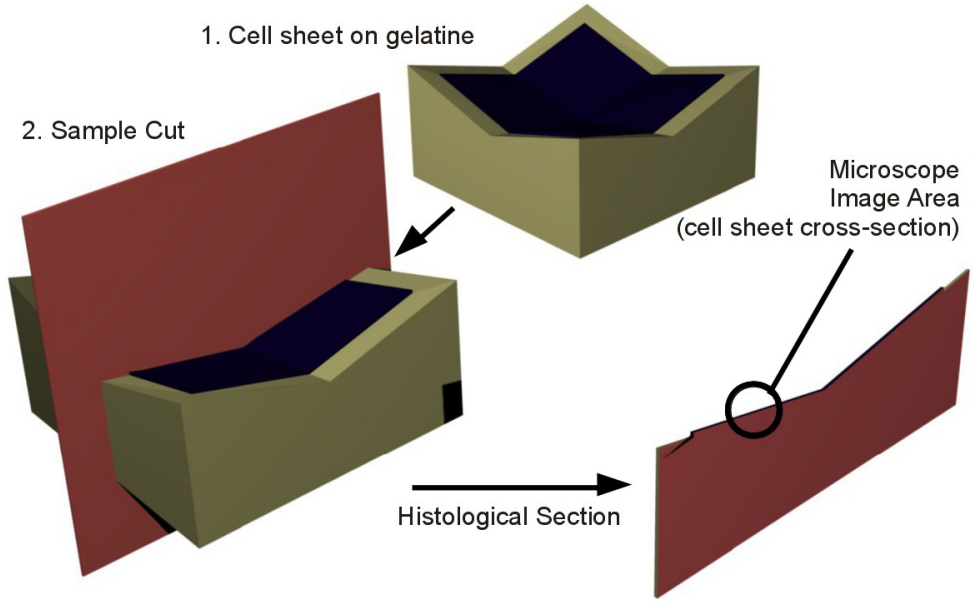

Figure 3.33: scheme of the vertical cross-section (gelatine in yellow, cell-sheet in black, and the plane of section in red).

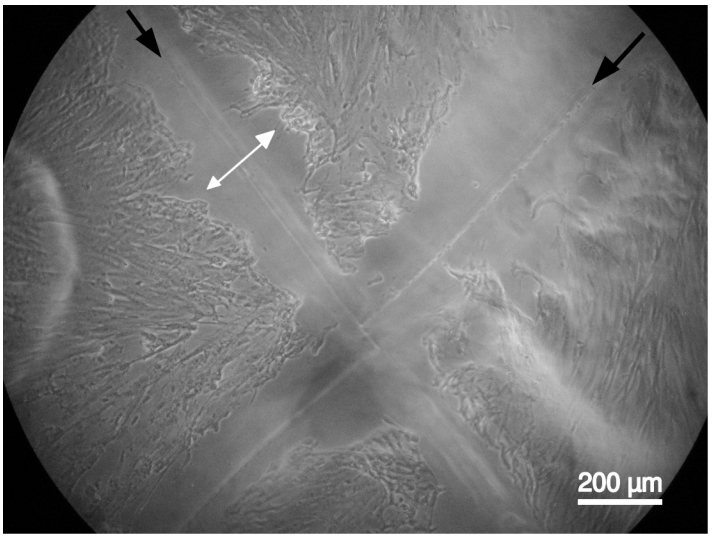

Figure 3.34: cell sheet after the cut with the bistoury (black arrows), prior to the fixation in formalin. Slight contraction of the sheet, mechanically detached from the surface by the cut, is clearly visible (white arrow). The image was acquired by using the phase contrast microscope.

of a continuous layer made of cells and ECM on the surface. After the cut this layer slightly contracted because of a mechanical detachment induced by the bistoury blade.

In figure 3.35 a horizontal cross-section of the sample cut as described in figure 3.32 is shown: the presence of cells is shown by nucleus stained in blue (by means of hematoxylin). The cut was not perfectly parallel to the cell sheet surface, due to difficulties in blade alignment and sample irregularity. However, it is possible to notice the presence of a dense cell layer on the sample surface.

In figures 3.36a and 3.36b a vertical cross-section of the sample, obtained as sketched in figure 3.33, is shown. It is possible to notice the cell sheet cross-section, which appears as a film slightly detached from the surface. This detachment was induced by mechanical stresses while preparing the histological sections. The sheet seems to be continuous and not formed by single cells attached to the surface of the gelatine substrate, indicating strong interactions

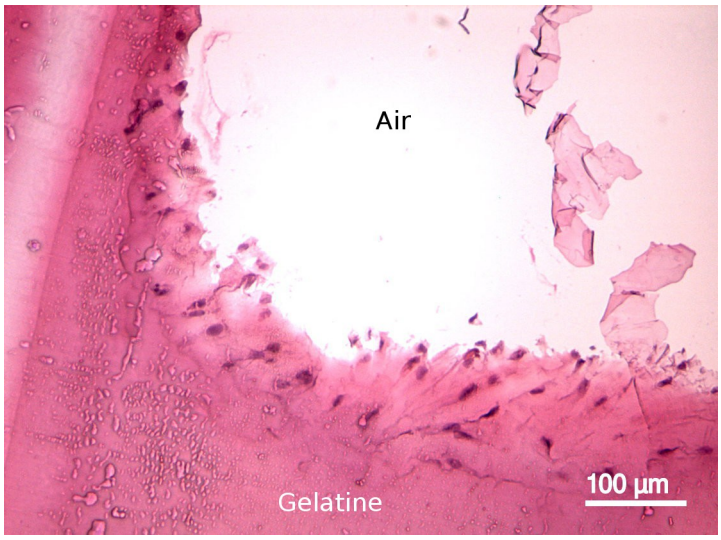

Figure 3.35: histological section (horizontal), stained with H&E, dark spots represent cell nuclei. The image was acquired at the optical microscope.

between the cells forming the layer. Moreover, cells are clearly confined into the superficial layer, indicating the use of ideal culture conditions for cell sheet formation.

Samples stained by using van Gieson protocol provided no additional results to what was deduced after analyzing samples stained with H&E.

3.4.6 Cell Sheet Transferring

In order to demonstrate the possibility to transfer the developed cell sheet on a wound or an injured organ (figure 3.1), it was necessary to test the transfer method on a substrate easy to analyze. The surface chosen to perform the transfer test, was a polystyrene TCP, since it gave the possibility to perform further analysis and to carry on with the culture.

To carry out the test cell sheet samples were prepared seeding the fibroblasts (MRC-5) on the gelatine gel (seeding density: $2 \cdot 10^4$ cells/cm^2) and culturing them at 31 °C (section 3.3.3 step 5). Such a cell sheet was then

a:

b:

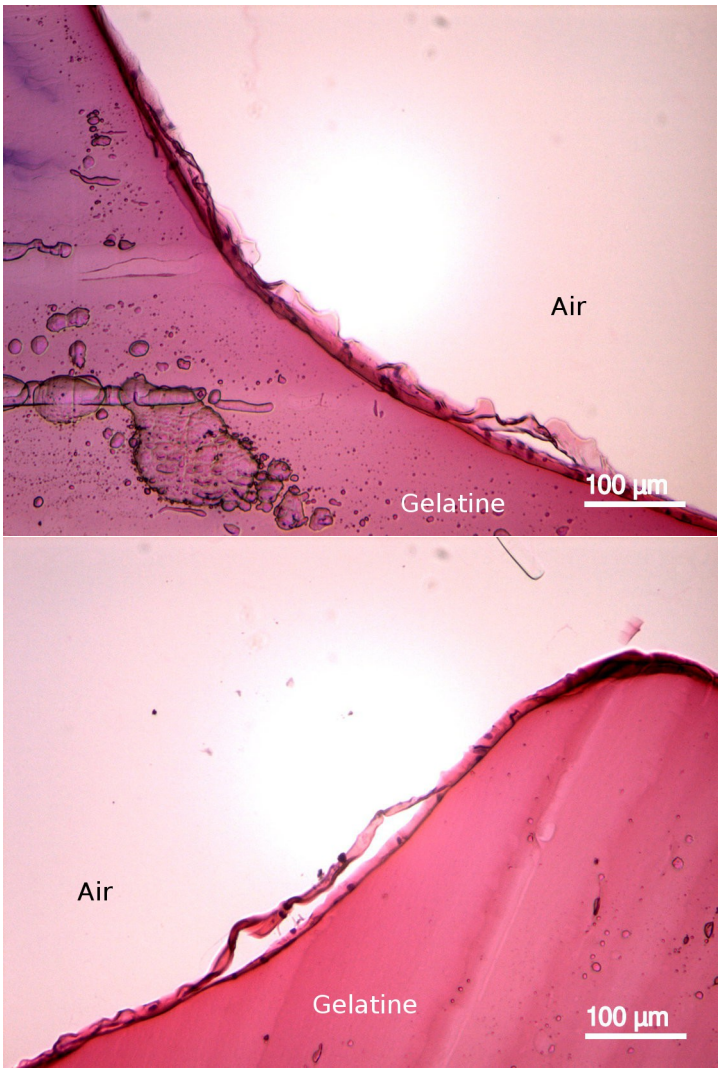

Figure 3.36: histological section (vertical), stained with H&E, dark spots represent cell nuclei. In (a) is shown the cell sheet almost completely adherent to the surface, in (b) a detachment of the cell sheet, induced during the preparation of the histological section is clearly visible. The images were acquired at the optical microscope.

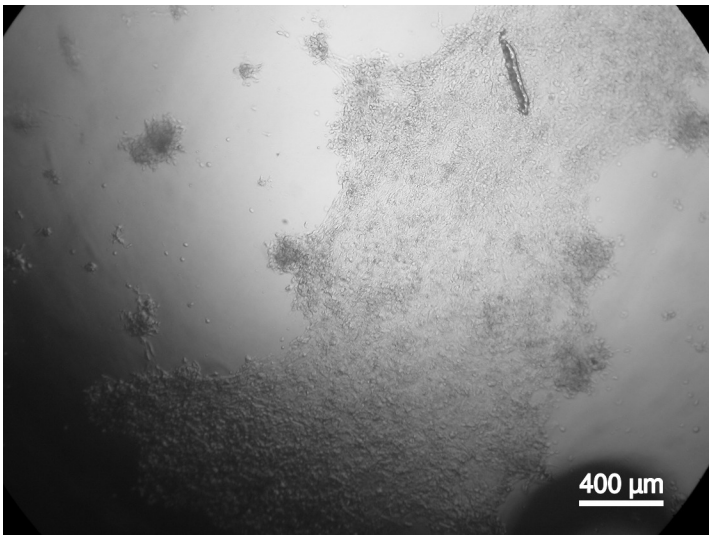

Figure 3.37: cell sheet cultured on gelatine at 31 °C for 72 hours, just placed in contact with the TCP at 37 °C (transfer start). The image was acquired by using the optical microscope.

transferred to a TCP and kept it in contact with the surface, as described in section 3.3.7. Once adhesion occurred (i.e., after 90 minutes), cells were rinsed repeatedly with culture medium to remove residual gelatine and confirm cell adhesion. Cell culture was carried on in standard culture conditions to demonstrate cell activity and mobility once re-incubated at 37 °C [56, 62].

Results Figure 3.37 shows a cell sheet cultured on gelatine at 31 °C for 72 hours. This picture was acquired after placing it on the TCP (i.e., the moment at which the transfer process started). In order to assess the shrinkage occurring during the transfer process, a cell sheet, which was small enough to be fully comprised into the picture, was chosen. Images were acquired without the phase contrast objective, to allow lower magnification, and therefore the availability of a bigger area inside the picture.

After 60 minutes at 37 °C gelatine appeared to be melted, but cells had not shrunk yet (figure 3.38).

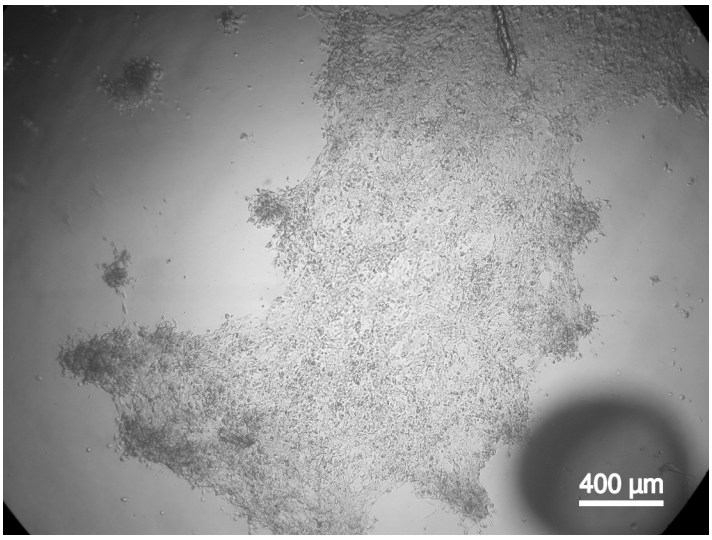

Figure 3.38: cell sheet cultured on gelatine at 31 °C for 72 hours, 60 minutes after the transfer start. The image was acquired by using the optical microscope.

After 90 minutes shrinkage started, indicating the complete melting of the substrate. Melted gelatine was then aspirated and the TCP, with the attached cell sheet, was rinsed with medium. In figure 3.39 a small shrinkage is clearly visible, which is typical of fibroblast cell sheets detached from the culture substrate [63]. The small entity of the shrinkage indicates the sheet adhesion to the new substrate (i.e. the TCP); differently, cells would shrink completely, forming a big cell cluster.

In the following images, specially in figure 3.41, acquired after 24 hours of incubation at 37 °C, cell clusters were evident, indicating a sub-optimal adhesion or a light detachment in these sheet areas, as confirmed by the position of these clusters. They were in fact distributed on the sheet boundaries, which are the most stressed zones and which can be detached by the medium flow while rinsing. However, the presence of these clusters indicated a good interaction between cells in the sheet, otherwise they would be washed away by the

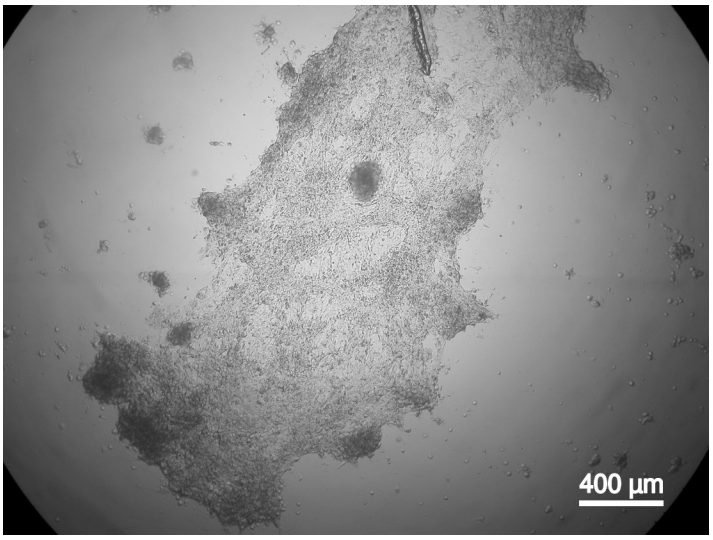

Figure 3.39: cell sheet cultured on gelatine at 31°C for 72 hours, 90 minutes after the transfer start. Melted gelatine was removed. The image was acquired, after rinsing with warm medium (37°C), by using the optical microscope.

medium.

After 48 hours of incubation at 37 °C cells were reorganizing on the surface and migrating from the clusters to the surface, making clusters less visible (figure 3.42). Since it was difficult to observe cells spread on the TCP without phase contrast, they were stained with Calcein AM. This one allows to verify their living state too.

In figure 3.43, the spreading on the surface is evident, even if clusters are still visible.

3.5 Conclusions

The importance of avoiding gelatine melting during cell culturing is evident. Moreover, the experimental results shown in section 3.4.2 step 1 pointed out also the importance of avoiding the swelling on the culture surface. Swollen

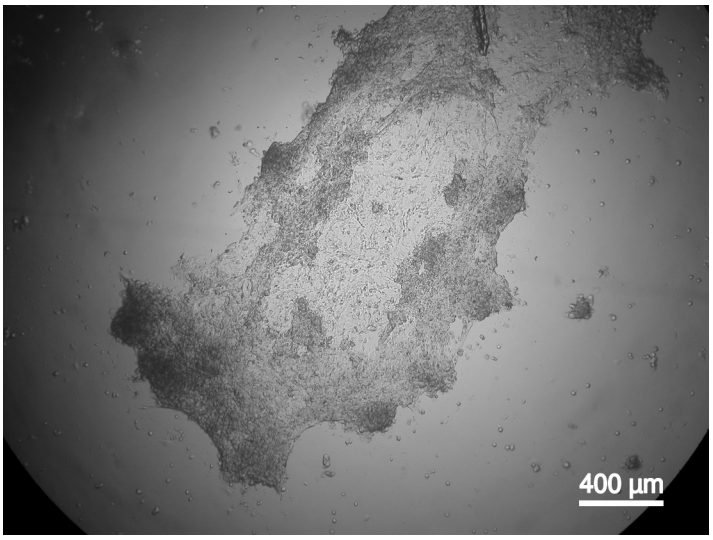

Figure 3.40: cell sheet cultured on gelatine at 31°C for 72 hours, 180 minutes after the transfer start. The image was acquired by using the optical microscope.

gelatine presented a much lower stiffness, further reduced at higher temperature, as shown by the compression test (section 2.3.1). This stiffness decrease, associated with a lower concentration of "protein" inside the swollen gel, greatly reduced cell adhesion, as deduced by the round shape of the cells. Gels incubated at 31 °C showed a much better behavior, with less swelling and, therefore, good cell spreading in the first 24 hours, if compared with samples cultured at 32 °C and 34 °C.

Initially the cell culture on dry surface (section 3.4.2, step 2) seemed to be a promising technique, since cells were cultured on a substrate constituted by 85% of cell culture medium, in an incubator with 100% RH: unfortunately it was not possible to keep cells alive for more than 24 hours without medium additions. Adding medium 24 hours after incubation started, led to an intermediate condition: after 24 more hours of incubation (figure 3.17), cells were able to spread again, but with an unusual shape, probably due to some de-

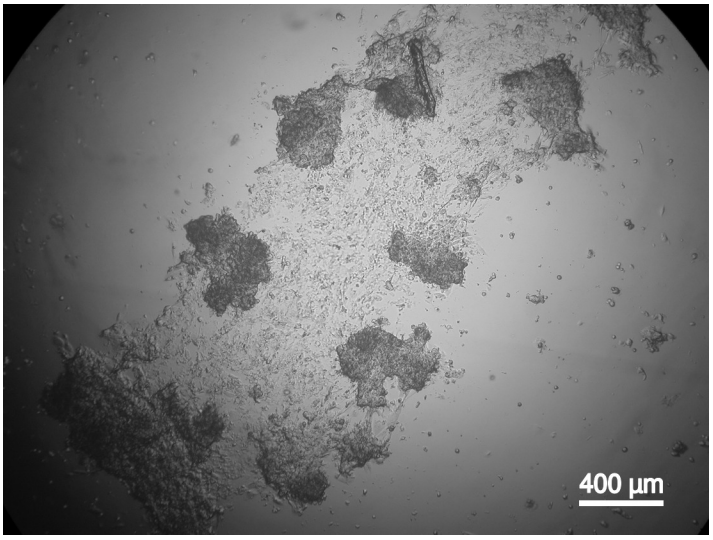

Figure 3.41: cell sheet cultured on gelatine at 31°C for 72 hours, 24 hours after the transfer start. Clusters caused by small detachments and shrinkage on boundaries are evident. The image was acquired by using the optical microscope.

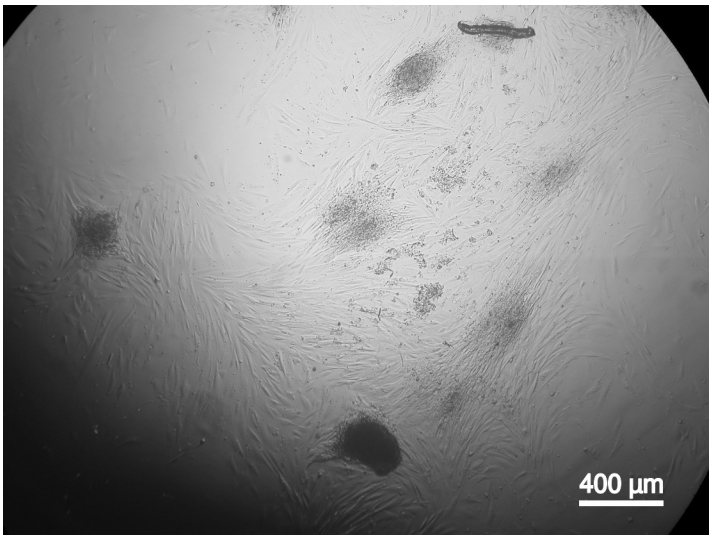

Figure 3.42: cell sheet cultured on gelatine at 31°C for 72 hours, 48 hours after the transfer start. Cell clusters are disappearing due to cell migration to empty surface. The image was acquired by using the optical microscope.

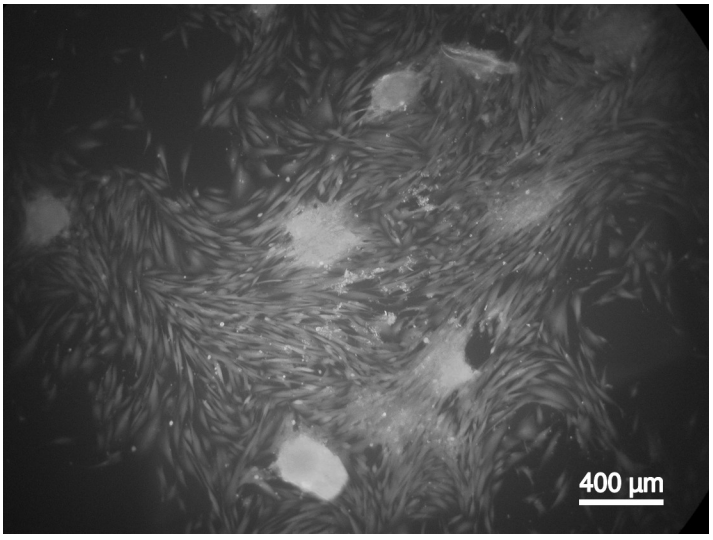

Figure 3.43: cell sheet cultured on gelatine at 31°C for 72 hours, 48 hours after the transfer start. Living cells were stained with Calcein. The image was acquired by using the fluorescence microscope.

gree of migration inside the gel during the drying. However, this test proved that cells were still alive, even if round in shape, after 24 hours on the dry gel surface.

In case of cells cultured on an uncross-linked gelatine, the adding of the right amount of medium on the surface greatly affected the cell spreading. As shown in section 3.4.2 step 3, cells unable to spread on the surface if completely covered by the medium, spread perfectly when the medium periodically added to the samples was barely sufficient to wet the surface. The ideal quantity of medium was carefully added to the culture to reach an ideal dry surface just before the next addition, i.e. avoiding the excessive drying showed in figure 3.15 and 3.16. An excessively dry surface can be easily detected at the phase contrast microscope, since, in these conditions, cells appear as blisters protruding from the surface; on the contrary, whet a correct hydration is reached, a smooth surface is visible.

As easily predictable, the seeding density is a fundamental parameter for reaching confluence in low temperature cell culture. The results shown in section 3.4.2 step 4, underlined the importance not to exceed a threshold value identified as the optimal seeding density. Exceeding the optimal seeding density brings to an irreversible cell sheet detachment and to a successive contraction, which transform it into a huge cell cluster. Fibroblast contraction is natural, but since it brings about the formation of scar tissue it should be avoided (using the right seeding density) [64], in order to reach the best conditions for the culture and the cell sheet transferring.

It is known that fibroblasts can produce proteolytic enzymes able to cleave collagen and, therefore, gelatine. This degradation allows them to migrate across the surface and remodel the extracellular matrix and the gelatine hydrogel [65, 66, 67, 68]. As shown in section 3.4.4, cells cultured on gelatine hydrogels at 31 °C for 3 weeks were able to migrate into the gelatine matrix forming a 3D network. By exploiting this cell behavior would be possible to produce 3D structures made of cells and gelatine, while retaining the ability to remove the scaffold (i.e., gelatine) by melting, once cells have produced a

consistent extracellular matrix. This feature would be even more interesting considering how "traditional" cell-sheet engineering solved the problem of obtaining 3D structures: by stacking cell layers [63, 51, 69], which implies low interpenetration between layers. It is also interesting to notice the different orientations of cells in the 3D structure (figure 3.31), similarly to what happens in the connective tissue. However, culturing cells into thick gelatine scaffolds present some problems: firstly the diffusion of nutrients and wastes, which limits the depth of cell migration, secondly, the reduced proliferation rate typical of such a low culture temperature [56, 62]. Multi-step seeding would be probably needed to obtain higher cell density in the matrix, to avoid the cell sheet contraction shown in high seeding density (section 3.4.2, step 4).

The main preoccupation given by these experimental procedures came largely from the possibility to damage cells with the permanence at reduced temperature for a relatively long time. Thompson et al. [57] studied the effect of temperature on the longevity of MRC-5 human fibroblasts as number of passages before senescence. A passage is roughly the number of duplications a cell had, so it is an indicator of how old the cell is. In that work, Thompson showed an irreversible diminution of cell longevity when culture temperature is higher than 37 °C (40 °C). This reduction was probably induced from errors in the protein synthesis related to the temperature increase. On the contrary, in the case of culture at lower temperature, a different behavior was observed: cells maintained at 32 °C showed a reduced proliferation, and a reduced mitotic activity. However, moving back the cells to 37 °C, their proliferation rate was recovered and they reached the same number of passages as cells kept at 37 °C for the whole culture process [57]. Similar results were obtained by Enniga et al.: they showed a decrease in the fibroblast proliferation rate at 30 °C, with a sharp decrease after 25 hours of culturing. They also indicated that mitosis was stopped in the G_1 phase (gap 1 phase). However, after reverting to 37 °C, cells started to proliferate again, recovering their normal state [56, 62].

The main aim of this thesis was to develop a new material for the production of cell sheets, able to transport living cells into the body and degrade

/ dissolve in a few days. In section 3.4.6 it was demonstrated the possibility to transfer fibroblast cell sheets from the uncross-linked gelatine substrate, on which they were cultured, to a target surface (i.e., a polystyrene TCP used as a model). Once transfer ended, gelatine melted and ensured an easy removal. Finally one should not underestimate that staining with calcein made it possible to show the cell viability on the transferred cell sheet.

Chapter 4

Films for bioactive molecule release

Gelatine gels showed interesting *in-vivo* dissolution-degradation time, when loaded with plasma derivatives (see chapter 5), and the consequent possibility to use them as depot, to release proteins *in-situ* for a time ranging from hours to weeks. Therefore, in collaboration with the department of Oncology, Biology and Genetics, University of Genoa, with the Ludwig Boltzmann Institute for Experimental and Clinic Traumatology of Vienna, and the National Cancer Research Institute of Genoa, we decided to test the *in-vivo* release of pro-angiogenic factors from gelatine hydrogels, in a model of ischemic fascio-cutaneous flap.

4.1 Introduction to skin flaps

Skin flaps are routinely used by plastic surgeons for the functional and cosmetic repair of wounds and defects left behind after traumatic injuries and malignancy removals [70]. A fascio-cutaneous flap consists of three layered vascularized tissues: reticular dermis, hypodermis and the underlying fascia. A flap grafting failure can occur because of surgery complications such as in-

fections, denervations, inadequate fluid drainage (hematoma/seroma). Flap survival mainly depends on the blood supply, either non specifically (random flap) or specifically (pedicle flap) provided through vessels of the dermal and subdermal plexus [71]. A lack of oxygen and nutrients especially in the distal part of the flap often results in a partial necrosis with devastating results for the patient. The complexity of events associated with ischemia, such as production of reactive oxygen species, neutrophil influx, depletion of NO and apoptosis have directed the counteracting therapy towards pharmacological approaches, including use of antioxidants [72], vasodilators [73], and anti-inflammatory drugs [74]. The recent concept of therapeutic angiogenesis has emerged as another attractive approach to enhance blood supply and perfusion in compromised flap tissues. Therapeutic angiogenesis is defined as the administration of pro-angiogenic factors in order to convert an ischemic tissue into a viable and functional tissue through the maintenance of existing vasculature or by stimulating the formation of new vessels [75, 76]. Local and systemic application of angiogenic proteins, such as PDGF [77], basic FGF [78] and VEGF [79] have been demonstrated to improve the survival of compromised flaps, while fibrin sealants have been investigated for their hemostatic and adhesive properties and for the ability to locally deliver and sustainably release growth factors [80, 81], thus providing an important role as a biomatrix in pursuing the angiogenic effect.

In line with the current regenerative medicine trend, we recently demonstrated that Amniotic Fluid Stem Cells (AFSC) can mediate the tissue repair by recruiting host reparative cells [82] and that their secreted factors, contained in conditioned media, can be responsible for a cell paracrine effect on vessel growth [83]. We strongly believe that the increased blood flux achieved by the administration of the AFSC soluble factors is a keystone of the whole regenerative process, not only because of the increased nutrients perfusion, but especially for the establishment of an “activated” regeneration niche. In the present study, we embedded AFSC Conditioned Media (ACM) into a 15% gelatin-membrane to topically deliver angiogenic growth factors and cytokines

in a rat model of ischemic full-thick skin flap elevated in the epigastric region. We studied the vascular perfusion rate, the vessel distribution and the survival of ACM/membrane- and only membrane-treated flaps and demonstrated an ACM-mediated recruitment of endothelial-like progenitors occurring only in the subcutaneous tissues of ACM/membrane-treated flaps. We want to underline the benefits of a cell free therapy with no needs to differentiate uncommitted stem cells into a specialized tissue both in terms of avoiding allo-rejection and vi potential tumorigenic risks for the patient, and in terms of cost and operating time savings.

4.2 Material and Methods

Cell Culture, Conditioned Media and Membrane Fabrication Human AFSC were supplied by the Cytogenetic Laboratory of Galliera Hospital (Genoa, Italy) as normal karyotype amniocentesis samples from 15-17 weeks pregnant women, after obtaining written informed consent. AFSC were isolated as previously described [84, 83] Briefly, back-up cultures from a total of 20 donors were expanded in αMEM medium (Gibco, Milan, Italy) containing 15% ES-FBS, 1% glutamine and 1% penicillin/streptomycin (Gibco), supplemented with 18% Chang B and 2% Chang C (Irvine Scientific, Santa Ana, CA, USA), at 37°C within a 5% CO_2 atmosphere. Once confluent, cells were pooled, labeled with CD117 MicroBeads (Milteyi Biotec, Bergisch Gladbach. Germany) and immunoselected based on cKit expression on a Mini-MACS apparatus (Miltenyi Biotec) following manifacturer instructions. Selected cells were plated at clonal density ($10/cm^2$) and about 7-10 days after seeding, clones were isolated and replated and passaged few times in dishes with a larger diameter. Two AFSC clonal lines, from the same primary culture and showing a similar phenotype, were arbitrarily used at a culture passage between passages 6 and 10 in our experiments. Cultured cells were tested for the expression of lineage specific surface e molecules in a Cyan ADP Cytofluorimeter (Beckman Coulter) and the absence of hematopoietic markers together with the presence

of mesenchymal markers were confirmed (Supplementary Figure 1). Murine monoclonal anti-human antibodies used for this study were: anti-CD117 (cKit) PE-conjugated (clone A3C6E2, Miltenyi Biotec), anti-CD45 (TA218/12, IgM), anti-CD31 (89D3, Ig2a) and anti-CD44 (T61/12, IgG1), kindly provided by M. R. Zocchi (San Raffaele Scientific Institute), anti-CD90 (clone Thy-1A1, IgG2a from R and D System Inc.), anti-CD146 (P1H12, IgG1 from BD PharMingen), anti-SH2 (CD105, IgG1) and anti-SH3 (CD73, IgG2b) producing hybridoma, purchased from the American Type Culture Collection (ATCC, Manassas, VA), followed by the addition of anti-isotype specific goat anti-mouse (GAM) antisera (Southern Biotechnology) conjugated with phycoerythrin (PE) (Invitrogen). Control samples were stained with isotype-matched irrelevant mAb (Becton Dickinson) followed by anti-isotype specific GAM-PE. To obtain conditioned media, eighty % confluent AFSC were plenty washed in PBS and incubated in serum free αMEM for 16 hours [83]. AFSC conditioned media (ACM) were collected and stored in 5 milliliter aliquots equivalent to the medium conditioned by 4 X 106 AFSC. This concentration (1 mL medium conditioned by 800 000 AFSC during a 16 hour culture) was used for all in vivo studies. Lyophilized gelatine film membranes (5 x 5 cm and 1.5 mm thick) were prepared by casting from a solution of 15% by wt. type A gelatine (from porcine skin, Sigma Aldrich, Milan, Italy) in water as follows. Briefly, a gelatine/water solution was prepared under gentle stirring at the temperature of 50°C for 1 hour, then cast into a polystyrene Petri dish kept at 23°C for 24 hours. Afterwards, the cast membrane was freeze-dried at -80°C for 72 hours. Each membrane was regenerated before further use by its soaking with 5 ml of ACM or saline as control (CTRL). Such a membrane is easy to handle, resorbable within 24-48 h in vivo, it can entrap and slowly release proteins and finally it is a useful delivering substrate suitable for the fascio-cutaneous flap experiment protocol.

Fascio-cutaneous Flap Model and Treatment All experiments performed on animals were approved by the local legislative committee in Vienna to the

Ludwig Boltzmann Institute and all experimental procedures were consistent with the Guide for the Care and Use of Laboratory Animals of the National Institute of Health (Publication No. 85–23, revised 1996). Ten (five per group) male Sprague Dawley rats weighing 300–350 g (Harlan– Winkelmann, Borchen, Germany) were used to recreate the previously established epigastric flap model [85]. The rats were anaesthetized with ketamine (100mg/kg BW) and xylazine (10mg/kg BW). Briefly, abdominal skin of rats was depilated and a squared fascio-cutaneous flap (approximately 7 X 7 cm) was elevated in a cranial to caudal direction so that the flap was well detached from the abdominal muscular layer. Conditioned medium containing (ACM) or non containing (control - CTRL) membranes were carefully positioned on the muscular layer (figure 4.1C). To render the flap half ischemic, the left or the right (according to a randomization protocol) inferior epigastric neurovascular bundle was ligated before the split of the epigastric pedicle into a medial and a lateral branch. To avoid neighboring anastomoses, the entire flap was isolated from the surrounding tissues except for the contralateral inferior epigastric neurovascular pedicle that remained pervious and perfused the rest of the flap. The flap was then sutured back to its anatomical location. Animals were followed-up for 1 week, afterwards they were sacrificed to take samples for Phistological and biological studies.

Flap Perfusion and Survival These two parameters were evaluated by two independent observers on three different vertical zones (Vital, Border, Ischemic; 2.5 X 7 cm/each) of the flap (figure 4.1D) at different times: before operation (Pre-OP), immediately after operation (Post-OP) and 1, 2, 3 and 7 days after surgery. To evaluate flap perfusion, we used the LDI (Moor Instruments Ltd., Devon, UK) system with a low-intensity (2 mW) laser light beam (wavelength 632.8 nm). The skin surface of supine positioned, anaesthetized rats was scanned at a standardized working distance of 20 cm. Blood flow through the flap was documented as 2D color-coded image (setting of scan modus 10 ms/pixel with resolution at 256X256 pixels). Results are expressed

as fold increase/decrease of perfusion units (PU) respect to the pre-operative baseline (=1), through the time and for each sector of the flap. The flap survival, as percentage (%) of necrosis, was calculated dividing the flap necrotic area to the entire flap area, multiplied by 100. Flap areas were photo-imaged by Moor^{TM} at standardized conditions of light, distance, and magnification, and analyzed with ImageJ 1.44 software (National Institutes of Health, Bethesda, Maryland, US). To be considered necrotic, an area should have macroscopically visible brown- to black-colored tissue accompanied by loss of elasticity. As a quality control, areas identified as necrotic were checked for having a Laser Doppler pixel distribution curves ranging between 50-70 over a scale 0-255.

Histological Analysis Full-thickness skin samples, proximal to the necrotic area of flaps, were excised from each animal after euthanasia on day 7 and over night fixed in buffered neutral formalin 10% (Sigma), dehydrated in ethanol 70% (2 h), ethanol 80% (2 h), ethanol 96% (2 h), absolute ethanol (2 h), cleared in xylol and embedded in paraffin into an upright position. Fascio-cutaneous cross sections were stained with Mallory's trichrome (Bioptica, Milan, Italy) in order to evaluate the inflammatory infiltrates (masses of red nuclei), the vascularization of subcutaneous plexus (red blood cells in gold yellow), the thickness of superficial necrotic layers (orange - red) and the organization of cutaneous structures (glands in pale pink and collagen fibers in deep blue). Density of subdermal plexus vessels with a diameter ≥ 40 μm vi was determined on five random fields (400 X magnification), on six 7 mm thick-cross sections for each sample. Thickness of cutaneous dead layers was measured along 3mm of each section using the Axiovision Rel 4.4 software and distribution curves were generated for each group of treatment.

Recruitment Studies and Progenitors Isolation Recruitment studies and progenitor isolation were performed on 10 rats. To study the recruitment of progenitor cells into the injured/repaired site, we excised the piece of flap (2 X 1 cm) showed in figure 4.1E. Briefly, we considered a square delimited by

the medial line of the whole flap area and the outlining border of the necrotic area. This squared piece corresponds to the healing region of the flap. In fact, since after the ligation of one epigastric bundle just half flap is perfused, the medial line can be considered the "growth plate" of new vessels that from a pre-existing vasculature move toward an ischemic region. That full-thickness skin piece was then sliced according to depth [86]. The upper part (from the surface to a 0.15-0.20 mm depth) contained the epidermis and the papillary dermis and was discarded. The rest of the skin, corresponding to the reticular dermis, hypodermis and fascia, being the most vascularised part of the skin, was used in our studies to isolate and identify endothelial progenitors. Samples were minced, washed in HBSS/30 mM HEPES (Euroclone, Milan, Italy) plus penicillin and streptomycin, digested in 0.25% trypsin (Gibco) and 200 U/mL type 2 Collagenase (Biochrom, AG Berlin, Germany) for 60 minutes in 37°C water bath and finally passed through a 70 μm nylon mesh to obtain a single cell suspension. Cells were centrifuged at 300 X g and the lipid phase was removed from the top and discarded. Freshly isolated cells were either analyzed with a Cyan ADP cytofluorimeter (Beckman-Coulter, Brea CA, USA) for the presence of different cell surface antigen markers or plated at a density of 8,000 cells/cm^2 onto fibronectin-coated Petri dishes (BD Biosciences, Erembodegem, Belgium). This pre-plating step was introduced to separate cells of the stromal-vascular fraction (SVF) from the less adherent endothelial progenitors. Forty eight hours after plating, nonadherent suspended cells were collected and re-plated (25 cells/cm^2) onto fibronectin-coated plates in order to assess the presence of clonogenic progenitors [87]. We chose a fibronectin coating in order to provide the endothelial-lineage cells with a matrix suitable for their attachment and expansion. Medium (DMEM/F12_10% FBS, without any supplemental Growth Factors) was changed every three days. Seven days after the replating, colonies were fixed in 10% formalin and stained for the specific endothelial marker Von Willebrand Factors (Rabbit polyclonal anti-vWF by DAKO, Glostrup, Denmark and TRITC-conjugated goat anti-rabbit IgG by Jackson Immunoresearch Labs, Baltimore Pike West Grove, PA, USA).

Suppliers Antibodies used for the cytofluorimetric analysis were: APC-conjugated anti-CD31 (clone 390), PE-conjugated anti-CD34 (clone RAM34) by E Bioscience, San Diego, CA, USA, and PE-conjugated anti-Flk1/VEGFR2 (clone Avas 12a1) by BD PharMingen San Diego, CA, USA. Control samples were stained with isotype-matched irrelevant mAb. Data were analyzed using the Summit 4.3.1 computer program and are reported as Log fluorescence intensity vs. number of cells.

Statistical Analysis All values are expressed as mean ± standard error. Statistical differences between groups were assessed by the use of unpaired t-test and Mann Whitney U test. We considered a p-value < 0.05 to be significant.

4.3 Results

Vascularization of flap sectors Blood perfusion through the flap was evaluated at LDI by measuring the perfusion units (PU) average of each sector and was expressed as fold increase/decrease respect to the preoperative baseline assumed to be equal to 1 (figure 4.2B). As a confirmation of the correctly executed ligation of the epigastric neurovascular bundle, in the immediate Post-OP the Vital zone of the flap was perfused as before the operation, while in the Border zone and even more in the Ischemic zone the perfusion was strongly decreased. In the Vital zone the perfusion was doubled starting from Day 1 and remained steady through the whole week without significant differences between the control and the treated animal groups. This increased perfusion in the zone of the flap vascularized by the not ligated artery (Vital zone) must be considered compensative of the absence of vascularization in the flap ischemic counterpart. In the Border zone a similar hyper-reaction occurred at Day 1, but the increasing trend of the perfusion was mantained through the week only in the ACM animal group . At Day 7 the Vital and the Border parts of the CTRL-treated flaps showed a reduced hyper-perfusion effect, while the

same parts of the ACM-treated flaps continued to show an increased perfusion effect. We conclude that the observed effect was treatment-dependent rather than a physiological response of the body consequent to the ongoing injury. In the Ischemic zone, the CTRL membrane never recovered the initial perfusion (baseline level), while in the same ACM- treated zone the perfusion level at Day 7 was 50% higher than the initial baseline. We concluded that, although the simple injury (ligation of the epigastric bundle) triggered an angiogenic response, this was not sufficient to re-vascularize an ischemic area. On the contrary, the ACM treatment mediated the growth and the sprouting of new vessels toward the ischemic regions.

Necrosis development through the flap We measured the necrotic areas developed through the flap and calculated the percentage (%) of necrosis to the entire flap area. Necrosis started to be evident in the ischemic (ligated) part at Day 1 for the flaps treated with the CTRL membrane and at Day 2 for the ACM-treated flaps (figure 4.3). Once started, necrosis spread through the flap toward the midline and the CTRL membrane failed to stop its development. The survival of the flap is linked to the blood supply and, looking at the perfusion data (figure 4.2) of the ischemic zone, one can notice that in the CTRL group the perfusion increased very slowly during the week, never getting to the baseline. On the contrary, in the ACM group the ischemic zone suffered a less severe blood supply deficiency during the first 3 days post surgery and recovered a complete perfusion at Re Day 7 (figure 4.2). Indeed, in the CTRL group, where the ischemic zone was never recovered, the necrosis % was progressively increasing, while in the ACM group, where vessels finally crossed the ischemic part, at Day 7 the necrosis % was significantly lower (figure 4.3).

Histological Analysis of cutaneous and subcutaneous structures We excised full-thickness skin samples proximally to the necrotic area of flaps. Looking at the cutaneous structures of the CTRL group (figure 4.4A, upper right panel), it is of notice the thickness of the dead upper epidermal

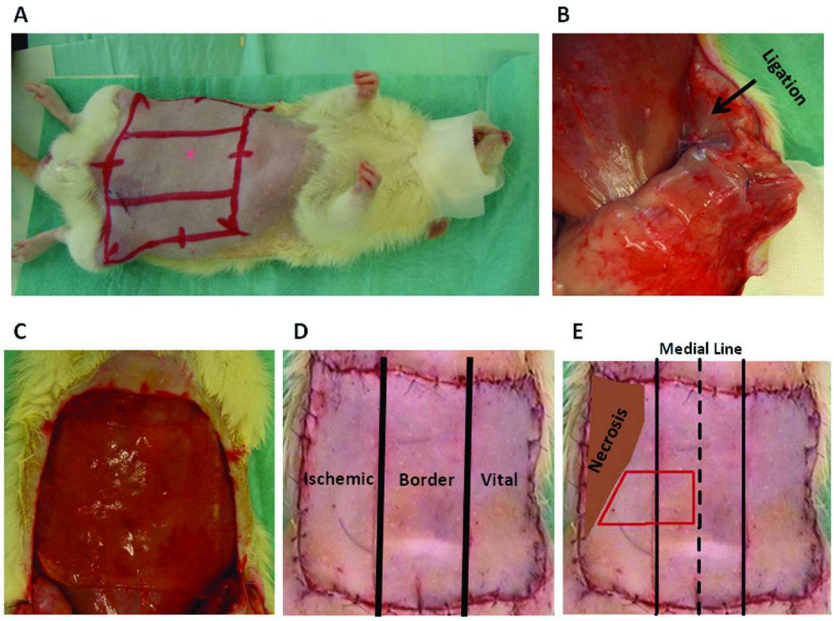

Figure 4.1: Experimental Procedure: Most important passages of the experimental procedure. (A) The rat abdomen is depilated and the flap perimeter (7 X 7 cm) is outlined. (B) The epigastric bundle is ligated. (C) The membrane is positioned under the elevated skin flap; (D) Flaps are sutured back and divided into the three sectors (Ischemic, Border, Vital), based on the proximity to the ligated bundle. (E) The red line indicates the flap area excised after 7days and considered for the recruitment studies and the progenitor isolation;

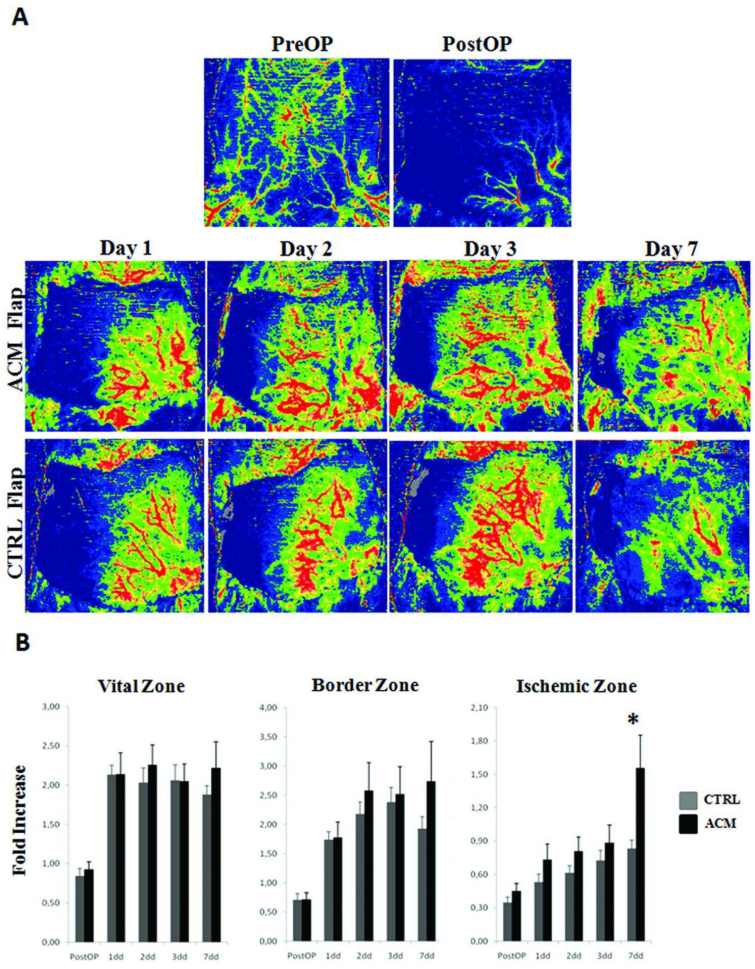

Figure 4.2: Flap Perfusion: (A) Laser Doppler Imaging of flaps before (PreOP), immediately after the Operation (PostOP) and at different times after ligation of the epigastric bundle for the ACM group (upper panel) and the CTRL group (bottom panel); (B) Perfusion is measured as fold increase/decrease of the perfusion respect to the Pre-operative baseline (assumed to be =1) at different times after ligation of the epigastric bundle and for each sector of the flap. *p-value < 0.05

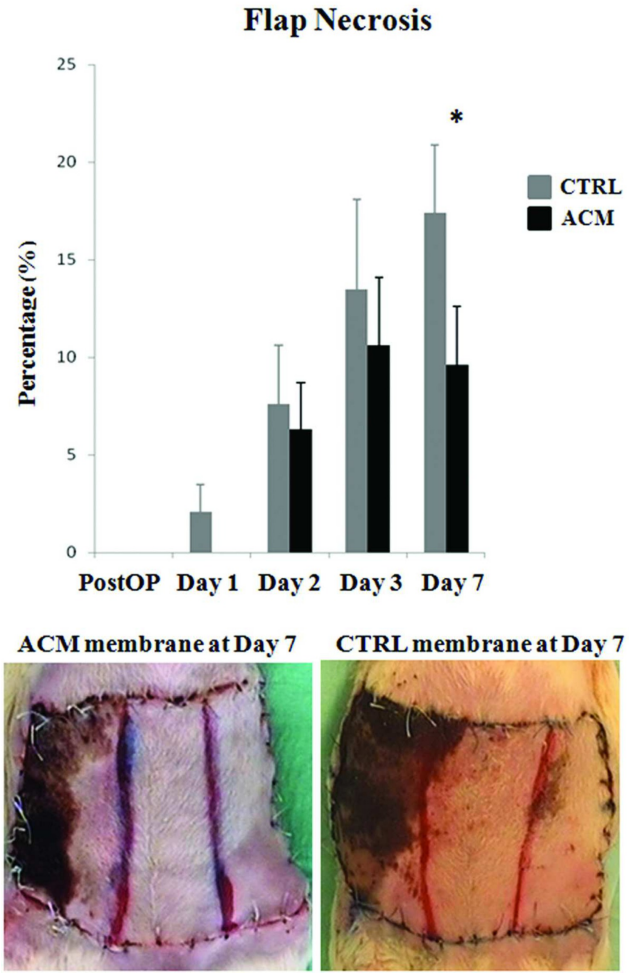

Figure 4.3: Necrosis development: Histograms represent the percentage of developed necrosis throughout the whole flap area immediately after the operation (PostOP) and at different times after ligation of the epigastric bundle. Photos represent a macroscopic view of the ACM and CTRL-treated flap at day 7 post surgery . * p-value < 0.05

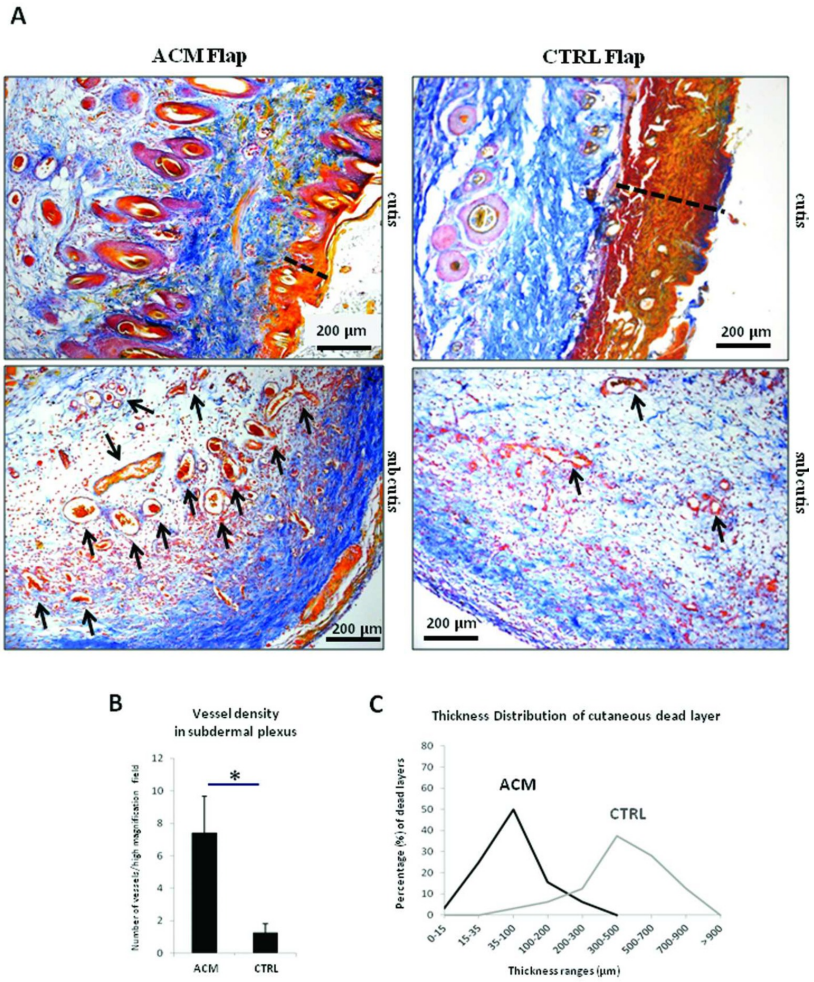

Figure 4.4: Histological analysis: (A) Histology of cutaneous (upper panels) and subcutaneous (lower panels) tissues of ACM-treated (right panels) and CTRL-treated (left panels) flaps. Mallory's trichrome staining. Dashed lines indicate thickness of the superficial necrotic layer. Arrows point to vessels of the subdermal plexus. Scale Bar 200μm. Photos by an Axiovert 200M microscope (Zeiss). (B) Density of subdermal vessels is indicated in histograms. (C) Distribution curves of cutaneous dead layer thickness (black curve for ACM group, grey curve for the CTRL group). * p-value < 0.01

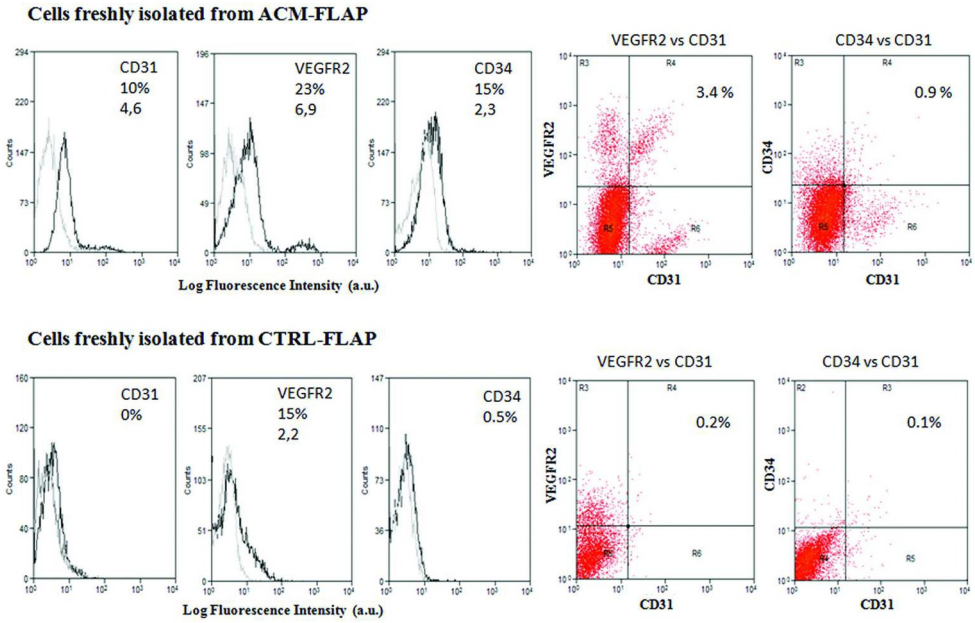

Figure 4.5: Vascular Progenitor Recruitment: Cytofluorimetric analysis of cells extracted from the ACM-treated (upper panel) and the CTRL-treated (lower panel) flaps. Histograms on the left show single staining analysis for the markers CD31, VEGFR2, CD34 (grey histograms are the isotype-matched mAb used as control). Dot charts on the right show double staining analysis for CD31/VEGFR2 and CD31/CD34 positive cells. Percentage of positive cells and mean fluorescence intensity are shown as well. Shown results are representative of independent determinations performed on cells recovered from each animal. Data analysis with Summit 4.3.1 software.

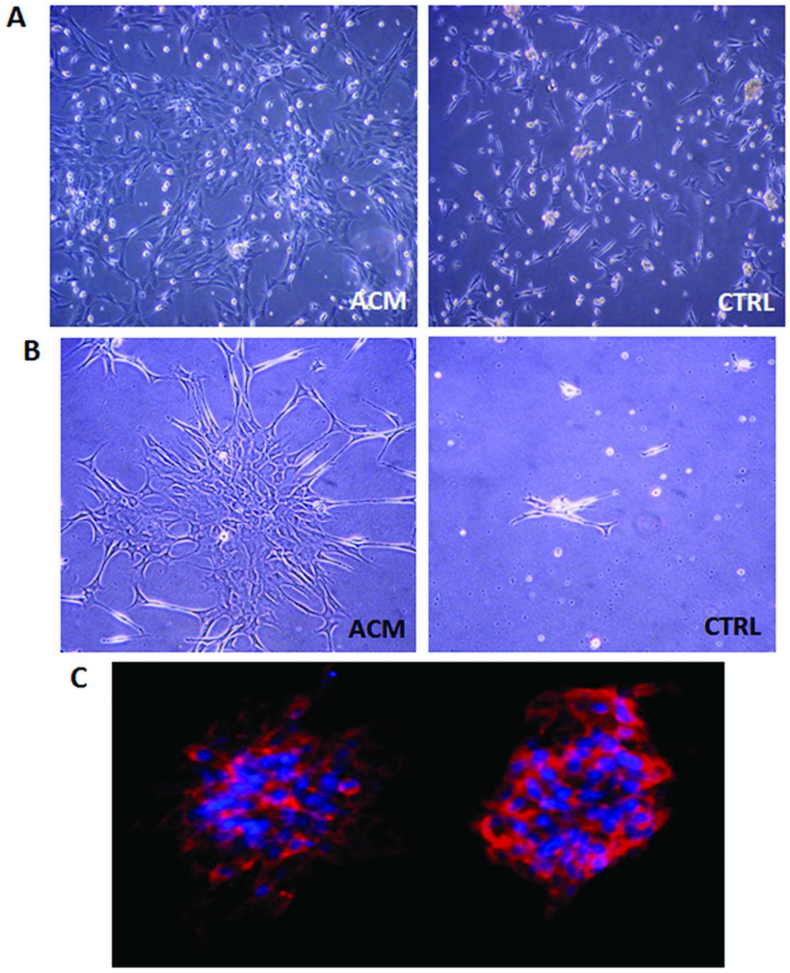

Figure 4.6: Isolation of EPCs: (A) Cells extracted from ACM and CTRL-treated flaps after 48 hours of culture (100 X magnification); (B) CFU formed after plating the floating fraction at a clonogenic density (200 X magnification); (C) vWF-staining of two different CFU obtained from cells extracted from the ACM-treated flaps (200 X magnification). Photos by an Axiovert 200M microscope (Zeiss).

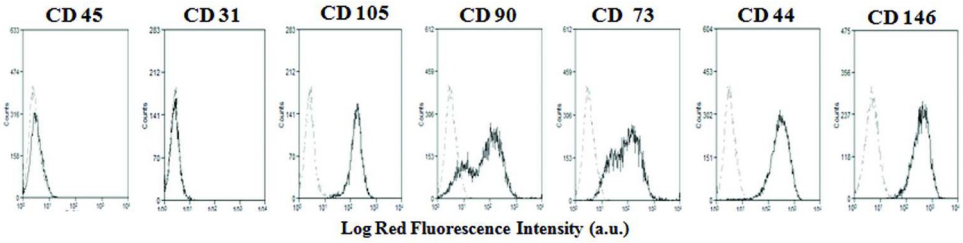

Figure 4.7: Human AFSC Cytofluorimetric Characterization: Surface expression of the indicated molecules. Human AFSCs were stained with mAbs to different markers (black histograms). In each panel it is shown (grey histogram) the isotype matched mAb used as control. Results are expressed as Log fluorescence intensity arbitrary units (a.u.) vs number of cells. Data analysis with Summit 4.3.1 software.

layer (orange), the disorganization of the collagen fibers (blue) in the papillary layer and the dermal glands (pale pink) that appears less numerous and atrophied. Instead, the ACM-treated group (figure 4.4A, upper left panel), showed some detached dead *stratum corneum*, a normal epithelialization of the *stratum spinosum* and *basale*, and a correct arrangement of the collagen fibers and glands in the underlying dermis. In the subcutaneous tissues (figure 4.4A, lower panel) where hypoderm and underlying fascia are visible, the vessel density was about five folds increased in the ACM group respect to the CTRL group (figure 4.4B), as well as the presence of inflammatory infiltrates. The high vascularization, histologically detected in the ACM-treated subcutis, well explain the survival of the upper structures of the skin. Thickness distribution curves of dead cutaneous layers (figure 4.4C) are right side-located in the CTRL group because necrotic layers are thicker in not- treated rats, ranging from 300 to 700 μm. Instead, necrotic layers of ACM group have a distribution curve averaged on 35-100 μm (50% of layers).

Recruitment of endothelial progenitors The flap area we chose for these studies is showed in figure 4.1E and described in Materials and Methods.

Subcutaneous tissues were excised from each animal and digested to obtain a single cell suspension (cells freshly isolated). Cells suspensions were analyzed at the cytofluorimeter for the presence of endothelial cell (EC) and endothelial progenitor cell (EPC) markers [88, 89, 90], such as CD31, CD34 and Flk1 (VEGFR2) (figure 4.5). Cells isolated from ACM-treated flaps included about 10% of CD31, 23% of VEGFR2 and 15% of CD34 positive cells. Furthermore, a double positive population for CD31/CD34 (0.9% of the total amount of extracted cells) and a double positive population for CD31/VEGFR2 (3.4% of the total) were isolated from the ACM group.

While ACM contains soluble factors capable to chemoattract circulating progenitors and mediate the blood vessels growth, the not treated ischemia alone was not able to recruits EPCs in the subcutaneous tissues of the flap. In fact, cells isolated from the flaps of the CTRL group were negative for the markers CD31 and CD34, and only 15% of them expressed the VEGFR2. When we searched for double positive cells, only 0.2% of CD31+/VEGFR2+ cells and 0.1% of CD31+/CD34+ cells were observed.

Isolation of endothelial progenitors Cells derived from the subcutaneous tissues of ischemic flaps were cultured with a two steps procedure. First cells were pre-plated onto fibronectin-coated dishes for 48 h (figure 4.6A) in order to separate adherent from floating cells. Adherent cells extracted from the CTRL group grew slowly, while cells from ACM group got the 70% of confluence in 48 h and presented both polygonal and spindle morphology (figure 4.6A). The nonadherent cells were re-plated at a clonogenic density (25 cells/cm^2) onto fibronectin-coated dishes. After 7 days of culture colonies were analyzed (figure 4.6B). From ACM group we isolated several colonies (1.7 er CFU/cm^2) with the typical cobblestone morphology surrounded by radiating thin cells and characterized by a central cluster of rounded cells. These clusters were found positive for the vWF (figure 4.6C), confirming their endothelial nature. We did not obtain colonies from the CTRL group in agreement with the observed absence of double positive progenitors in the freshly isolated subcutaneous cells

from this animal group.

4.4 Discussion

Ischemia of the operated tissues is a very common and difficult to handle complication of many surgeries. Necrosis of tissues occurs secondary to an early reperfusion injury or a prolonged absence of blood supply. The animal model we chose provides a very serious (half flap-extended and 1 week-protracted) ischemic damage, since the vascularization of the flap is prevented by the chronic epigastric artery ligation and the complete elevation of the whole flap area. Several studies have used angiogenic growth factors [91], in local or systemic administration [92], as recombinant proteins or by gene delivery [93], to pursue a therapeutic angiogenesis of ischemic flaps. We previously demonstrated [83] that the AFSC secretome is responsible for the paracrine vascularizing effect that these cells showed in vivo. We described the conditioned media of human AFSC as a potent cocktail of combined chemokines (such as MCP-1, IL-8, SDF-1α,) and growth factors (such as VEGF, TGFβ), synergically promoting the neovascularization of ischemic tissues. Here we used 5 mL of 16 hour conditioned media (each mL from 800 000 AFSC) for each 25 cm^2 gelatine membrane (secretome from 30 000 AFSC per cm2). This low ACM concentration was demonstrated to be effective in this formulation. The membrane we used, offers a good solid support for the local delivery of the ACM at the injury site. This approach was useful to potentiate [79] and at the same time topically limit the neovascularization, thus avoiding clinical concerns linked to a systemic administration of angiogenic growth factors, such as the targeting of non specific tissues or, on the other hand, the blood diluting effect and the reduced half-life of circulating proteins.

The support membrane that we chose, made of gelatine, i) is a biodegradable, biocompatible and nonimmunogenic product, suitable for many medical applications; ii) its hydrophilic nature enables absorption of ACM; iii) in the adopted formulation it can undergo a gel/sol transition at body tempera-

ture thus releasing proteins in a controlled way. The gelatin membrane alone, soaked with saline, was implanted in rats of the CTRL group, where no recovery of the ischemic sector of the flap occurred. Postnatal growth of new vessels is activated during pathological conditions, such as wound healing, tumorigenesis and tissue ischemia [94]. In our CTRL group the ischemic injury per se triggered a neovascularization, as the compensative hyper-perfusion effect in the Vital and Border zones showed, nevertheless this was not sufficient to re-establish a normo-perfusion in the Ischemic zone within the first week. The initial baseline level of perfusion was never achieved, the subsequent necrosis reached the 18% of the whole flap area with peaks of 23%, and no progenitors were detected (cytofluorimetric analisys) or isolated (CFU analysis) from the ischemic subcutis. The post-injury vascularization can be enhanced by the administration of growth factors and cytokines [76] that recruit EPC into the injury site, thus accelerating the wound healing. In the ACM group, at Day 7, the ischemic area was re-vascularized with a perfusion level 50% higher than the initial baseline and, as a consequence, presented a less developed necrosis respect to the CTRL group. The histology of ACM-treated flaps revealed a thin dead *stratum corneum*, a normal arrangement of the epidermal and dermal structures and a high density of vessels in the subcutaneous tissues. More important, we showed that ACM recruited CD31+/VEGFR2+ and CD31+/CD34+ cells into the ischemic subcutaneous tissues, where growth and sprouting of new vessels occurred. Since subcutaneous tissues contain blood, adipose cells and other derivatives of mesodermal origin, we used a double staining analysis for the quantification of endothelial progenitors from the freshly isolated cell population. In fact, CD31 cannot be considered a specific marker of endothelial cells, since it is expressed also by circulating monocytes [95]. Similarly, CD34 cannot be considered a solely marker of EPC since CD34-positive cells can be abundantly isolated also from the total non-endothelial population within the stromal-vascular fraction (SVF) of adipose tissues [96]. Even the VEGFR2 is not a unique marker for hematovascular lineage cells, since it is expressed also by developing and mature mesoderm

derivatives [97]. We found that out of the 23% VEGFR2 positive cells and the 15% CD34 positive cells extracted from the ACM-treated flap, 3.4% were CD31/VEGFR2 double positive and 0.91% were CD31/CD34 double positive. To confirm the ACM-mediated recruitment of endothelial progenitor cells, we identified vWF-positive cell clones derived from the free floating cell fraction obtained from the digestion of subcutaneous tissues. Given the extraction of a high percentage of CD34 single positive and VEGFR2 single positive cells from subcutaneous tissues of ACM group, together with the isolation of a high proliferative SVF, one could speculate that the ACM also stimulated stem/progenitor cells residing in the subdermal adipose tissue and dermis [98]. Many studies have demonstrated that a variety of growth factors and cytokines are involved in the cutaneous wound healing; IL-6 is necessary for tissue granulation, VEGF for the wound angiogenesis, TGF-β for the reepithelialisation. AFSC conditioned media contain these growth factors [83] together with other soluble factors, such as chemokines (IL-8, MCP-1, SDF-1α) responsible for the migration of inflammatory cells and for the mobilization, homing and incorporation of endothelial progenitors into the vasculature [99]. Again, since AFSC secrete the mentioned growth factors and chemokines, as our and other groups have demonstrated [100, 101, 102, 83, 103, 104][100, 101, 102, 83, 103, 104], we hypothesize that the endogenous repair triggered by the AFSC secretome could involve both the recruitment of EPC and the activation of local niches.

4.5 Conclusions

AFSC conditioned media loaded in a gelatine hydrogel, as a cocktail of "navigation cues and niche signals" [105], are effective, safe, simple and reproducible to formulate, convenient, easy to deliver, being good candidate for a translational treatment that could be: i) in situ-directed; ii) based on the activation of endogenous mechanisms of repair; iii) cell-free, thus avoiding the ex vivo manipulation of autologous or heterologous cells.

Chapter 5

Perspective on anti-adhesion applications

5.1 Introduction

During the water absorption test (section 2.3.4), samples of gelatine gels were prepared with PRP instead of water. Despite similarities in the kinetic of absorption, the resistance of these samples to the temperature was clear, therefore additional test followed in collaboration with the University of Genova. The purpose was to discover the resistance of PRP loaded gelatine gels when surgically implanted *in-vivo*.

5.2 Materials and Methods

Three different gelatine gel samples were compared in order to study the influence of PRP in gelatine hydrogels on the kinetic of *in-vivo* resorption.

Sample 1 was prepared as described in section 2.2.1, step 5, and rehydrated with water.

Also sample 2 was prepared following the same procedure used before, but, instead of using water, it was rehydrated by soaking in PRP for 2 hours at room

temperature on an orbital shaker. The obtained PRP gel was then frozen at -80 °C for at least 16 hours, and freeze-dried again for 15 hours.

Sample 3 was prepared dissolving gelatine powder in PRP at 37 °C, at a 15% concentration, under constant stirring for 1 hour; the solution was then cast into a petri dish and left for 1 hour at room temperature to allow gelation to take place. Successively the hydrogel was frozen at -80 °C, and freeze-dried as already described (section 2.2.1, step 5).

After freeze drying procedure, all the three samples were sterilized by γ-radiation (0.1 Gy) and rehydrated with sterile water.

Gels where successively implanted subcutaneously in six different CD-1 mice, weighing 20 - 25 g. Each mouse was implanted with every all the 3 samples of gelatine previously described (gelatine, PRP-loaded gelatine, and gelatine prepared using PRP instead of water).

The implanted samples were retrieved after 6 hours, 24 hours and 7 days. The resorption of the membranes was evaluated by visual inspection.

5.3 Results and Discussion

Three different samples of gelatine gels, normal and loaded with platelet rich plasma (PRP), were prepared and implanted as described in section 5.2 and compared to study the influence of the PRP on the gelatine gel resorption kinetic *in-vivo*.

Results 6 hours after the implantation, all the gels were still present and in sufficiently good conditions (figure 5.1), no evident degradation occurred.

At the successive check, 24 hours after implantation, some degree of degradation and partial resorption were evident on all the samples (figure 5.2). In the case of the PRP containing hydrogels (2 and 3), corners and surface were smoother, indicating some erosion but no degradation of the "bulk". On the contrary on the pure gelatine gel (1) it was possible to notice cracks passing through the material, and sharp borders, indicating detachment of fragments:

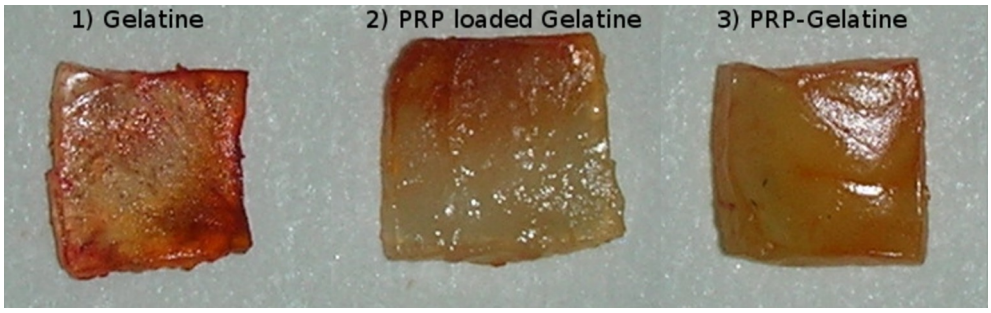

Figure 5.1: Gelatine gel samples after 6 hours from the implantation

Figure 5.2: Gelatine gel samples after 24 hours from the implantation

in this case the degradation was much quicker.

7 days after implantation (figure 5.3) samples 1 and 2 were completely resorbed while sample 3 was still present, indicating a strong interaction between PRP and gelatine specially when they PRP is added to the liquid suspension of gelatine.

Conclusions This preliminary *in-vivo* degradation test allowed to discover the interesting interaction between gelatine and PRP. Appropriately modifying the quantity of PRP used to prepare the membrane it was possible to tailor the *in-vivo* degradation rate.

Gelatine is known to be biodegraded by several enzymes [106]. Therefore an appropriate tuning of the *in-vivo* degradation rate would allow to have a

Figure 5.3: PRP-Gelatine sample after 7 days. Gelatine and "PRP Loaded Gelatine" were completely resorbed

good material to employ as barrier to prevent surgical adhesions, and to stay in place for the time needed. Successively it dissolves and degrades rapidly without hard debrises production.

Chapter 6

Final Remarks

This thesis investigated the production of uncross-linked gelatine hydrogels. Different applications were analyzed in order to exploit the gel-sol transition of these gels.

Gelatine hydrogel based patches, with melting temperature in the range 36 °C - 39 °C, were obtained by solution casting. These gels were dried to allow long (months to years) shelf-life, retaining their distinctive property, that is the ability to be rehydrated forming a hydrogel when needed and to be melted / dissolved at a biologically tolerable temperature. The use of these patches for wound and burn healing would help keeping a moist environment on the injury allowing a better healing process to occur. After the treatment or before any medication, the gelatine patch was demonstrated to be easily removable by washing with warm sterile water, allowing a gentle detachment which preserves the new formed tissue.

In order to culture cell sheets on the gelatine gel substrate, it was developed a novel cell culture protocol. By using this procedure, it was possible to realize confluent fibroblast layers. These layers, cultured on the gelatine surface, were demonstrated to be integrally transferable to different surfaces, without the use of any proteolytic enzyme, simply by exploiting the gelatine melting at body temperature (37 °C). This cell sheet culture substrate, unlike traditional

PNIPAAm grafted TCPs, can be implanted in-vivo where it can degrade / dissolve with no need for removal. Moreover, gelatine hydrogels are inexpensive and much easier to prepare. Additionally, the possibility to obtain 3D cell structures in these hydrogels was demonstrated.

Finally, uncross-linked gelatine hydrogel, loaded with pro-angiogenic factors, were tested in-vivo on a model of ischemic fasciocutaneous flap, demonstrating the possibility to use these bioresorbable hydrogels as depot for situations which require an in-situ rapid release (less than one week). Additionally, gelatine gels loaded with PRP showed an in-vivo degradation rate which suggests their use as separator to avoid surgical adhesions.

Concluding, uncross-linked gelatine hydrogels showed interesting properties and versatility for many biomedical applications. Their main property, the ability to melt at body temperature, is still almost completely unexploited in the medical field. For this reason the work described in this thesis was protected by two patent deposits: EP 11 183 232 “Therapeutic use of gelatin hydrogels with a gel-sol transition at body temperature” and EP 11 183 233 “Medical uses of lyophilized polymeric membranes containing blood derivatives”.

Appendix A

Materials

- Gelatine Powder: provided by Sigma-Aldrich, Gelatin from porcine skin, Type A - G8150 batch n.:059K0019
- Sterile Water: provided by Euroclone(ECM0970D).
- D-PBS without Calcium and Magnesium: provided by Euroclone (ECB4004L).
- Trypsin 0.05% - EDTA 0.02% in PBS: provided by Euroclone (ECB3052D).
- Fibroblasts. Human Fetal Lung Fibroblast Line (MRC-5): provided by Istituto Zooprofilattico Sperimentale della Lombardia e dell'Emilia Romagna "Bruno Ubertini" - Brescia
- The Culture Medium Composition used for cell culture is described in table A.1.
- Phase Contrast and Fluorescence Microscope: Zeiss Axiovert 25
- Optical Microscope: Zeiss Axiotech
- Laser Confocal Microscope: Nikon A1
- Ultra-sonication device: Hielscher UP400S

NAME	SUPPLIER	CAT. N.	CONC.
Minimum Essential Medium	Invitrogen	21090022	
Fetal Bovine Serum (FBS)	Gibco	10106	1:10 FBS:MEM
Sodium Pyruvate	Euroclone	ECM0542D	1 mM
L-Glutamine	Euroclone	ECB3000D	2 mM
Non Essential Amino Acids	Gibco	11140	0.1 mM
Antibiotic Antimycotic	Gibco	15240	1:10000 AA-MEM

Table A.1: MRC-5 Culture Medium Composition

- Mechanical Testing Machine: Instron 4502
- Dynamic Scanning Calorimetry, Mettler DSC 30

Appendix B

Publications

Patents

- EP 11 183 232 - THERAPEUTIC USE OF GELATIN HYDROGELS WITH A GEL-SOL TRANSITION AT BODY TEMPERATURE - Christian Lorandi, Claudio Migliaresi, Antonella Motta, Ranieri Cancedda, Maddalena Mastrogiacomo, Anita Muraglia

- EP 11 183 233 - MEDICAL USES OF LYOPHILIZED POLYMERIC MEMBRANES CONTAINING BLOOD DERIVATIVES - Christian Lorandi, Claudio Migliaresi, Antonella Motta, Ranieri Cancedda, Maddalena Mastrogiacomo, Anita Muraglia

Articles

- Pro-angiogenic soluble factors from Amniotic Fluid Stem Cells mediate the recruitment of endothelial progenitors in a model of ischemic fasciocutaneous flap. - Teodelinda Mirabella, Joachim Hartinger, Christian Lorandi, Chiara Gentili, Martijn van Griensven, and Ranieri Cancedda. Stem Cells and Development. Ahead of print. doi:10.1089/scd.2011.0639.

Congresses

- Natural polymer gels for biomedical uses - Claudio Migliaresi, Michael Floren, Christian Lorandi, Michele Preghenella and Antonella Motta - ACS Meeting, San Diego, March 2012

Acknowledgment

I would like to thank all of them that have contributed to the realization of this work.

First of all, my supervisors Prof. Claudio Migliaresi and Dr. Antonella Motta, for their trust, their support, and for giving me the possibility to focus my work on the argument I preferred.

I acknowledge all the people of the BIOtech group, together with Matteo Traina and Alfredo Casagranda for the work discussions, the help, the support and the happiness, but especially: for putting up with me.

A special thank goes to Giorgina for her invaluable help, support, pizza and patience.

Last but not least, I want thank my parents Sandro and Lucia for their continuous support along these years.

Bibliography

[1] R. Langer and C. Vacanti, "Tissue Engineering," *Science*, vol. 260, no. 5110, pp. 920–926, 1993.

[2] P. Chu and X. Liu, *Biomaterials fabrication and processing handbook*. CRC Press, 2008.

[3] D. Hutmacher, "Scaffold design and fabrication technologies for engineering tissues state of the art and future perspectives," *Journal of Biomaterials Science, Polymer Edition*, vol. 12, no. 1, pp. 107–124, 2001.

[4] J. D. Bronzino, *Tissue engineering of artificial organs*. crc press ed., 2006.

[5] P. Gunatillake, R. Adhikari, and Others, "Biodegradable synthetic polymers for tissue engineering," *Eur Cell Mater*, vol. 5, no. 1, pp. 1–16, 2003.

[6] B. Seal, T. Otero, and A. Panitch, "Polymeric biomaterials for tissue and organ regeneration," *Materials Science and Engineering: R: Reports*, vol. 34, no. 4-5, pp. 147–230, 2001.

[7] D. W. Hutmacher, "Scaffolds in tissue engineering bone and cartilage," *Biomaterials*, vol. 21, pp. 2529–2543, Dec. 2000.

[8] B.-S. Kim and D. J. Mooney, "Development of biocompatible synthetic extracellular matrices for tissue engineering," *Trends in Biotechnology*, vol. 16, pp. 224–230, Dec. 1998.

[9] T. Hadlock, C. Sundback, D. Hunter, M. Cheney, and J. P. Vacanti, "A Polymer Foam Conduit Seeded with Schwann Cells Promotes Guided Peripheral Nerve Regeneration," July 2004.

[10] M. Sokolsky-Papkov, K. Agashi, A. Olaye, K. Shakesheff, and A. J. Domb, "Polymer carriers for drug delivery in tissue engineering.," *Advanced drug delivery reviews*, vol. 59, pp. 187–206, May 2007.

[11] J. S. Temenoff and A. G. Mikos, "Injectable biodegradable materials for orthopedic tissue engineering," *Biomaterials*, vol. 21, pp. 2405–2412, Dec. 2000.

[12] J. Drury and D. Mooney, "Hydrogels for tissue engineering: scaffold design variables and applications," *Biomaterials*, vol. 24, no. 24, pp. 4337–4351, 2003.

[13] F. H. Silver and G. Pins, "Cell growth on collagen: a review of tissue engineering using scaffolds containing extracellular matrix.," *Journal of long-term effects of medical implants*, vol. 2, pp. 67–80, Jan. 1992.

[14] L. Buttafoco, N. G. Kolkman, P. Engbers-Buijtenhuijs, A. A. Poot, P. J. Dijkstra, I. Vermes, and J. Feijen, "Electrospinning of collagen and elastin for tissue engineering applications.," *Biomaterials*, vol. 27, pp. 724–34, Feb. 2006.

[15] T. A. E. Ahmed, E. V. Dare, and M. Hincke, "Fibrin: a versatile scaffold for tissue engineering applications.," *Tissue engineering. Part B, Reviews*, vol. 14, pp. 199–215, June 2008.

[16] Y. Wang, H.-J. Kim, G. Vunjak-Novakovic, and D. L. Kaplan, "Stem cell-based tissue engineering with silk biomaterials.," *Biomaterials*, vol. 27, pp. 6064–82, Dec. 2006.

[17] J. S. Temenoff and A. G. Mikos, "Review: tissue engineering for regeneration of articular cartilage," *Biomaterials*, vol. 21, pp. 431–440, Mar. 2000.

[18] J.-K. Francis Suh and H. W. Matthew, "Application of chitosan-based polysaccharide biomaterials in cartilage tissue engineering: a review," *Biomaterials*, vol. 21, pp. 2589–2598, Dec. 2000.

[19] P. B. Malafaya, G. A. Silva, and R. L. Reis, "Natural-origin polymers as carriers and scaffolds for biomolecules and cell delivery in tissue engineering applications.," *Advanced drug delivery reviews*, vol. 59, pp. 207–33, May 2007.

[20] J. F. Mano and R. L. Reis, "Osteochondral defects: present situation and tissue engineering approaches.," *Journal of tissue engineering and regenerative medicine*, vol. 1, no. 4, pp. 261–73.

[21] A. Mikos, L. McIntire, J. Anderson, and J. Babensee, "Host response to tissue engineered devices.," *Advanced drug delivery reviews*, vol. 33, pp. 111–139, Aug. 1998.

[22] J. M. Anderson, A. Rodriguez, and D. T. Chang, "Foreign body reaction to biomaterials.," *Seminars in immunology*, vol. 20, pp. 86–100, Apr. 2008.

[23] G. B. Ryan and G. Majno, "Acute inflammation. A review.," *The American journal of pathology*, vol. 86, pp. 183–276, Jan. 1977.

[24] D. L. Coleman, R. N. King, and J. D. Andrade, "The foreign body reaction: a chronic inflammatory response.," *Journal of biomedical materials research*, vol. 8, pp. 199–211, Oct. 1974.

[25] Y. Onuki, U. Bhardwaj, F. Papadimitrakopoulos, and D. J. Burgess, "A review of the biocompatibility of implantable devices: current challenges to overcome foreign body response.," *Journal of diabetes science and technology*, vol. 2, pp. 1003–15, Nov. 2008.

[26] J. M. Anderson and J. J. Langone, "Issues and perspectives on the biocompatibility and immunotoxicity evaluation of implanted controlled release systems.," *Journal of controlled release : official journal of the Controlled Release Society*, vol. 57, pp. 107–13, Feb. 1999.

[27] S. Albelda and C. Buck, "Integrins and other cell adhesion molecules," *FASEB J*, vol. 4, pp. 2868–2880, Aug. 1990.

[28] R. O. Hynes and A. D. Lander, "Contact and adhesive specificities in the associations, migrations, and targeting of cells and axons.," *Cell*, vol. 68, pp. 303–22, Jan. 1992.

[29] E. H. J. Danen and A. Sonnenberg, "Integrins in regulation of tissue development and function.," *The Journal of pathology*, vol. 201, pp. 632–41, Dec. 2003.

[30] P. X. Ma, "Biomimetic materials for tissue engineering.," *Advanced drug delivery reviews*, vol. 60, pp. 184–98, Jan. 2008.

[31] C. A. Buck and A. F. Horwitz, "Cell surface receptors for extracellular matrix molecules.," *Annual review of cell biology*, vol. 3, pp. 179–205, Jan. 1987.

[32] R. L. Juliano, "Signal transduction by cell adhesion receptors and the cytoskeleton: functions of integrins, cadherins, selectins, and immunoglobulin-superfamily members.," *Annual review of pharmacology and toxicology*, vol. 42, pp. 283–323, Jan. 2002.

[33] R. Schrieber, H. Gareis, and I. Practice, *Gelatine Handbook*.

[34] V. Ottani, D. Martini, M. Franchi, a. Ruggeri, and M. Raspanti, "Hierarchical structures in fibrillar collagens.," *Micron (Oxford, England : 1993)*, vol. 33, pp. 587–96, Jan. 2002.

[35] R. Chambers, "Basic Collagen Info," *Molecular Cell*, pp. 5–8, 2004.

[36] R. T. Jones, *Gelatin: physical and chemical properties*. London: Pharmaceutical Press, 1989.

[37] F. Podczeck and B. Jones, *Pharmaceutical capsules*. PHARMACEUTICAL PRESS, 2004.

[38] M. Djabourov and P. Papon, "Influence of thermal treatments on the structure and stability of gelatin gels," *Polymer*, vol. 24, pp. 537–542, May 1983.

[39] M. Djabourov, J. Leblond, and P. Papon, "Gelation of aqueous gelatin solutions. I. Structural Investigation," *J. Phys. France*, vol. 49, pp. 319–332, 1988.

[40] F. a. Osorio, E. Bilbao, R. Bustos, and F. Alvarez, "Effects of Concentration, Bloom Degree, and pH on Gelatin Melting and Gelling Temperatures Using Small Amplitude Oscillatory Rheology," *International Journal of Food Properties*, vol. 10, pp. 841–851, Oct. 2007.

[41] H. Takahashi, T. Miyoshi, and K. Boki, "Study on hydrophilic properties of gelatin as a clinical wound dressing. I. Hydrophilic properties of gelatin as a wound dressing," *The Tokushima Journal of Experimental Medicine*, vol. 40, pp. 159–167, Dec. 1993.

[42] Y. Ikada and Y. Tabata, "Protein release from gelatin matrices.," *Advanced drug delivery reviews*, vol. 31, pp. 287–301, May 1998.

[43] M. S. Ponticiello, R. M. Schinagl, S. Kadiyala, and F. P. Barry, "Gelatin-based resorbable sponge as a carrier matrix for human mesenchymal stem

cells in cartilage regeneration therapy.," *Journal of biomedical materials research*, vol. 52, pp. 246–55, Nov. 2000.

[44] C. H. Lee, a. Singla, and Y. Lee, "Biomedical applications of collagen.," *International journal of pharmaceutics*, vol. 221, pp. 1–22, June 2001.

[45] I. J. Haug, K. I. Draget, and O. Smidsrø d, "Physical and rheological properties of fish gelatin compared to mammalian gelatin," *Food Hydrocolloids*, vol. 18, pp. 203–213, Mar. 2004.

[46] C. Michon, G. Cuvelier, P. Relkin, and B. Launay, "Influence of thermal history ont the stability of gelatin gels," *International Journal of Biological Macromolecules*, vol. 20, pp. 259–264, 1997.

[47] S. M. Tosh, A. G. Marangoni, F. Ross Hallett, and I. J. Britt, "Aging dynamics in gelatin gel microstructure," *Food Hydrocolloids*, vol. 17, pp. 503–513, July 2003.

[48] S. Van Vlierberghe, P. Dubruel, and E. Schacht, "Effect of Cryogenic Treatment on the Rheological Properties of Gelatin Hydrogels," *Journal of Bioactive and Compatible Polymers*, vol. 25, pp. 498–512, Aug. 2010.

[49] T. Ushiki, "Collagen fibers, reticular fibers and elastic fibers. A comprehensive understanding from a morphological viewpoint," *Archives of histology and cytology*, 2002.

[50] R. Narayani and K. P. Rao, "Controlled release of anticancer drug methotrexate from biodegradable gelatin microspheres.," *Journal of Microencapsulation*, vol. 11, no. 1, pp. 69–77.

[51] M. Yamato and T. Okano, "Cell sheet engineering," *Materials Today*, vol. 7, no. 5, pp. 42–47, 2004.

[52] T. Shimizu, H. Sekine, J. Yang, Y. Isoi, M. Yamato, A. Kikuchi, E. Kobayashi, and T. Okano, "Polysurgery of cell sheet grafts overcomes

diffusion limits to produce thick, vascularized myocardial tissues.," *The FASEB journal : official publication of the Federation of American Societies for Experimental Biology*, vol. 20, pp. 708–10, Apr. 2006.

[53] Y. Haraguchi, T. Shimizu, and M. Yamato, "Scaffold-free tissue engineering using cell sheet technology," *RSC Adv.*, pp. 2184–2190, 2012.

[54] H. Liang, W. Chang, H. Liang, M. Lee, and H. Sung, "Crosslinking structures of gelatin hydrogels crosslinked with genipin or a water-soluble carbodiimide," *Journal of applied polymer science*, vol. 91, no. 6, pp. 4017–4026, 2004.

[55] N. Matsuda, T. Shimizu, M. Yamato, and T. Okano, "Tissue Engineering Based on Cell Sheet Technology," *Advanced Materials*, vol. 19, pp. 3089–3099, Oct. 2007.

[56] I. C. Enninga, R. T. Groenendijk, a. a. van Zeeland, and J. W. Simons, "Use of low temperature for growth arrest and synchronization of human diploid fibroblasts.," *Mutation research*, vol. 130, pp. 343–52, Oct. 1984.

[57] K. Thompson, "Effect of temperature on the longevity of human fibroblasts in culture," *Experimental Cell Research*, vol. 80, 1973.

[58] M. Abercrombie and J. E. Heaysman, "Observations on the social behaviour of cells in tissue culture," *Experimental Cell Research*, vol. 5, pp. 111–131, Jan. 1953.

[59] R. W. Holley and J. a. Kiernan, ""Contact inhibition" of cell division in 3T3 cells.," *Proceedings of the National Academy of Sciences of the United States of America*, vol. 60, pp. 300–4, May 1968.

[60] M. Sakaguchi, M. Miyazaki, Y. Inoue, T. Tsuji, H. Kouchi, T. Tanaka, H. Yamada, and M. Namba, "Relationship between contact inhibition and intranuclear S100C of normal human fibroblasts.," *The Journal of cell biology*, vol. 149, pp. 1193–206, June 2000.

[61] R. Wieser, "Contact inhibition of growth of human diploid fibroblasts by immobilized plasma membrane glycoproteins.," *The Journal of cell biology*, vol. 103, no. August, pp. 361–367, 1986.

[62] R. Weidemann, A. Ludwig, and G. Kretzmer, "Low temperature cultivation–a step towards process optimisation.," Jan. 1994.

[63] T. Shimizu, M. Yamato, A. Kikuchi, and T. Okano, "Cell sheet engineering for myocardial tissue reconstruction," *Biomaterials*, vol. 24, no. 13, pp. 2309–2316, 2003.

[64] F. Grinnell, "Fibroblasts, myofibroblasts, and wound contraction.," *The Journal of cell biology*, vol. 124, pp. 401–4, Feb. 1994.

[65] P. Billings, J. Habres, and D. Liao, "Human fibroblasts contain a proteolytic activity which is inhibited by the Bowman-Birk protease inhibitor," *Cancer research*, pp. 5539–5543, 1991.

[66] I. M. Clark and T. E. Cawston, "Fragments of human fibroblast collagenase. Purification and characterization.," *The Biochemical journal*, vol. 263, pp. 201–6, Oct. 1989.

[67] E. E. Golds, V. Santer, J. Killackey, and P. J. Roughley, "Mononuclear cell factors stimulate the concomitant secretion of distinct latent proteoglycan, gelatin and collagen degrading enzymes from human skin fibroblasts and synovial cells.," *The Journal of rheumatology*, vol. 10, pp. 861–71, Dec. 1983.

[68] G. P. Stricklin, E. A. Bauer, J. J. Jeffrey, and A. Z. Eisen, "Human skin collagenase: isolation of precursor and active forms from both fibroblast and organ cultures," *Biochemistry*, vol. 16, pp. 1607–1615, Apr. 1977.

[69] J. Yang, M. Yamato, C. Kohno, A. Nishimoto, H. Sekine, F. Fukai, and T. Okano, "Cell sheet engineering: recreating tissues without biodegradable scaffolds," *Biomaterials*, vol. 26, no. 33, pp. 6415–6422, 2005.

[70] S. Mathes and S. Hansen, *Flap Classification and Applications. In: Plastic Surgery. Vol. I: General Principles.* Philadelphia : Saunders, 2005.

[71] H. Nakajima, T. Fujino, and S. Adachi, "A new concept of vascular supply to the skin and classification of skin flaps according to their vascularization.," *Annals of plastic surgery*, vol. 16, pp. 1–19, Jan. 1986.

[72] J. R. Kosko, P. B. Williams, and M. F. Pratt, "Correlation of neutrophil activation and skin flap survival in pharmacologically altered pigs.," *The Annals of otology, rhinology, and laryngology*, vol. 106, pp. 790–4, Oct. 1997.

[73] C. Y. Pang, C. R. Forrest, and S. F. Morris, "Pharmacological augmentation of skin flap viability: a hypothesis to mimic the surgical delay phenomenon or a wishful thought.," *Annals of plastic surgery*, vol. 22, pp. 293–306, May 1989.

[74] M. K. Wax, D. D. Reh, and M. M. Levack, "Effect of celecoxib on fasciocutaneous flap survival and revascularization.," *Archives of facial plastic surgery : official publication for the American Academy of Facial Plastic and Reconstructive Surgery, Inc. and the International Federation of Facial Plastic Surgery Societies*, vol. 9, no. 2, pp. 120–4.

[75] M. Höckel, K. Schlenger, S. Doctrow, T. Kissel, and P. Vaupel, "Therapeutic angiogenesis.," *Archives of surgery (Chicago, Ill. : 1960)*, vol. 128, pp. 423–9, May 1993.

[76] J. M. Isner and T. Asahara, "Angiogenesis and vasculogenesis as therapeutic strategies for postnatal neovascularization.," *The Journal of clinical investigation*, vol. 103, pp. 1231–6, May 1999.

[77] D. M. Brown, S. P. Hong, C. L. Farrell, G. F. Pierce, and R. K. Khouri, "Platelet-derived growth factor BB induces functional vascular anastomoses in vivo.," *Proceedings of the National Academy of Sciences of the United States of America*, vol. 92, pp. 5920–4, July 1995.

[78] D. B. Hom, T. C. Simplot, K. J. Pernell, J. C. Manivel, and C. W. Song, "Vascular and epidermal effects of fibroblast growth factor on irradiated and nonirradiated skin flaps.," *The Annals of otology, rhinology, and laryngology*, vol. 109, pp. 667–75, July 2000.

[79] A. Scalise, M. G. Tucci, G. Lucarini, F. Giantomassi, F. Orlando, M. Pierangeli, A. Pugnaloni, A. Bertani, G. Ricotti, and G. Biagini, "Local rh-VEGF administration enhances skin flap survival more than other types of rh-VEGF administration: a clinical, morphological and immunohistochemical study.," *Experimental dermatology*, vol. 13, pp. 682–90, Dec. 2004.

[80] S. Jorgensen, D. A. Bascom, A. Partsafas, and M. K. Wax, "The effect of 2 sealants (FloSeal and Tisseel) on fasciocutaneous flap revascularization.," *Archives of facial plastic surgery : official publication for the American Academy of Facial Plastic and Reconstructive Surgery, Inc. and the International Federation of Facial Plastic Surgery Societies*, vol. 5, no. 5, pp. 399–402.

[81] R. Mittermayr, T. Morton, M. Hofmann, S. Helgerson, M. van Griensven, and H. Redl, "Sustained (rh)VEGF(165) release from a sprayed fibrin biomatrix induces angiogenesis, up-regulation of endogenous VEGF-R2, and reduces ischemic flap necrosis.," *Wound repair and regeneration : official publication of the Wound Healing Society [and] the European Tissue Repair Society*, vol. 16, no. 4, pp. 542–50.

[82] T. Mirebella, A. Poggi, M. Scaranari, M. Mogni, M. Lituania, C. Baldo, R. Cancedda, and C. Gentili, "Recruitment of host's progenitor cells to sites of human amniotic fluid stem cells implantation.," *Biomaterials*, vol. 32, pp. 4218–27, June 2011.

[83] M. Teodelinda, C. Michele, C. Sebastiano, C. Ranieri, and G. Chiara, "Amniotic liquid derived stem cells as reservoir of secreted angiogenic

factors capable of stimulating neo-arteriogenesis in an ischemic model.," *Biomaterials*, vol. 32, pp. 3689–99, May 2011.

[84] P. De Coppi, G. Bartsch, M. M. Siddiqui, T. Xu, C. C. Santos, L. Perin, G. Mostoslavsky, A. C. Serre, E. Y. Snyder, J. J. Yoo, M. E. Furth, S. Soker, and A. Atala, "Isolation of amniotic stem cell lines with potential for therapy.," *Nature biotechnology*, vol. 25, pp. 100–6, Jan. 2007.

[85] W. Michlits, R. Mittermayr, R. Schäfer, H. Redl, and S. Aharinejad, "Fibrin-embedded administration of VEGF plasmid enhances skin flap survival.," *Wound repair and regeneration : official publication of the Wound Healing Society [and] the European Tissue Repair Society*, vol. 15, no. 3, pp. 360–7.

[86] S. Mine, N. O. Fortunel, H. Pageon, and D. Asselineau, "Aging alters functionally human dermal papillary fibroblasts but not reticular fibroblasts: a new view of skin morphogenesis and aging.," *PloS one*, vol. 3, p. e4066, Jan. 2008.

[87] J. M. Hill, G. Zalos, J. P. J. Halcox, W. H. Schenke, M. A. Waclawiw, A. A. Quyyumi, and T. Finkel, "Circulating endothelial progenitor cells, vascular function, and cardiovascular risk.," *The New England journal of medicine*, vol. 348, pp. 593–600, Mar. 2003.

[88] T. Asahara, H. Masuda, T. Takahashi, C. Kalka, C. Pastore, M. Silver, M. Kearne, M. Magner, and J. M. Isner, "Bone marrow origin of endothelial progenitor cells responsible for postnatal vasculogenesis in physiological and pathological neovascularization.," *Circulation research*, vol. 85, pp. 221–8, Aug. 1999.

[89] M. Lamparter, A. K. Hatzopoulos, E. Deindl, and C. Kupatt, *Therapeutic Neovascularization–Quo Vadis?* Dordrecht: Springer Netherlands, 2007.

[90] C. Sunderkötter, K. Steinbrink, M. Goebeler, R. Bhardwaj, and C. Sorg, "Macrophages and angiogenesis.," *Journal of leukocyte biology*, vol. 55, pp. 410–22, Mar. 1994.

[91] F. Zhang, W. Waller, and W. C. Lineaweaver, "Growth factors and flap survival.," *Microsurgery*, vol. 24, pp. 162–7, Jan. 2004.

[92] Z. Kryger, F. Zhang, T. Dogan, C. Cheng, W. C. Lineaweaver, and H. J. Buncke, "The effects of VEGF on survival of a random flap in the rat: examination of various routes of administration.," *British journal of plastic surgery*, vol. 53, pp. 234–9, May 2000.

[93] P. Y. Liu, W. Tong, K. Liu, S. H. Han, X. T. Wang, E. Badiavas, K. Rieger-Christ, and I. Summerhayes, "Liposome-mediated transfer of vascular endothelial growth factor cDNA augments survival of random-pattern skin flaps in the rat.," *Wound repair and regeneration official publication of the Wound Healing Society and the European Tissue Repair Society*, vol. 12, no. 1, pp. 80–85.

[94] P. Carmeliet, "Angiogenesis in health and disease.," *Nature medicine*, vol. 9, pp. 653–60, June 2003.

[95] S.-J. Kim, J.-S. Kim, J. Papadopoulos, S. Wook Kim, M. Maya, F. Zhang, J. He, D. Fan, R. Langley, and I. J. Fidler, "Circulating monocytes expressing CD31: implications for acute and chronic angiogenesis.," *The American journal of pathology*, vol. 174, pp. 1972–80, May 2009.

[96] V. Planat-Benard, J.-S. Silvestre, B. Cousin, M. André, M. Nibbelink, R. Tamarat, M. Clergue, C. Manneville, C. Saillan-Barreau, M. Duriez, A. Tedgui, B. Levy, L. Pénicaud, and L. Casteilla, "Plasticity of human adipose lineage cells toward endothelial cells: physiological and therapeutic perspectives.," *Circulation*, vol. 109, pp. 656–63, Feb. 2004.

[97] V. L. Bautch, "Flk1 expression: promiscuity revealed," *Blood*, vol. 107, pp. 3–4, Jan. 2006.

[98] K. L. Kroeze, W. J. Jurgens, B. Z. Doulabi, F. J. van Milligen, R. J. Scheper, and S. Gibbs, "Chemokine-mediated migration of skin-derived stem cells: predominant role for CCL5/RANTES.," *The Journal of investigative dermatology*, vol. 129, pp. 1569–81, June 2009.

[99] S. WERNER and R. GROSE, "Regulation of Wound Healing by Growth Factors and Cytokines," *Physiol Rev*, vol. 83, pp. 835–870, July 2003.

[100] S. Bollini, K. K. Cheung, J. Riegler, X. Dong, N. Smart, M. Ghionzoli, S. P. Loukogeorgakis, P. Maghsoudlou, K. N. Dubé, P. R. Riley, M. F. Lythgoe, and P. De Coppi, "Amniotic fluid stem cells are cardioprotective following acute myocardial infarction.," *Stem cells and development*, vol. 20, pp. 1985–94, Nov. 2011.

[101] J. D. Klein, C. G. B. Turner, S. A. Steigman, A. Ahmed, D. Zurakowski, E. Eriksson, and D. O. Fauza, "Amniotic mesenchymal stem cells enhance normal fetal wound healing.," *Stem cells and development*, vol. 20, pp. 969–76, July 2011.

[102] E. C. Moorefield, E. E. McKee, L. Solchaga, G. Orlando, J. J. Yoo, S. Walker, M. E. Furth, and C. E. Bishop, "Cloned, CD117 selected human amniotic fluid stem cells are capable of modulating the immune response.," *PloS one*, vol. 6, p. e26535, Jan. 2011.

[103] B. S. Yoon, J.-H. Moon, E. K. Jun, J. Kim, I. Maeng, J. S. Kim, J. H. Lee, C. S. Baik, A. Kim, K. S. Cho, J. H. Lee, H. H. Lee, K. Y. Whang, and S. You, "Secretory profiles and wound healing effects of human amniotic fluid-derived mesenchymal stem cells.," *Stem cells and development*, vol. 19, pp. 887–902, July 2010.

[104] D. S. Zagoura, M. G. Roubelakis, V. Bitsika, O. Trohatou, K. I. Pappa, A. Kapelouzou, A. Antsaklis, and N. P. Anagnou, "Therapeutic potential of a distinct population of human amniotic fluid mesenchymal stem cells

and their secreted molecules in mice with acute hepatic failure.," *Gut*, Oct. 2011.

[105] F.-M. Chen, L.-A. Wu, M. Zhang, R. Zhang, and H.-H. Sun, "Homing of endogenous stem/progenitor cells for in situ tissue regeneration: Promises, strategies, and translational perspectives.," *Biomaterials*, vol. 32, pp. 3189–209, Apr. 2011.

[106] A. Courts, "The N-terminal amino acid residues of gelatin. 3. Enzymic degradation," *Biochemical Journal*, no. 1948, pp. 1948–1952, 1955.